

---

# Tokens-per-Parameter Coverage Is Critical for Robust LLM Scaling Law Extrapolation

---

Joshua Shay Kricheli<sup>||</sup>, Alexander Lawrence Reid<sup>||</sup>, Venkata Gandikota & Paulo Shakarian  
 Syracuse University  
 {jkrichel, areid04, vsgandik, pashakar}@syr.edu

Soumajyoti Sarkar \*  
 Amazon AGI Foundations

## Abstract

Neural scaling laws approximate a language model’s loss as a power-law function of parameter count  $N$  and token count  $D$ . Following Chinchilla-style compute-optimal training, many studies fit scaling laws from runs performed under a fixed tokens-per-parameter (TPP) ratio  $k$  and set  $D = kN$ . We show that this collinear design, combined with the empirically common near-equality of the exponents governing  $N$  and  $D$ , induces an inherent ill-conditioning in the Gauss-Newton least-squares problem: the condition number of the design grows as the inverse square of the gap between the  $N$  and  $D$ -exponents. The scale coefficients become practically unidentifiable, with confidence intervals inflating by an order of magnitude or more, yielding a “sloppy” model whose extrapolations degrade sharply off the training ray. We prove this for four scaling-law formalisms and derive a closed-form TPP-diversity threshold that is necessary and sufficient for well-conditioned estimation. Empirically, non-collinear designs outperform collinear ones on held-out splits with a 97.3% win rate across four laws, five corpora, multiple floating point precision modes. We further show the degeneracy is rooted in Jacobian geometry and is not an artifact of the loss function: any smooth estimation objective whose curvature involves the Jacobian inherits the same ill-conditioning.

## 1 Introduction

Scaling laws have become a cornerstone of large language model (LLM) research, providing a predictive framework for estimating model performance as a function of compute, dataset size, and parameter count (Hestness et al., 2017; Rosenfeld et al., 2019; Kaplan et al., 2020; Alabdulmohsin et al., 2022; Caballero et al., 2023; Bahri et al., 2024). The seminal Chinchilla study (Hoffmann et al., 2022) proposed that model size  $N$  and training tokens  $D$  scale linearly under a fixed compute budget with  $D \approx 20N$ . A recent survey of 50+ studies finds the fitted law shifts substantially under changes to the included  $D/N$  range, with the optimal ratio a recurring source of disagreement (Li et al., 2025b). These works established the fixed TPP (*Tokens-per-Parameter*) heuristic in the compute-optimal setting. This ratio is a prescription for how to allocate compute when *training a single model*, not a design for the experimental grid from which scaling laws are derived. Yet fixed-TPP grids are widely used for exactly this purpose. Cerebras-GPT (Dey et al., 2023) trains 111M-13B models at  $D = 20N$ ; Gadre et al. (2024) parameterize over-trained scaling along constant- $M$  lines where each slice is itself collinear; the OLMo ladder fits Chinchilla at fixed Chinchilla multiples (Bhagia et al., 2025); and DataDecide reports that eight scaling-law variants fitted at  $D = 100N$  fail to beat a naïve single-scale baseline (Magnusson et al., 2025). The practical stakes are high: Choshen et al. (2025)

---

<sup>||</sup> Equal contribution. \* This work does not relate to the author’s position at Amazon.

fit over 1,000 laws to 485 published models and find estimates sensitive to the choice and coverage of training configurations. When all training runs lie on a single ray  $D = kN$  in the  $(N, D)$  plane, the predictor variables become collinear, and combined with the empirically common near-equality of the  $N$  and  $D$  exponents this renders the scaling-law parameters *practically unidentifiable*. We prove this for four scaling-law formalisms - Chinchilla, repeated-data (Muennighoff et al., 2025), Kaplan (Kaplan et al., 2020), and Droppo-Elibol (Droppo and Elibol, 2021) - via Gauss-Newton analysis. Because the degeneracy is in the Jacobian geometry rather than in the loss, any smooth estimation objective inherits the same ill-conditioning (Section 3). The law becomes a “sloppy” model (Section 2): a near-continuum of parameters fits training data indistinguishably yet diverges off the training ray. This directly corrupts isoFLOP prediction: isoFLOP curves cut across the training ray and thereby probe the sloppy direction that collinear fitting leaves unconstrained. Constructively, we give an identified reduced model recovering the combined effect along a single ray (Definition 2), and show empirically that non-collinear designs beat collinear ones when evaluated on the same held-out models (Section 4).

**Key contributions.** (i) A Gauss-Newton analysis proving that collinear designs are inherently ill-conditioned when the exponents governing model size and data size are close, with the condition number growing as the inverse square of the exponent gap - established for four scaling-law formalisms, with a corresponding confidence-interval inflation result (Proposition 1, Corollary 1); (ii) a closed-form TPP-diversity threshold that is necessary and sufficient for well-conditioned estimation (Proposition 2); (iii) a holdout-prediction ordering separating collinear from non-collinear designs (Theorem 1), validated at a 97.3% win rate; (iv) an identified reduced parametrisation that recovers what a single-ray design can constrain (Definition 2); and (v) a fully reproducible experimental suite -  $\sim 1,900$  trained LLMs, all checkpoints, training metrics, accompanied by training and analysis code - provided via an anonymized live online repository link; supplementary material includes a ZIP file with a screenshot of that repository.<sup>2</sup>

**Paper road-map.** The rest of this paper is as follows. Section 3 develops the Gauss-Newton framework, proves condition-number bounds for the four formalisms under collinear designs, derives confidence-interval inflation for individual scale coefficients, and establishes the isoFLOP prediction-error amplification that separates collinear from non-collinear training; proofs are in Appendix B. Section 4 validates the analysis with controlled experiments across five corpora, four laws, and multiple precision regimes. Section 5 synthesises the empirical patterns and cautions against interpreting separate data versus model contributions from single-ray fits.

## 2 Related work

Predictable power-law scaling of generalization error was first reported by Hestness et al. (2017) and formalized for autoregressive language models by Kaplan et al. (2020) using bivariate fits whose grids were often close to fixed-TPP for large subsets. Bahri et al. (2024) linked the observed exponents to data-manifold structure via variance - and resolution-limited regimes. Follow-ups to Chinchilla examined data availability (Villalobos et al., 2024), overtraining (Touvron et al., 2023), and unbounded compute with fixed data (Kim et al., 2025); we extend our analysis to repeated-data regimes (Muennighoff et al., 2025) in Appendix B.7. Sardana et al. (2025) sweep ratios up to 10,000 TPP, producing inherently non-collinear designs that our diagnosis predicts should be well-identified (Section 3) - yet the most widely cited scaling-law parameters were estimated under the collinearity conditions we formalize. Besiroglu et al. (2024) could not reconcile Chinchilla’s reported estimates with two of three replication methods, and Porian et al. (2025) attribute the Kaplan-Chinchilla discrepancy to minor recipe differences (last-layer cost, warm-up, scale-dependent tuning); our ill-conditioning result explains *why* such small perturbations shift coefficients by orders of magnitude. Reinforcing this, Bergsma et al. (2025) show even optimizer hyperparameters (weight decay, batch size) obey power laws in the TPP ratio  $D/N$ , so fixing a single ray couples recipe with scale. Concurrently, Volkova et al. (2026) report that fitting separate Chinchilla-style laws across optimizers yields ill-conditioned, highly correlated parameters - the same pathology we formalize from Jacobian geometry, observed along the optimizer axis. Schaeffer et al. (2026) propose sidestepping multicollinearity via compute-envelope or gold-reference parameterizations - both

<sup>2</sup>Code: [https://anonymous.4open.science/r/Tokens-per-Parameter\\_Coverage\\_Is\\_Critical\\_for\\_Robust\\_LLM\\_Scaling\\_Law\\_Extrapolation-CC76](https://anonymous.4open.science/r/Tokens-per-Parameter_Coverage_Is_Critical_for_Robust_LLM_Scaling_Law_Extrapolation-CC76). Checkpoints and metrics: [https://huggingface.co/datasets/TPPIsCriticalFor/collinear\\_scaling\\_models](https://huggingface.co/datasets/TPPIsCriticalFor/collinear_scaling_models).

abandon the  $(N, D)$  decomposition. Zhang et al. (2026) pursue a related goal at the downstream-evaluation level, estimating compute-to-capability boundaries via quantile regression on post-trained models. Our work is complementary: we prove the condition number grows as  $\Theta(\varepsilon^{-2})$  in the exponent gap from Jacobian geometry alone (Proposition 1, Lemma 2), and give designs that *restore* identifiability within the multivariate framework (Proposition 4). Yue et al. (2025)’s Relative-Based Scaling Law is largely a single-axis sweep in model size, which our analysis flags as insufficient for multivariate identifiability. Farseer (Li et al., 2025a) adds an  $N$ - $D$  coupling term and trains  $\sim 1,000$  models on a diverse  $(N, D)$  grid - the two-dimensional coverage our analysis requires - reporting a 433% reduction in extrapolation error over Chinchilla; even such interaction terms remain unidentifiable under  $D = kN$  (Section 3; Appendix B.16). Shukor et al. (2025) similarly extend scaling laws to data-mixture weights, enlarging the multivariate design space where collinearity matters. Hu et al. (2026) sidestep parametric fitting altogether by training a neural extrapolator over checkpoint trajectories - orthogonal to our diagnosis of *why* the parametric fit is fragile. Statistically, the pathology we analyze is the nonlinear-regression analog of multicollinearity (Kim, 2019; Vatcheva et al., 2016; Dormann et al., 2013; Montgomery et al., 2012; O’Brien, 2007) and of the “sloppy” model phenomenon (Transtrum et al., 2010, 2015), in which narrow model-manifold cross-sections yield fragile estimates - here induced by fixed-TPP sampling.

### 3 Formal analysis

The standard Chinchilla scaling law (Hoffmann et al., 2022, Eq. 2) approximates the loss as a sum of two power-law terms - capturing limited model capacity and data size - plus an irreducible loss  $E$ , a form observed across deep learning domains (Hestness et al., 2017; Kaplan et al., 2020, Sec. 3):

$$L(N, D) = AN^{-\alpha} + BD^{-\beta} + E, \quad (1)$$

where  $A, B, \alpha, \beta, E \in \mathbb{R}_{>0}$  and  $N, D \in \mathbb{R}_{>0}$ .

**Definition 1** (Scaling-law experimental dataset). Let  $\mathcal{A}$  be a training scheme (architecture, optimizer, algorithm, etc.). Each experiment records loss  $L_i$  for a model of size  $N_i$  on  $D_i$  tokens, yielding  $\mathcal{D} = \{(N_i, D_i, L_i)\}_{i=1}^m$ . Let  $N_1 < \dots < N_n \in \mathbb{N}_{>0}$  be the model sizes and  $k_1 < \dots < k_K \in \mathbb{R}_{>0}$  the TPP ratios. A *collinear* design pairs each  $(N_i, k_\ell)$  as  $(N_i, k_\ell N_i, L_{i\ell})$ , so  $m = nK$ ; the special case  $K = 1$  is fully collinear. A parametric law  $\hat{L}(N, D; \theta)$  with  $\theta \in \mathbb{R}^p$  is fit to  $\mathcal{D}$  by minimizing the discrepancy between predicted and observed losses; observations are split into a training set  $\mathcal{D}_{\text{train}}$  and a holdout  $\mathcal{H}$  of  $n_{\mathcal{H}}$  points (possibly at TPP ratios off the training manifold).

On a single ray ( $K = 1$ ) - the dominant practical case ( $k \approx 20$  for Chinchilla (Hoffmann et al., 2022; Villalobos et al., 2024)) - substituting  $D = kN$  into (1) gives  $L(N, kN) = AN^{-\alpha} + Bk^{-\beta}N^{-\beta} + E$ . Setting  $\beta = \alpha$  collapses the two power-law terms, yielding a *reduced model*:

**Definition 2** (Reduced Chinchilla model under fixed TPP).

$$L(N; \psi, \alpha, E) = (A + Bk^{-\alpha})N^{-\alpha} + E = \psi N^{-\alpha} + E, \quad (2)$$

where  $\psi := A + Bk^{-\alpha}$  combines the Chinchilla-scale coefficients from (1) and  $k \in \mathbb{R}_{>0}$  is the fixed TPP ratio on that ray.

**Definition 3** (Exponent gap by scaling law). Define  $\varepsilon$  as a *law-specific exponent gap* in each law’s native notation (see Table 1): **Chinchilla** (and repeated-data on effective  $(N', D')$ ):  $\varepsilon := |\alpha - \beta|$ ; **Kaplan** (exponents  $\alpha_N, \alpha_D$ ):  $\varepsilon := |\alpha_D - \alpha_N|$ ; **Droppo-Elibol** (exponents  $\alpha_N, \alpha_D, \alpha$  with  $\gamma_N := \alpha_N/\alpha, \gamma_D := \alpha_D/\alpha, \alpha > 0$ ):  $\varepsilon := |\gamma_N - \gamma_D|$ . For example, Chinchilla reports  $\alpha \approx 0.34$  and  $\beta \approx 0.28$ ; Kaplan-scale fits use  $\alpha_N \approx 0.076$  and  $\alpha_D \approx 0.095$ .

#### 3.1 Gauss-Newton (GN) framework on a single ray

We fit by nonlinear least squares: minimize  $S(\theta) := \frac{1}{2}\|\mathbf{r}(\theta)\|^2$  over  $\theta \in \mathbb{R}^p$ , where the residuals  $r_i := L_i - \hat{L}(N_i, D_i; \theta)$  stack into  $\mathbf{r}(\theta)$ , with *Jacobian*  $J \in \mathbb{R}^{m \times p}$  given by  $J_{ij} = \partial r_i / \partial \theta_j$ . We write  $\kappa(M) := \lambda_{\max}(M) / \lambda_{\min}(M)$  for the condition number of a symmetric positive-definite matrix  $M$ . GN linearizes  $\mathbf{r}$ , giving the normal equations  $(J^T J) \Delta \theta = -J^T \mathbf{r}$  (Appendix B.1). For each law’s scale coefficients  $(A, B)$ , let  $\kappa_{A,B} := \kappa((J^T J)_{A,B})$  on the  $(A, B)$  principal submatrix of  $J^T J$ . Throughout the paper, we assume the  $(A, B)$  pair is the dominant source of ill-conditioning

Table 1: Jacobian columns at the  $i$ -th data point under  $D = kN$  (with  $i$  subscripts dropped for brevity). Rows correspond, in order, to Chinchilla (Hoffmann et al., 2022), Repeated-data (Muennighoff et al., 2025), Kaplan (Kaplan et al., 2020), and Droppo-Elibol (Droppo and Elibol, 2021). For each law,  $\mathbf{j}_2$  is a scalar multiple of  $\mathbf{j}_1$  times  $N^\varepsilon$ , exposing the shared collinearity structure.

Law ( $\hat{L}$ )	Collinear pair	$\mathbf{j}_1$	$\mathbf{j}_2$	$\varepsilon$
$AN^{-\alpha} + BD^{-\beta} + E$	$(A, B)$	$N^{-\alpha}$	$k^{-\beta} N^{-\alpha} N^\varepsilon$	$ \alpha - \beta $
$AN'^{-\alpha} + BD'^{-\beta} + E$	$(A, B)$	$N'^{-\alpha}$	$k^{-\beta} (D'/N')^{-\beta} N'^{-\alpha} N^\varepsilon$	$ \alpha - \beta $
$[(N_c/N)^{\alpha_N/\alpha_D} + D_c/D]^{\alpha_D}$	$(N_c, D_c)$	$\propto N^{-\alpha_D}$	$\propto N^{-\alpha_D} N^\varepsilon$	$ \alpha_D - \alpha_N $
$[(N_C/N)^{\alpha_N} + (D_C/D)^{\alpha_D} + E^{1/\alpha}]^\alpha$	$(N_C, D_C)$	$\propto N^{-\gamma_N}$	$\propto N^{-\gamma_N} N^\varepsilon$	$ \gamma_N - \gamma_D $

Table 2: Statistical identifiability of scale coefficients under single-TPP designs, using representative published exponent values.  $\varepsilon^{-1}$  and  $\varepsilon^{-2}$  are the leading-order asymptotic factors in  $\text{CI}(A)/\text{CI}(\psi) = \Theta(\varepsilon^{-1})$  (Corollary 1) and  $\kappa_{A,B} = \Theta(\varepsilon^{-2})$  (Proposition 1), respectively, both as  $\varepsilon \rightarrow 0$ . The indicative  $\kappa_{A,B}$  range is computed on our experimental grid of 14 model sizes spanning  $N \in [5.04, 76.5] \text{ M}$  ( $N_{\max}/N_{\min} \approx 15.2$ ; Appendix C, weighted  $\sigma_w^2(\log N) \approx 0.74$  at  $\alpha=0.34$ ). The repeated-data law inherits Chinchilla’s exponents and is omitted.

Law	Exponents	$\varepsilon$	$\varepsilon^{-1}$	$\varepsilon^{-2}$	$\kappa_{A,B}$	CI inflation
Chinchilla	$\alpha \approx 0.34, \beta \approx 0.28$	0.06	17	278	$10^3$ - $10^4$	$\gtrsim 17\times$
Kaplan	$\alpha_N \approx 0.076, \alpha_D \approx 0.095$	0.019	53	$\sim 2.8 \times 10^3$	$10^4$ - $10^5$	$\gtrsim 53\times$
Droppo-Elibol	$\gamma_N \approx \gamma_D$	$\sim 0.05$ - $0.10$	10-20	100-400	$10^3$ - $10^4$	$\gtrsim 10$ - $20\times$

in  $J^T J$  (verified case-by-case in Appendices B.5-B.9), so  $\kappa(J^T J) \asymp \kappa_{A,B}$  and the two are used interchangeably in the formal statements that follow. This dominance turns the lower bounds of Propositions 1-2 and Corollary 1 into matching two-sided ( $\Theta$ ) rates.

**Proposition 1** (Full-matrix conditioning). *Let  $J \in \mathbb{R}^{m \times p}$  have columns  $\mathbf{j}_1, \dots, \mathbf{j}_p$ , and suppose two columns  $a \neq b$  satisfy  $\mathbf{j}_b = c\mathbf{j}_a + \boldsymbol{\delta}$  with  $c \neq 0$  and  $\|\boldsymbol{\delta}\| = O(\varepsilon)$  for some scalar  $c$  and  $\boldsymbol{\delta} \in \mathbb{R}^m$ , where  $\varepsilon$  is the law-specific exponent gap (Definition 3). Let  $\lambda_{\max}(J^T J)$  and  $\lambda_{\min}(J^T J)$  denote the largest and smallest eigenvalues of  $J^T J$ . Then as  $\varepsilon \rightarrow 0$ ,  $\lambda_{\max}(J^T J) = \Theta(1)$ ,  $\lambda_{\min}(J^T J) = \Theta(\varepsilon^2)$ , and*

$$\kappa(J^T J) = \Theta(\varepsilon^{-2}). \quad (3)$$

*Proof.* Appendix B.3. The bound applies to all four laws in Table 1: on a collinear ray  $D = kN$ , every law’s Jacobian satisfies the near-proportionality assumption of Proposition 1 (Appendices B.5-B.9).

On a single ray, the reduced model (2) is identified (Proposition 4) while the full model is ill-conditioned (Proposition 1). The LS estimator’s uncertainty comes from inverting  $J^T J$  (Björck, 1996, §2.8.3, eq. (2.8.7), p. 118): when the data cannot distinguish  $A$  from  $B$ , only their combination  $\psi$  is pinned down, leaving each coefficient individually highly uncertain. The confidence interval on  $A$  therefore widens by a factor  $\Theta(\varepsilon^{-1})$  relative to the one on  $\psi$ :

**Corollary 1** (Confidence interval inflation). *Under i.i.d. Gaussian noise with variance  $\sigma^2$ , on a single ray  $D = kN$ , the least-squares confidence intervals for  $A$  in the full Chinchilla model (1) and for the combined coefficient  $\psi$  in the reduced model (2) satisfy, as  $\varepsilon \rightarrow 0$ ,*

$$\frac{\text{CI}_{0.95}(A)}{\text{CI}_{0.95}(\psi)} = \Theta(\varepsilon^{-1}). \quad (4)$$

*Proof.* Appendix B.11.

The approximated CI inflation for the four scaling laws is collected in Table 2.

### 3.2 Multi-ray designs and holdout prediction

We generalize to  $K \geq 1$  collinear rays - the practically relevant setting of training at several TPP ratios - and ask how much TPP diversity suffices to restore well-conditioned estimation.

**Proposition 2** (TPP diversity and full-matrix conditioning). *For any of the four scaling laws in Table 1, assume observed losses have i.i.d. Gaussian residuals with variance  $\sigma^2$  (well-specified law). For any  $\kappa_{\text{target}} > 0$  and ordered training ratios  $k_1 \leq \dots \leq k_K$  ( $K \geq 1$ ), to leading order as  $\varepsilon \rightarrow 0$ , we have*

$$\kappa(J^T J) \leq \kappa_{\text{target}} \iff \underbrace{\frac{1}{K} \sum_{\ell=1}^K k_\ell^{-2\beta_{\text{eff}}} - \left( \frac{1}{K} \sum_{\ell=1}^K k_\ell^{-\beta_{\text{eff}}} \right)^2}_{V_K} \geq \underbrace{\frac{\left( K + \sum_{\ell=1}^K k_\ell^{-2\beta_{\text{eff}}} \right)^2}{K^2 \kappa_{\text{target}}}}_{\tau_K}, \quad (5)$$

where  $V_K$  is the second central moment (or variance) of  $\{k_\ell^{-\beta_{\text{eff}}}\}_{\ell=1}^K$ , and  $\beta_{\text{eff}}$  is the law-specific data-size exponent:  $\beta$  for Chinchilla/repeated-data,  $\alpha_D$  for Kaplan,  $\gamma_D$  for Droppo-Elibol. For  $K = 1$ ,  $V_1 = 0 < \tau_1$ , so (5) never holds; for  $K = 2$  with  $R := k_2/k_1$  it reduces to  $R \geq R_{\text{min}}$  (Eq. (95), Table 9); for  $K > 2$  interior rays reduce  $V_K$  at fixed endpoint spread, so  $K = 2$  with mass at the endpoints is near-optimal at fixed  $R$  and  $K \geq 3$  does not relax the spread requirement (Appendix B.15).

*Proof.* Appendix B.12; explicit  $V_K, \tau_K$  algebra and the two-ray reduction are in Appendix B.15.

With  $K \geq 2$  training rays, per-ray  $(A, B)$  collinearity (Proposition 1) is cured at the full-matrix level iff  $V_K \geq \tau_K$  (Proposition 2). Since (5) can be evaluated *before* training using a literature estimate of  $\beta_{\text{eff}}$  (the data-side power-law exponent governing  $L \propto D^{-\beta_{\text{eff}}}$  at leading order; e.g.  $\beta \approx 0.28$  for Chinchilla), it is an a-priori design diagnostic. Theorem 1 translates the conditioning into a holdout-RMSE ordering.

**Theorem 1** (Holdout prediction regimes). *Under Proposition 2, assume  $\kappa_{\text{target}}$  is small enough that  $\kappa(J^T J) \leq \kappa_{\text{target}}$  ensures numerically well-conditioned NLS and faithful Gauss-Newton linearization (Appendix B.13). Let CO denote a collinear design ( $K \geq 1$ ), NC a non-collinear design with at least two distinct training ratios and dense two-dimensional  $(N, D)$  coverage, and let  $\mathcal{H}$  denote a holdout with a nonzero fraction of off-ratio points ( $k' = D'/N'$  differs from every training ratio). For  $X \in \{\text{CO}, \text{NC}\}$ ,  $\text{RMSE}_{\mathcal{H}}^X$  is the root-mean-square prediction error of  $\hat{L}$  on  $\mathcal{H}$  under that training design, and  $R_{\mathcal{H}}^{2X}$  the corresponding coefficient of determination on  $\mathcal{H}$ . The regimes below hold at leading order as  $\varepsilon \rightarrow 0$ .*

**Regime A** (ill-conditioned,  $V_K < \tau_K$ ; for the CO ray design, includes all  $K = 1$  and any  $K \geq 2$  with insufficient diversity):

$$\mathbb{E}[\text{RMSE}_{\mathcal{H}}^{\text{NC}}] < \mathbb{E}[\text{RMSE}_{\mathcal{H}}^{\text{CO}}], \quad (6)$$

and thus  $\mathbb{E}[R_{\mathcal{H}}^{2\text{NC}}] > \mathbb{E}[R_{\mathcal{H}}^{2\text{CO}}]$  (misspecification extension: Appendix B.13).

**Regime B** (well-conditioned,  $V_K \geq \tau_K$ ; requires  $K \geq 2$ ):  $\mathbb{E}[\text{RMSE}_{\mathcal{H}}^{\text{CO}}]/\mathbb{E}[\text{RMSE}_{\mathcal{H}}^{\text{NC}}] = \Theta(1)$ , i.e., neither design has systematic asymptotic RMSE dominance.

*Proof.* Appendix B.13 (Gauss-Newton linearization, spectral decomposition, RMSE ordering).

### 3.3 Applying to respective scaling laws

Table 1 collects the collinear pair, Jacobian columns on a single ray  $D = k_\ell N$ , and exponent gap for each law. Proposition 1 then yields  $\kappa(J^T J) = \Theta(\varepsilon^{-2})$  in all four cases; per-law derivations are in Appendices B.5, B.7, B.8, and B.9. The resulting CI inflation is *statistical* (Corollary 1); per-law factors appear in Table 2. **First**, Kaplan is the most degenerate under single-TPP: its gap 0.019 is  $\sim 3\times$  smaller than Chinchilla's 0.06, amplifying  $\varepsilon^{-2}$  by an order of magnitude ( $\sim 2.7 \times 10^3$  vs.  $\sim 278$ ) and CI inflation by  $\sim 3\times$  ( $\sim 53\times$  vs.  $\sim 17\times$ ) - matching its strong empirical degeneracy. **Second**, Chinchilla and repeated-data are problematic: small, near-equal exponents ( $\alpha, \beta < 0.4$ ) yield CI inflation  $\sim 17\times$ , leaving individual  $A, B$  estimates noise-dominated. **Third**, Droppo-Elibol is fit-dependent: for language data  $|\gamma_N - \gamma_D|$  is comparable to Chinchilla's 0.06, and the well-identified outer envelope ( $\alpha, L_\infty$ ) does not relieve the  $(N_C, D_C)$  degeneracy. The reduced model (Definition 2) is therefore most critical for Kaplan- and Chinchilla-class fits, with Kaplan the most degenerate.

### 3.4 IsoFLOP prediction under collinearity

*IsoFLOP* curves are contours of constant training compute  $C = 6ND$  (Hoffmann et al., 2022). They cut across the training ray and probe the sloppy parameter direction that collinear training leaves unconstrained, making them an informative diagnostic.

**Definition 4** (Induced isoFLOP curves plot). Let  $\hat{L}(N, D; \theta)$  be a fitted scaling law and  $\mathcal{H} = \{(N_i, D_i, L_i)\}_{i=1}^{n_{\mathcal{H}}}$  a holdout set of size  $n_{\mathcal{H}}$  with induced compute budgets  $C_i := 6N_iD_i$ . The *induced isoFLOP curves* are the family

$$\{N \mapsto \hat{L}(N, C_i/(6N); \theta) : N \in [N_{\min}, N_{\max}]\}_{i=1}^{n_{\mathcal{H}}}, \quad (7)$$

with  $N_{\min} := \min_j N_j$  and  $N_{\max} := \max_j N_j$ . The *induced isoFLOP curves plot* draws this family on the  $(N, L)$ -plane with each holdout point  $(N_i, L_i)$  overlaid on its curve.

**Proposition 3** (RMSE invariance under isoFLOP reparameterization). *With  $\hat{L}, \mathcal{H}, \{C_i\}$  as in Definition 4, the RMSE of  $\hat{L}$  on  $\mathcal{H}$  is invariant under  $(N, D) \mapsto (N, C)$ : evaluating the  $i$ -th induced isoFLOP curve at  $N = N_i$  yields the same error as evaluating  $\hat{L}(N_i, D_i)$  directly (Appendix B.14).*

## 4 Empirical evaluation

**Empirically evaluating dense TPP coverage.** To validate the formal statements of Section 3, we fit each scaling law under two training designs - collinear (CO) and non-collinear (NC) - and measure holdout error on a shared CO/NC split across five pre-training corpora: three common and two specialized (see Appendix C.5). All models are LLaMA-style transformers trained with AdamW on a cosine schedule; full hyperparameters are in Appendix C. Model sizes span 5.04-76.5M parameters across 14 log-spaced configurations ( $N_{\max}/N_{\min} \approx 15$ ; see Table 10). Tokenization uses `cl100k_base` ( $V=100,277$ ), and  $N$  counts all trainable parameters (embeddings included) per the Hoffmann-Chinchilla convention (Hoffmann et al., 2022); we apply this convention uniformly when fitting all four laws - including Kaplan (Kaplan et al., 2020), which originally defines  $N$  on non-embedding parameters - and our analysis does not involve a FLOPs budget  $C$ . We log cross-entropy loss per epoch.

**Experimental designs.** Both designs share identical architectures, optimizers, and schedules; the *only* difference is how  $(N, D)$  pairs are sampled, and total run counts are comparable. **Collinear (CO):** Every run sets  $D = kN$  for  $k \in \mathcal{K}_{\text{train}} := \{1, 1.5, 1.9, 2, 2.5, 2.7, 3, 3.3, 3.5, 4, 4.5, 5\}$ . Although 12 ratios are used, each defines a ray through the origin; the configurations form a *fan of rays* rather than filling a two-dimensional region, producing the collinearity diagnosed in Section 3.

**Non-Collinear (NC):** The same 14 model sizes are crossed with 12 dataset sizes ( $\sim 10\text{M}$ - $\sim 276\text{M}$  tokens), yielding a  $14 \times 12$  grid spanning a two-dimensional region. The implied ratio  $k = D/N$  varies freely, decoupling the two axes and eliminating the rank deficiency. The grid is visualized in Appendix D.1. We fit the four mentioned scaling laws via nonlinear least squares with 100 random restarts and a differential-evolution polish, repeated across 30 independent optimizer seeds (see Appendix D.6). For Repeated-Data, each epoch’s checkpoint is a separate observation; for the remaining three we fit per-epoch losses independently (epochs 1, 2, 3). To verify robustness to numerical precision, we run a **BF16** round ( $k \in \mathcal{K}_{\text{train}}$ , mixed precision). The NC advantage persists in this regime (Appendix D.4). Additionally, we provide a preliminary high-TPP experiment (small-scale,  $k \in \mathcal{K}_{\text{big}} := \{10, 11, 12, 13, 14, 15\}$ , holdouts up to 20) with Wikipedia and Chinchilla, achieving a 63.3% NC win rate (CI [45.5%, 78.1%]); see Appendices D.7 and C.8).

Table 3:  $R^2$  and RMSE summary across training designs with different seed-to-seed optimizer setup. 95% CI: confidence interval on the mean. Best per split in **bold**.

Split	Design	$R^2$				RMSE			
		Mean	95% CI	Median	Std	Mean	95% CI	Median	Std
Train ( $\mathcal{D}$ )	CO	<b>0.9848</b>	<b>[0.985, 0.985]</b>	<b>0.9850</b>	<b>0.0047</b>	<b>0.1737</b>	<b>[0.173, 0.174]</b>	<b>0.1616</b>	<b>0.0430</b>
	NC	0.9526	[0.952, 0.953]	0.9542	0.0172	0.2023	[0.202, 0.203]	0.1869	0.0443
Holdout ( $\mathcal{H}$ )	CO	0.8370	[0.832, 0.842]	0.8811	0.1129	0.2373	[0.233, 0.241]	0.2163	0.1229
	NC	<b>0.9319</b>	<b>[0.930, 0.934]</b>	<b>0.9392</b>	<b>0.0269</b>	<b>0.1561</b>	<b>[0.154, 0.158]</b>	<b>0.1242</b>	<b>0.0599</b>

**Evaluation splits.** The collinear design reserves five TPP ratios  $k \in \mathcal{K}_{\text{test}} := \{6, 6.2, 6.5, 6.7, 7\}$ , forming a collinear holdout  $\mathcal{H}_{\text{col}}$  on rays just beyond the training fan. The non-collinear design

reserves dataset sizes  $D \in [300, 401]$  M tokens, forming a non-collinear holdout  $\mathcal{H}_{\text{nc}}$  that requires extrapolation into the  $(N, D)$  plane beyond the training fan. We evaluate both designs on a single *unified holdout*  $\mathcal{H} = \mathcal{H}_{\text{col}} \cup \mathcal{H}_{\text{nc}}$ , so that every comparison is head-to-head, with test points from both geometries. All paper metrics and tables use this  $\mathcal{H}$  when reporting holdout performance; per-split breakdowns appear in Appendix D.

Table 4: Win rate breakdown (NC vs. CO design) on holdout with seed-paired comparisons. Overall NC (non-collinear) win rate: 97.3% (1,460/1,500). 95% CI: [96.4%, 98.0%].

Dataset		Scaling Law		Epoch	
C4	93.0%	Chinchilla	97.6%	first	99.8%
Cosmopedia	94.7%	Droppo-Elibol	98.0%	second	97.6%
peS2o	99.3%	Kaplan	95.6%	final	93.8%
RedPajama	100.0%	Repeated-Data	100.0%		
Wikipedia	99.7%				

**TPP coverage tracking.** To quantify how design coverage affects fit quality, we incrementally widen each design’s data axis - progressively including additional TPP ratios (CO) or dataset sizes (NC) - and refit each scaling law at each step, recording holdout  $R^2$ . The coverage fraction reports the fraction of levels included: 1.0 means all of  $\mathcal{K}_{\text{train}}$  (CO) or all 12  $D$  sizes (NC). Because the two designs draw from distinct value sets, CO and NC curves trace independent trajectories through the  $(N, D)$  plane. Setup details and paired convergence plots appear in Appendices D.5 and D.8, respectively.

Table 5:  $R^2$  and RMSE summary for bf16 across training designs, averaged with seed-to-seed optimizer std (30 seeds). 95% CI: confidence interval on the mean. Best per split in **bold**.

Split	Design	$R^2$				RMSE			
		Mean	95% CI	Median	Std	Mean	95% CI	Median	Std
Train ( $\mathcal{D}$ )	CO	0.9896	[0.990, 0.990]	0.9916	0.0029	0.1854	[0.185, 0.185]	0.1606	0.0353
	NC	<b>0.9907</b>	<b>[0.991, 0.991]</b>	<b>0.9915</b>	<b>0.0020</b>	<b>0.1457</b>	<b>[0.145, 0.146]</b>	<b>0.1428</b>	<b>0.0171</b>
Holdout ( $\mathcal{H}$ )	CO	0.9412	[0.940, 0.942]	0.9473	0.0172	0.2546	[0.252, 0.257]	0.2402	0.0396
	NC	<b>0.9657</b>	<b>[0.965, 0.967]</b>	<b>0.9663</b>	<b>0.0068</b>	<b>0.1949</b>	<b>[0.192, 0.198]</b>	<b>0.1921</b>	<b>0.0203</b>

**Aggregate metrics.** Table 3 reports mean, median, and standard deviation of  $R^2$  and RMSE across all law-dataset combinations for each design-split pair. Table 4 tallies pairwise wins (higher  $R^2$  or lower RMSE) for NC vs. CO, broken down by dataset, law, and epoch mode. Table 5 confirms the effect is precision-invariant: under BF16 mixed-precision training on Wikipedia, NC achieves a unified holdout  $R^2$  of 0.966 vs. CO’s 0.941. The BF16 winrate (98.7%, CI: [96.6%, 99.5%]) is comparable to the full-precision results, presented in Appendix D.4 (Table 16). Full per-dataset breakdowns for FP and BF16 runs are in Appendices D and E.

**Representative plots.** Figure 1 complements the aggregate statistics with a representative three-panel view: fitted loss surface, holdout  $R^2$  vs. TPP coverage, and induced isoFLOP curves (more three-panel views in Appendix D.8). TPP coverage is the fraction of  $\mathcal{K}_{\text{train}}$  for CO (or available  $D$  sizes for NC) included in the fit; see Section 4. The contrast is stark: the Kaplan CO fit on RedPajama (first-epoch loss) achieves a holdout  $R^2$  of only 0.51, while NC reaches 0.91. The surface panel (Figure 1a) shows CO residuals growing toward the small- $N$  region, where Proposition 1’s sloppy direction dominates predicted loss. The convergence panel (Figure 1b) aligns with the predictions of Theorem 1 and Corollary 1: (i) CO sits strictly below NC at every TPP coverage level because, at  $\kappa_{\text{target}} = 100$ , Kaplan’s full CO satisfies  $V_K \approx 1.6 \times 10^{-3} \ll \tau_K \approx 3.4 \times 10^{-2}$ , while NC yields  $V_K \approx 9.3 \times 10^{-3}$ ,  $\tau_K \approx 3.1 \times 10^{-2}$  (Proposition 2); both sit in Regime A of Theorem 1, which predicts NC > CO (6); (ii) CO’s CI bars are  $\sim 53\times$  wider than NC’s - matching the  $\Theta(\varepsilon^{-1})$  inflation predicted by Corollary 1 (numerically  $\varepsilon^{-1} \approx 53$  at Kaplan’s  $\varepsilon \approx 0.019$ ; Table 2); (iii) CO’s bars shrink monotonically with coverage but never close the gap, because  $\kappa(J^T J) = \Theta(\varepsilon^{-2})$  (numerically  $\sim 2.8 \times 10^3$ ) is design-level, independent of  $n$  (Proposition 1); (iv) CO’s central  $R^2$  oscillates while NC’s rises smoothly because Kaplan’s scale-coefficient estimates  $(\hat{N}_c, \hat{D}_c)$  wander along the sloppy direction of Proposition 1, whereas NC’s 2D coverage keeps  $\kappa(J^T J) \leq \kappa_{\text{target}}$

(Theorem 1), bounding the sloppy direction; (v) the isoFLOP panel (Figure 1c) makes the same separation visible at the budget level: CO’s dashed curves splay apart at high  $N$  along the sloppy direction of Proposition 1, while NC’s solid curves stay tight.

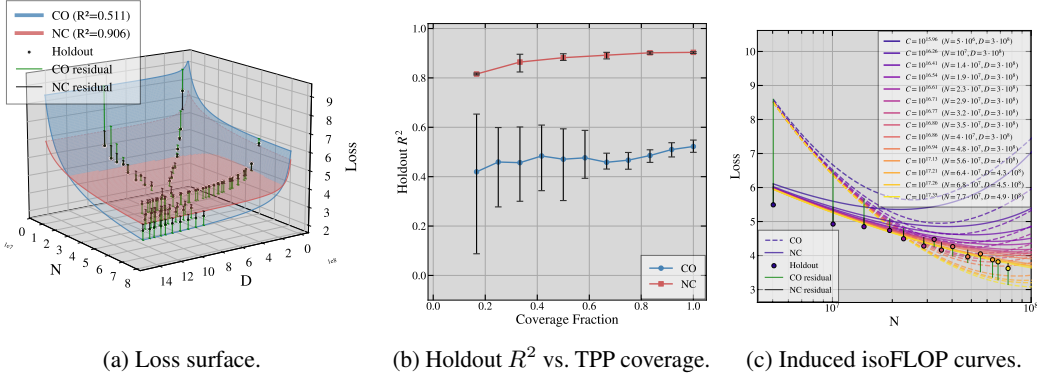


Figure 1: Kaplan law on RedPajama, first epoch (CO holdout  $R^2 = 0.51$ , NC  $R^2 = 0.91$ ; CO blue, NC red; seed 0 in (a) and (c), median across 30 seeds with 5th-95th percentile bands in (b)). (a) Fitted loss surface  $\hat{L}(N, D; \theta)$  over the  $(N, D)$  plane with holdout points and residual bars overlaid. (b) Holdout  $R^2$  vs. TPP coverage. (c) Induced isoFLOP curves (Definition 4), one per kept holdout point (highest  $D$  per unique  $N$ ), with residual bars at each  $N_i$ ; curves and markers share a colormap ordered by  $C_i = 6N_i D_i$ .

**Empirical evaluation of Theorem 1 through budget-matched subset enumeration.** Table 6 supports Theorem 1, which predicts that within Regime A ( $V_K < \tau_K$ ; (6)) an NC design achieves smaller expected holdout RMSE than a budget-matched CO design. We enumerate all  $2^{12} - 1 = 4,095$  non-empty subsets  $S \subseteq \{1, \dots, 12\}$  of available TPP ratios. Each  $\text{CO}(S)$  (Definition 10) is paired with a bounding-box NC design of identical cardinality (Appendix D.3) and classified a priori via  $V_K < \tau_K(\kappa_{\text{target}})$  using literature  $\beta_{\text{eff}}$  (Definition 3). Because the theorem doesn’t fix a single  $\kappa_{\text{target}}$ , we average the NC-win rate over 2,000 values drawn log-uniformly from  $[1, 10^9]$ . Each  $\kappa_{\text{target}}$  is repeated under 22 seeds that vary the bounding-box construction and the random restarts of the fit optimizer (300 restarts per fit; random 70% subsample of  $\mathcal{H}$ ). When Regime A is empty for a given  $\kappa_{\text{target}}$ , that seed is skipped. NC beats CO consistently within Regime A for all three laws: 68.5% (Chinchilla), 57.4% (Droppo-Elibol), and 66.0% (Kaplan) averaged across corpora, all with CIs excluding 50%. The effect is strongest on the web-crawled corpora C4, RedPajama, and Wikipedia (NC wins 77-88% for Chinchilla); the two specialized corpora (Cosmopedia and peS2o) show systematically smaller margins, which we interpret as a scope limitation in Section 5.

Table 6: Regime A NC-win rate (%) by law and dataset, first-epoch fits. Each cell: fraction of paired comparisons where  $\text{RMSE}_{\mathcal{H}}^{\text{NC}} < \text{RMSE}_{\mathcal{H}}^{\text{CO}}$  within predicted Regime A. **Dataset Avg.:** mean across corpora with 95% bootstrap CI.

Law	Web-crawled			Specialized		Dataset Avg.
	C4	RedPajama	Wikipedia	Cosmopedia	peS2o	
Chinchilla	77.1	78.6	88.0	51.8	47.1	<b>68.5</b> [67.3, 69.8]
Droppo-Elibol	62.2	67.2	65.9	45.5	46.2	<b>57.4</b> [56.1, 58.7]
Kaplan	76.1	79.9	72.9	50.9	50.3	<b>66.0</b> [64.1, 67.9]

## 5 Discussion and conclusions

The formal statements of Section 3 establish that collinear designs will produce deceptively confident fits that fail to generalize. The experiments of Section 4 confirm this statement quantitatively and reveal how severe the failure is in practice.

**Collinear designs overfit, non-collinear designs generalize:** on training data CO achieves higher  $R^2$  than NC in nearly every experiment (Table 3: aggregate 0.985 vs. 0.953), as a five-parameter fit along a 1D manifold near-interpolates, but on held-out data the ranking reverses - NC raises unified-holdout  $R^2$  from 0.837 to 0.932 and cuts RMSE from 0.237 to 0.156, with seed-paired per-trial RMSE gaps of 3-8 $\times$  that rule out an averaging artifact, sitting below Theorem 1’s  $\Theta(\varepsilon^{-1}) \approx 16.7\times$  ceiling at Chinchilla exponents (Eqs. (81)-(84)) with the slack absorbed by the design-independent misspecification floor (87). **Scaling 12 TPP ratios does not rescue collinearity:** our CO design spans  $\mathcal{K}_{\text{train}}$  (12 ratios) yet NC still wins 97.3% of 1,500 seed-paired comparisons (Table 4) because  $\kappa \propto \varepsilon^{-2}$  depends on the exponent gap, not the number of rays (Proposition 1). **The effect is precision-invariant:** a BF16 mixed-precision replication on Wikipedia gives unified-holdout  $R^2 = 0.966$  vs. CO’s 0.941 (Table 5) and a seed-paired NC win rate of 98.7% (296/300, 95% CI [96.6%, 99.5%]; Table 16), consistent with the FP32 Wikipedia win rate of 99.7% (Table 4). **The pattern is consistent across corpora, laws, and epochs:** Table 4 reports NC win rates above 93% on every corpus (min 93.0% C4, max 100% RedPajama), above 95% for every scaling law, and above 93% for every evaluation epoch. The combined **takeaway** is that single-TPP fits do not support coefficient-level interpretation - along  $D = kN$  rays only the combined effect of  $N$  and  $D$  is well constrained, so claims such as “model size contributes  $X\%$  and data  $Y\%$  of the reducible loss” require training to span a two-dimensional region of  $(N, D)$ , and even 12 collinear rays are insufficient (Table 3: CO’s training- $R^2$  advantage flips to a 0.03-0.10 holdout deficit); when the design is collinear, the reduced parameterization (Definition 2) is the appropriate reporting target.

**Limitations.** Theorem 1 gives an ordering, not a quantitative gap, so the observed seed-paired RMSE spread is consistent with but not predicted by the theorem; under misspecification, a design-independent approximation-bias floor bounds the ratio (87). Corollary 1’s closed-form CI inflation assumes i.i.d. Gaussian residuals; checkpoint-level temporal correlation and shared-corpus noise would under-state, not invert, the pathology. Empirically, we use small-scale models (5.04-76.5M parameters), a single LLaMA-style architecture, English-only text, one run per  $(N, D)$ , and a single fitter (multi-start L-BFGS-B with DE polish; Appendices C, D.6). Training hyperparameters were not swept per- $(N, D)$ ; following Gadre et al. (2024) we adopt a fixed recipe applied identically to CO and NC, so the head-to-head comparison is controlled even if absolute losses are not optimal. The budget-matched validation (Section 4, Table 6) softens to near-50% on Cosmopedia and peS2o, plausibly due to non-power-law loss surfaces attenuating variance inflation (untested); Regime A transfers most cleanly to web-crawled and reference text. Finally, the analysis targets pre-training loss; downstream-task and cross-domain extensions (Bhagia et al., 2025) inherit the Jacobian argument but are not validated here.

**Safeguards.** All corpora (C4, RedPajama, Wikipedia, Cosmopedia, peS2o) are public and pre-filtered; no new data collection. Released checkpoints (5.04-76.5M; Appendix C) are diagnostic data points, not deployable models, and the code targets scaling-law fitting and small-scale training runs, not serving production models. The paper’s deflationary posture against single-TPP coefficient claims offsets any marginal acceleration from better-identified scaling laws.

**Broader impact.** Scaling laws guide multi-billion-dollar pre-training decisions and inform claims about the relative importance of capacity vs. data volume; under single-TPP designs those claims are unidentifiable (Section 3, Corollary 1). Our diagnostics (Proposition 2, (5)) flag such fits, and the framework reframes the Kaplan-Chinchilla replication gap (Besiroglu et al., 2024; Porian et al., 2025) as a predictable consequence of  $\Theta(\varepsilon^{-2})$  ill-conditioning -  $A$ ’s CIs inflate  $\geq 17\times$  at Chinchilla exponents and  $\geq 53\times$  at Kaplan exponents (Table 2). Because the degeneracy is purely Jacobian-geometric, the analysis transfers to generative vision (Henighan et al., 2020; Alabdulmohsin et al., 2022), time-series (Edwards et al., 2025; Yao et al., 2025), and scientific ML; IsoFLOP-grid designs (Section 3.4) naturally avoid the pitfall.

**LLM usage.** All research questions, results, design, and analyses originated with the authors. The primary non-trivial use of LLMs was as a sounding board for candidate proof steps: the authors drafted the structure of each derivation, asked an LLM to propose intermediate algebraic manipulations or identities, and then independently verified, rewrote, or discarded each suggestion before incorporation. Auxiliary uses included exposition, L<sup>A</sup>T<sub>E</sub>X typesetting, boilerplate code, and prose editing, all reviewed by the authors. LLMs did not generate any claims, theorems, or experimental conclusions. We acknowledge Anthropic’s Claude Opus 4.7 for its assistance in this capacity.

## **Acknowledgments and Disclosure of Funding**

Funded by ARO grant W911NF-24-1-0007 and NSF ACCESS grant CIS230318.

## References

- Ibrahim Alabdulmohsin, Behnam Neyshabur, and Xiaohua Zhai. Revisiting neural scaling laws in language and vision. 2022. URL <https://arxiv.org/abs/2209.06640>.
- Yasaman Bahri, Ethan Dyer, Jared Kaplan, Jaehoon Lee, and Utkarsh Sharma. Explaining neural scaling laws. *Proceedings of the National Academy of Sciences*, 121(27), 6 2024. ISSN 1091-6490. doi: 10.1073/pnas.2311878121. URL <http://dx.doi.org/10.1073/pnas.2311878121>.
- Douglas M. Bates and Donald G. Watts. *Nonlinear Regression Analysis and Its Applications*. John Wiley & Sons, 1988.
- Loubna Ben Allal, Anton Lozhkov, Guilherme Penedo, Thomas Wolf, and Leandro von Werra. Cosmopedia, February 2024. URL <https://huggingface.co/datasets/HuggingFaceTB/cosmopedia>. Hugging Face dataset.
- Shane Bergsma, Nolan Dey, Gurpreet Gosal, Gavia Gray, Daria Soboleva, and Joel Hestness. Power lines: Scaling laws for weight decay and batch size in llm pre-training. 2025. URL <https://arxiv.org/abs/2505.13738>.
- Tamay Besiroglu, Ege Erdil, Matthew Barnett, and Josh You. Chinchilla scaling: A replication attempt. 2024. URL <https://arxiv.org/abs/2404.10102>.
- Akshita Bhagia, Jiacheng Liu, Alexander Wettig, David Heineman, Oyvind Tafjord, Ananya Harsh Jha, Luca Soldaini, Noah A. Smith, Dirk Groeneveld, Pang Wei Koh, Jesse Dodge, and Hannaneh Hajishirzi. Establishing task scaling laws via compute-efficient model ladders, 2025. URL <https://arxiv.org/abs/2412.04403>.
- Åke Björck. *Numerical Methods for Least Squares Problems*. Society for Industrial and Applied Mathematics (SIAM), 1996. ISBN 9780898713602.
- Ethan Caballero, Kshitij Gupta, Irina Rish, and David Krueger. Broken neural scaling laws. 2023. URL <https://arxiv.org/abs/2210.14891>.
- Leshem Choshen, Yang Zhang, and Jacob Andreas. A hitchhiker’s guide to scaling law estimation. 2025. URL <https://arxiv.org/abs/2410.11840>.
- Nolan Dey, Gurpreet Gosal, Zhiming, Chen, Hemant Khachane, William Marshall, Ribhu Pathria, Marvin Tom, and Joel Hestness. Cerebras-gpt: Open compute-optimal language models trained on the cerebras wafer-scale cluster. 2023. URL <https://arxiv.org/abs/2304.03208>.
- Carsten F. Dormann, Jane Elith, Sven Bacher, Carsten Buchmann, Gudrun Carl, Gabriel Carré, Jaime R. García Marquéz, Bernd Gruber, Bruno Lafourcade, Pedro J. Leitão, Tamara Münkemüller, Colin McClean, Patrick E. Osborne, Björn Reineking, Boris Schröder, Andrew K. Skidmore, Damaris Zurell, and Sven Lautenbach. Collinearity: a review of methods to deal with it and a simulation study evaluating their performance. *Ecography*, 36(1):27–46, 2013. doi: <https://doi.org/10.1111/j.1600-0587.2012.07348.x>. URL <https://nsojournals.onlinelibrary.wiley.com/doi/abs/10.1111/j.1600-0587.2012.07348.x>.
- Jasha Droppo and Oguz Elibol. Scaling laws for acoustic models. 2021. URL <https://arxiv.org/abs/2106.09488>.
- Thomas D. P. Edwards, James Alvey, Justin Alsing, Nam H. Nguyen, and Benjamin D. Wandelt. Scaling-laws for large time-series models. 2025. URL <https://arxiv.org/abs/2405.13867>.
- Wikimedia Foundation. Wikimedia downloads. URL <https://dumps.wikimedia.org>.
- Samir Yitzhak Gadre, Georgios Smyrnis, Vaishaal Shankar, Suchin Gururangan, Mitchell Wortsman, Rulin Shao, Jean Mercat, Alex Fang, Jeffrey Li, Sedrick Keh, Rui Xin, Marianna Nezhurina, Igor Vasiljevic, Jenia Jitsev, Luca Soldaini, Alexandros G. Dimakis, Gabriel Ilharco, Pang Wei Koh, Shuran Song, Thomas Kollar, Yair Carmon, Achal Dave, Reinhard Heckel, Niklas Muennighoff, and Ludwig Schmidt. Language models scale reliably with over-training and on downstream tasks, 2024. URL <https://arxiv.org/abs/2403.08540>.

- Tom Henighan, Jared Kaplan, Mor Katz, Mark Chen, Christopher Hesse, Jacob Jackson, Heewoo Jun, Tom B. Brown, Prafulla Dhariwal, Scott Gray, Chris Hallacy, Benjamin Mann, Alec Radford, Aditya Ramesh, Nick Ryder, Daniel M. Ziegler, John Schulman, Dario Amodei, and Sam McCandlish. Scaling laws for autoregressive generative modeling. 2020. URL <https://arxiv.org/abs/2010.14701>.
- Joel Hestness, Sharan Narang, Newsha Ardalani, Gregory Diamos, Heewoo Jun, Hassan Kianinejad, Md. Mostofa Ali Patwary, Yang Yang, and Yanqi Zhou. Deep learning scaling is predictable, empirically. 2017. URL <https://arxiv.org/abs/1712.00409>.
- Jordan Hoffmann, Sebastian Borgeaud, Arthur Mensch, Elena Buchatskaya, Trevor Cai, Eliza Rutherford, Diego de Las Casas, Lisa Anne Hendricks, Johannes Welbl, Aidan Clark, Tom Hennigan, Eric Noland, Katie Millican, George van den Driessche, Bogdan Damoc, Aurelia Guy, Simon Osindero, Karen Simonyan, Erich Elsen, Jack W. Rae, Oriol Vinyals, and Laurent Sifre. Training compute-optimal large language models. 2022. URL <https://arxiv.org/abs/2203.15556>.
- Michael Y. Hu, Jane Pan, Ayush Rajesh Jhaveri, Nicholas Lourie, and Kyunghyun Cho. Neural neural scaling laws. 2026. URL <https://arxiv.org/abs/2601.19831>.
- Jared Kaplan, Sam McCandlish, Tom Henighan, Tom B. Brown, Benjamin Chess, Rewon Child, Scott Gray, Alec Radford, Jeffrey Wu, and Dario Amodei. Scaling laws for neural language models. 2020. URL <https://arxiv.org/abs/2001.08361>.
- Jong Hae Kim. Multicollinearity and Misleading Statistical Results. *Korean Journal of Anesthesiology*, 72(6):558–569, 2019. doi: 10.4097/kja.19087.
- Konwoo Kim, Suhas Kotha, Percy Liang, and Tatsunori Hashimoto. Pre-training under infinite compute. 2025. URL <https://arxiv.org/abs/2509.14786>.
- Houyi Li, Wenzhen Zheng, Qiufeng Wang, Zhenyu Ding, Haoying Wang, Zili Wang, Shijie Xuyang, Ning Ding, Shuigeng Zhou, Xiangyu Zhang, and Daxin Jiang. Predictable scale: Part ii, farseer: A refined scaling law in large language models. 2025a. URL <https://arxiv.org/abs/2506.10972>.
- Margaret Li, Sneha Kudugunta, and Luke Zettlemoyer. (mis)fitting: A survey of scaling laws. 2025b. URL <https://arxiv.org/abs/2502.18969>.
- Ian Magnusson, Nguyen Tai, Ben Bogin, David Heineman, Jena D. Hwang, Luca Soldaini, Akshita Bhagia, Jiacheng Liu, Dirk Groeneveld, Oyvind Tafjord, Noah A. Smith, Pang Wei Koh, and Jesse Dodge. Datadecide: How to predict best pretraining data with small experiments, 2025. URL <https://arxiv.org/abs/2504.11393>.
- Douglas C. Montgomery, Elizabeth A. Peck, and G. Geoffrey Vining. *Introduction to Linear Regression Analysis*. John Wiley & Sons, 5th edition, 2012.
- Niklas Muennighoff, Alexander M. Rush, Boaz Barak, Teven Le Scao, Aleksandra Piktus, Nouamane Tazi, Sampo Pyysalo, Thomas Wolf, and Colin Raffel. Scaling data-constrained language models. 2025. URL <https://arxiv.org/abs/2305.16264>.
- Jorge Nocedal and Stephen J. Wright. *Numerical Optimization*. Springer Series in Operations Research and Financial Engineering. Springer, 2nd edition, 2006. ISBN 9780387400655.
- Robert O’Brien. A Caution Regarding Rules of Thumb for Variance Inflation Factors. *Quality & Quantity*, 41:673–690, 10 2007. doi: 10.1007/s11135-006-9018-6.
- Tomer Porian, Mitchell Wortsman, Jenia Jitsev, Ludwig Schmidt, and Yair Carmon. Resolving discrepancies in compute-optimal scaling of language models. 2025. URL <https://arxiv.org/abs/2406.19146>.
- Colin Raffel, Noam Shazeer, Adam Roberts, Katherine Lee, Sharan Narang, Michael Matena, Yanqi Zhou, Wei Li, and Peter J. Liu. Exploring the limits of transfer learning with a unified text-to-text transformer. *Journal of Machine Learning Research*, 21(140):1–67, 2020. URL <http://jmlr.org/papers/v21/20-074.html>.

- Jonathan S. Rosenfeld, Amir Rosenfeld, Yonatan Belinkov, and Nir Shavit. A constructive prediction of the generalization error across scales. 2019. URL <https://arxiv.org/abs/1909.12673>.
- Nikhil Sardana, Jacob Portes, Sasha Doubov, and Jonathan Frankle. Beyond chinchilla-optimal: Accounting for inference in language model scaling laws. 2025. URL <https://arxiv.org/abs/2401.00448>.
- Rylan Schaeffer, Noam Levi, Brando Miranda, and Sanmi Koyejo. Pretraining scaling laws for generative evaluations of language models. 2026. URL <https://arxiv.org/abs/2509.24012>.
- Mustafa Shukor, Louis Bethune, Dan Busbridge, David Grangier, Enrico Fini, Alaaeldin El-Nouby, and Pierre Ablin. Scaling laws for optimal data mixtures. 2025. URL <https://arxiv.org/abs/2507.09404>.
- Luca Soldaini and Kyle Lo. peS2o (Pretraining Efficiently on S2ORC) Dataset. Technical report, Allen Institute for AI, 2023. ODC-By, <https://github.com/allenai/pes2o>.
- Hugo Touvron, Thibaut Lavril, Gautier Izacard, Xavier Martinet, Marie-Anne Lachaux, Timothée Lacroix, Baptiste Rozière, Naman Goyal, Eric Hambro, Faisal Azhar, Aurelien Rodriguez, Armand Joulin, Edouard Grave, and Guillaume Lample. Llama: Open and efficient foundation language models. 2023. URL <https://arxiv.org/abs/2302.13971>.
- Mark K. Transtrum, Benjamin B. Machta, and James P. Sethna. Why are nonlinear fits to data so challenging? *Phys. Rev. Lett.*, 104:060201, Feb 2010. doi: 10.1103/PhysRevLett.104.060201. URL <https://link.aps.org/doi/10.1103/PhysRevLett.104.060201>.
- Mark K. Transtrum, Benjamin B. Machta, Kevin S. Brown, Bryan C. Daniels, Christopher R. Myers, and James P. Sethna. Perspective: Sloppiness and Emergent Theories in Physics, Biology, and Beyond. *The Journal of Chemical Physics*, 143:010901, 2015. doi: 10.1063/1.4923066.
- Kristina P. Vatcheva, MinJae Lee, Joseph B. McCormick, and Mohammad H. Rahbar. Multicollinearity in Regression Analyses Conducted in Epidemiologic Studies. *Epidemiology (Sunnyvale, Calif.)*, 6(2):227, 2016. doi: 10.4172/2161-1165.1000227.
- Pablo Villalobos, Anson Ho, Jaime Sevilla, Tamay Besiroglu, Lennart Heim, and Marius Hobbhahn. Will we run out of data? limits of llm scaling based on human-generated data. 2024. URL <https://arxiv.org/abs/2211.04325>.
- Alexandra Volkova, Mher Safaryan, Christoph H. Lampert, and Dan Alistarh. Towards robust scaling laws for optimizers. 2026. URL <https://arxiv.org/abs/2602.07712>.
- Maurice Weber, Daniel Fu, Quentin Anthony, Yonatan Oren, Shane Adams, Anton Alexandrov, Xiaozhong Lyu, Huu Nguyen, Xiaozhe Yao, Virginia Adams, Ben Athiwaratkun, Rahul Chalamala, Kezhen Chen, Max Ryabinin, Tri Dao, Percy Liang, Christopher Ré, Irina Rish, and Ce Zhang. Redpajama: an open dataset for training large language models. 2024. URL <https://arxiv.org/abs/2411.12372>.
- Qingren Yao, Chao-Han Huck Yang, Renhe Jiang, Yuxuan Liang, Ming Jin, and Shirui Pan. Towards neural scaling laws for time series foundation models. 2025. URL <https://arxiv.org/abs/2410.12360>.
- Baoqing Yue, Jinyuan Zhou, Zixi Wei, Jingtao Zhan, Qingyao Ai, and Yiqun Liu. Relative-based scaling law for neural language models. 2025. URL <https://arxiv.org/abs/2510.20387>.
- Hanlin Zhang, Jikai Jin, Vasilis Syrgkanis, and Sham Kakade. Prescriptive scaling reveals the evolution of language model capabilities. 2026. URL <https://arxiv.org/abs/2602.15327>.

## A Appendix - notation reference

Table 7 collects all symbols used throughout the paper and appendices.

Table 7: Summary of notation.

Symbol	Meaning	Defined in
<i>Scaling-law variables</i>		
$N$	Model parameter count	Eq. (1)
$D$	Training tokens (dataset size)	Eq. (1)
$L(N, D)$	Observed loss	Eq. (1)
$\hat{L}(N, D; \theta)$	Predicted loss (scaling law)	Def. 1
$k_1 < \dots < k_K$	Ordered TPP ratios in a $K$ -ray design	Def. 1
$k$	Tokens-per-parameter (TPP) ratio ( $K = 1$ case, $D = kN$ )	Sec. 3
$C$	Training compute, $C = 6ND$ (Chinchilla FLOPs)	Sec. 3.4
$C_i$	Induced compute budget $6N_i D_i$ for holdout point $i$	Def. 4
$N_{\min}, N_{\max}$	Min/max model sizes used for induced isoFLOP curves	Def. 4
$V$	Vocabulary size (cl100k_base; empirical count 100,277)	Sec. 4; App. C
<i>Chinchilla parameters</i>		
$A, B$	Scale coefficients (model, data)	Eq. (1)
$\alpha, \beta$	Power-law exponents	Eq. (1)
$E$	Irreducible loss	Eq. (1)
$\psi$	Combined coefficient $A + Bk^{-\alpha}$	Eq. (2)
$\varepsilon$	Exponent gap ( $ \alpha - \beta $ for Chinchilla)	Def. 3
<i>Observation model and optimization</i>		
$\mathcal{A}$	Training algorithm (architecture, optimizer, schedule)	Def. 1
$\mathcal{D}$	Scaling-law dataset $\{(N_i, D_i, L_i)\}_{i=1}^m$	Def. 1
$\mathcal{D}_{\text{train}}^{\text{train}}$	Training split of $\mathcal{D}$	Def. 1
$\mathcal{D}_{\text{train}}^{\text{CO}}, \mathcal{D}_{\text{train}}^{\text{NC}}$	Full collinear and non-collinear training pools before subset enumeration	Def. 10, Def. 11
$\mathcal{N}$	Shared ordered model sizes $\{N_1, \dots, N_n\}$	Def. 1; App. D.3
$m$	Number of observations in $\mathcal{D}$	Def. 1
$\theta$	Scaling-law parameter vector	Def. 1
$p$	Number of parameters in $\theta$	Def. 1
$n$	Number of distinct model sizes	Def. 1
$N_1 < \dots < N_n$	Ordered model sizes	Def. 1
$K$	Number of TPP ratios in collinear design	Def. 1
$\kappa(\cdot)$	Condition number ( $\lambda_{\max}/\lambda_{\min}$ )	Sec. 3.1
$r_i$	Residual: $L_i - \hat{L}(N_i, D_i; \theta)$	Sec. 3.1
$\mathbf{r}(\theta)$	Stacked residual vector $(r_i)_{i=1}^m$	Sec. 3.1
$S(\theta)$	GN objective $\frac{1}{2} \ \mathbf{r}(\theta)\ ^2$	Sec. 3.1
$J$	Jacobian of residuals	Sec. 3.1
$\Delta\theta$	Gauss-Newton update step	Sec. 3.1
$\kappa_{A,B}$	Condition number of $(A, B)$ sub-block of $J^T J$ ; equals $\kappa(J^T J)$ at leading order under the global dominance assumption (Sec. 3.1)	Sec. 3.1
$\mathbf{j}_a, \mathbf{j}_b$	Columns of $J$ (near-proportional pair)	Proposition 1
$c$	Proportionality scalar, $\mathbf{j}_b = c\mathbf{j}_a + \delta$	Proposition 1
$\delta$	Near-proportionality perturbation, $\ \delta\  = O(\varepsilon)$	Proposition 1
$\mathbf{j}_1, \mathbf{j}_2$	First two Jacobian columns in the column-ordering used in Table 1 (alias of the illustrative $(a, b)$ pair in Prop. 1)	Tab. 1
$\hat{\theta}$	Least-squares estimator	Lemma 1
$\mathbb{E}[\cdot]$	Expectation (Regime A/B inequalities and RMSE ratios)	Thm. 1
$\sigma^2$	Idealized homoscedastic variance of observational noise in non-linear least-squares (distinct from appendix-table $\sigma$ )	Lemma 1; Cor. 1
$\sigma$ (appendix tables)	Seed-to-seed std. dev. of Monte Carlo summaries across optimizer seeds	App. D; App. E
$\text{CI}_{0.95}(\cdot)$	Nominal 95% confidence interval half-width	Corollary 1
<i>Holdout prediction (Prop. 2; Theorem 1)</i>		
$\mathcal{H}$	General holdout set	Def. 1
$n_{\mathcal{H}}$	Holdout cardinality	Def. 1

Continued on next page

(Table 7 continued)

Symbol	Meaning	Defined in
$k_K, k_1$	Largest/smallest ordered TPP ratio in a design	Prop. 2
$R$	Two-ray TPP spread $k_2/k_1$ ( $K = 2$ )	Prop. 2
$\beta_{\text{eff}}$	Law-specific data-size exponent (Chinchilla/repeated-data: $\beta$ ; Kaplan: $\alpha_D$ ; Droppo-Elibol: $\gamma_D$ )	Prop. 2
$V_K$	Second central moment (variance) of $\{k_\ell^{-\beta_{\text{eff}}}\}_{\ell=1}^K$ across TPP rays; $V_1 = 0$	Prop. 2
$\tau_K$	Diversity threshold in (5); at leading order $\kappa(J^T J) \leq \kappa_{\text{target}} \Leftrightarrow V_K \geq \tau_K$	Prop. 2
$\kappa_K$	Shorthand for $\kappa(J^T J)$ on a collinear $K$ -ray design ( $\kappa_K \leq \kappa_{\text{target}} \Leftrightarrow V_K \geq \tau_K$ at leading order)	App. B.15
$\kappa_{\text{target}}$	Target condition number; $\tau_K$ in (5) depends on it; assumed small for NLS/GN in Thm. 1	Prop. 2; Thm. 1
$\text{RMSE}_{\mathcal{H}}^{\text{CO/NC}}$	Expected holdout RMSE (superscript: design)	Thm. 1
$R_{\mathcal{H}}^2$	Holdout $R^2$ under design CO or NC	Thm. 1
<i>Experimental design (Sec. 4)</i>		
$\mathcal{K}_{\text{train}}$	Full set of 12 collinear training TPP ratios used in the CO design	Sec. 4
$\mathcal{K}_{\text{test}}$	Set of 5 collinear holdout TPP ratios beyond the training fan	Sec. 4
$\mathcal{K}_{\text{big}}$	Set of 6 collinear training TPP ratios in the preliminary high-TPP CO design	Sec. 4; App. D.7
$\mathcal{H}_{\text{col}}$	Collinear holdout (empirical label)	Sec. 4
$\mathcal{H}_{\text{nc}}$	Non-collinear holdout (empirical label)	Sec. 4
$R_{\mathcal{H}}^2$	Unified-holdout $R^2$ on $\mathcal{H}$	Sec. 4; Tab. 3
$R_{\mathcal{H}_{\text{col}}}^2, R_{\mathcal{H}_{\text{nc}}}^2$	$R^2$ on CO-only vs. NC-only holdout splits	App. D
$R_{\text{train}}^2, R_{\text{holdout}}^2$	Coefficient of determination on train/holdout aggregates	Sec. 4
$d_{\text{model}}, d_{\text{ff}}, d_{\text{head}}, n_{\text{layers}}, n_{\text{heads}}$	Transformer shape hyperparameters (Table 10)	App. C
RMSE	Root mean squared error on a holdout split	Sec. 4
<i>Alternative scaling-law notation</i>		
$N', D'$	Effective quantities (repeated-data)	Def. 3
$N_c, D_c$	Scale parameters (Kaplan)	Def. 3
$\alpha_N, \alpha_D$	Separate exponents (Kaplan / Droppo-Elibol)	Def. 3
$N_C, D_C$	Scale parameters (Droppo-Elibol)	Def. 3
$\alpha$ (Droppo-Elibol)	Canonical composite exponent in that law	Def. 3; Tab. 1
$\gamma_N, \gamma_D$	Exponent ratios $\alpha_N/\alpha, \alpha_D/\alpha$ (Droppo-Elibol)	Def. 3
$L_\infty$	Irreducible loss (Droppo-Elibol)	Sec. 3; App. B.9
$R_D^*, R_N^*$	Decay constants (repeated-data)	App. B.7
<i>Appendix-only: design-dependent quantities</i>		
$\Phi_q$	Power-sum family $\sum_i N_i^{-q\alpha}$ (index $q$ )	App. B.5; Def. 5
$\Phi_2^{(2\varepsilon)}$	$\sum_i N_i^{-2\beta}$ (Chinchilla; $= \sum_i N_i^{-2\alpha+2\varepsilon}, \varepsilon = \alpha - \beta$ )	App. B.11
$T_q$	Log-weighted power sum (e.g. $T_2 = \sum_i N_i^{-2\alpha} \log N_i$ )	App. B.11
$U_q$	Log <sup>2</sup> -weighted power sum (e.g. $U_2 = \sum_i N_i^{-2\alpha} (\log N_i)^2$ )	App. B.11
$w_i$	Power-law weights $N_i^{-2\alpha}/\Phi_2$	App. B.10
$\sigma_w^2(\log N)$	Weighted log-variance of model sizes	App. B.10
<i>Appendix-only: experimental design</i>		
$R_{\text{min}}$	Minimum two-ray spread ( $V_2 \geq \tau_2$ ); $K > 2$ requires $R \geq R_{\text{min}}$	App. B.15
$\kappa_1$	Single-ray baseline $\kappa_K$ at $K = 1$ (enters $R_{\text{min}}$ via (95))	App. B.15
$R_{\text{eff}}$	Effective TPP spread ratio, $k_K/k_1$ , in multi-ray designs	Journal-only design-guidelines appendix
$\eta_k$	Singular-value ratio diagnostic, $\sigma_{\text{max}}/\sigma_k$	Journal-only design-guidelines appendix
$\Lambda(\mathcal{S})$	Sloppy leverage of test set $\mathcal{S}$	App. B.13, Def. 8
$G$	Training-design scalar $G = \sigma_w^2(\log N)^{-1} > 0$ in the coarse CO MSE bound (81)	Eq. (81)
$\eta$	Learning rate in optimizer setup	App. C

Continued on next page

(Table 7 continued)

Symbol	Meaning	Defined in
<i>Appendix-only: subset enumeration (App. D.3)</i>		
$\mathcal{L}$	Scaling-law family (Chinchilla, Kaplan, Droppo-Elibol)	App. D.3
$\mu$	Epoch/mode index in paired-comparison enumeration	Def. 12
$\mathbf{k}^{\text{all}}$	Full set of 12 collinear TPP ratios per dataset	Def. 9
$S$	Subset of TPP-ratio indices, $S \subseteq \{1, \dots, 12\}$	Def. 10
$\text{CO}(S)$	Collinear subset design induced by $S$	Def. 10
$n_S$	Cardinality of $\text{CO}(S)$	Def. 10
$K_S$	Effective TPP-ray count of subset design, $K_S =  S $	Def. 10
$\mathcal{N}_{\text{NC}}, \mathcal{D}_{\text{NC}}$	Row/column axes of the NC grid in $(N, D)$ space	Def. 11
$M_N, M_D$	NC-grid row/column counts, $ \mathcal{N}_{\text{NC}} ,  \mathcal{D}_{\text{NC}} $	Def. 11
$n^*, \mathbf{k}_S$	Target NC cardinality and target TPP ratios from $S$	Def. 11
$\text{NC}_{\square}(n^*, \mathbf{k}_S)$	Bounding-box NC design of cardinality $n^*$	Def. 11
$\mathcal{C}(\mathcal{L}, \mathcal{D}, \mu, S)$	Paired comparison tuple	Def. 12
$\mathcal{P}$	Set of all paired comparisons	Def. 12
$\kappa^*$	Target condition number for empirical regime classification	Def. 13
$\mathcal{P}_{\mathcal{L}, \mu}^A(\kappa^*)$	Predicted Regime A set ( $V_K < \tau_K$ ) at target $\kappa^*$	Def. 13
$\text{WR}(\mathcal{P}')$	NC win rate on a collection $\mathcal{P}' \subseteq \mathcal{P}$	Def. 13
$\text{WR}_A(\mathcal{L}, \mu; \kappa^*)$	Regime A NC win rate at target $\kappa^*$	Def. 13
$\mathbf{1}\{\cdot\}$	Indicator used in NC win-rate definition	Eq. (109)
$\kappa_{A,B}^{\text{design}}, \kappa_{\text{full}}^{\text{design}}$	Measured $(A, B)$ -block and full-matrix condition numbers (design $\in \{\text{CO}, \text{NC}\}$ )	Def. 14

## B Appendix - proofs and detailed derivations

The following proofs and derivations support the results in Section 3. For Kaplan, the Jacobian columns are derived for the additive simplification  $(N_c/N)^{\alpha_N} + (D_c/D)^{\alpha_D}$  in the proofs, while the empirical fit uses the original form.

### B.1 Appendix - Derivation of the Gauss-Newton normal equations

This subsection provides a self-contained derivation of the Gauss-Newton normal equations from the nonlinear least-squares objective (Section 3.1), following the treatment in (Nocedal and Wright, 2006, Chap. 10).

**Step 1: Objective and gradient.** Recall the objective:

$$S(\boldsymbol{\theta}) = \frac{1}{2} \|\mathbf{r}(\boldsymbol{\theta})\|^2 = \frac{1}{2} \sum_{i=1}^m r_i(\boldsymbol{\theta})^2, \quad (8)$$

where  $r_i(\boldsymbol{\theta}) = L_i - \hat{L}(N_i, D_i; \boldsymbol{\theta})$ . The gradient with respect to  $\boldsymbol{\theta}$  is obtained by the chain rule:

$$\frac{\partial S}{\partial \theta_j} = \sum_{i=1}^m r_i(\boldsymbol{\theta}) \frac{\partial r_i}{\partial \theta_j} = - \sum_{i=1}^m r_i(\boldsymbol{\theta}) \frac{\partial \hat{L}_i}{\partial \theta_j}, \quad (9)$$

since  $\partial r_i / \partial \theta_j = -\partial \hat{L}_i / \partial \theta_j$ . Define the residual Jacobian (equivalently, predictions satisfy  $\partial r_i / \partial \theta_j = -\partial \hat{L}_i / \partial \theta_j$ ):

$$J \in \mathbb{R}^{m \times p}, \quad J_{ij} := -\frac{\partial \hat{L}(N_i, D_i; \boldsymbol{\theta})}{\partial \theta_j} = \frac{\partial r_i}{\partial \theta_j}. \quad (10)$$

Thus  $J_{ij} = \partial r_i / \partial \theta_j$ , matching Section 3.1. With this convention, the gradient (9) can be written in matrix form as:

$$\nabla_{\boldsymbol{\theta}} S = J^T \mathbf{r}(\boldsymbol{\theta}). \quad (11)$$

**Step 2: Linearisation of the residuals.** At a current iterate  $\boldsymbol{\theta}_k$ , expand each residual to first order in the step  $\Delta \boldsymbol{\theta} = \boldsymbol{\theta} - \boldsymbol{\theta}_k$ :

$$r_i(\boldsymbol{\theta}_k + \Delta \boldsymbol{\theta}) \approx r_i(\boldsymbol{\theta}_k) + \sum_{j=1}^p \frac{\partial r_i}{\partial \theta_j} \Big|_{\boldsymbol{\theta}_k} \Delta \theta_j = r_{i,k} + (J_k \Delta \boldsymbol{\theta})_i, \quad (12)$$

where  $r_{i,k} := r_i(\boldsymbol{\theta}_k)$  and  $J_k := J(\boldsymbol{\theta}_k)$  is the Jacobian evaluated at  $\boldsymbol{\theta}_k$ . In vector notation:

$$\mathbf{r}(\boldsymbol{\theta}_k + \Delta \boldsymbol{\theta}) \approx \mathbf{r}_k + J_k \Delta \boldsymbol{\theta}. \quad (13)$$

**Step 3: Substitute into the objective.** Substituting (13) into (8):

$$\begin{aligned} S(\boldsymbol{\theta}_k + \Delta \boldsymbol{\theta}) &\approx \frac{1}{2} \|\mathbf{r}_k + J_k \Delta \boldsymbol{\theta}\|^2 \\ &= \frac{1}{2} (\mathbf{r}_k + J_k \Delta \boldsymbol{\theta})^T (\mathbf{r}_k + J_k \Delta \boldsymbol{\theta}) \\ &= \frac{1}{2} \mathbf{r}_k^T \mathbf{r}_k + \mathbf{r}_k^T J_k \Delta \boldsymbol{\theta} + \frac{1}{2} \Delta \boldsymbol{\theta}^T J_k^T J_k \Delta \boldsymbol{\theta}. \end{aligned}$$

This is an *exact* quadratic in  $\Delta \boldsymbol{\theta}$  (no higher-order terms remain because the linearization has already been applied). Denote this quadratic model as  $m_k(\Delta \boldsymbol{\theta})$ .

**Step 4: Stationarity condition.** At the minimizer of  $m_k$ , the gradient with respect to  $\Delta \boldsymbol{\theta}$  vanishes:

$$\nabla_{\Delta \boldsymbol{\theta}} m_k = J_k^T \mathbf{r}_k + J_k^T J_k \Delta \boldsymbol{\theta} = \mathbf{0}, \quad (14)$$

$$(J_k^T J_k) \Delta \boldsymbol{\theta} = -J_k^T \mathbf{r}_k. \quad (15)$$

This is the Gauss-Newton normal equation. When  $J_k^T J_k$  is non-singular, the unique solution is  $\Delta \boldsymbol{\theta} = -(J_k^T J_k)^{-1} J_k^T \mathbf{r}_k$ , and the parameter update is  $\boldsymbol{\theta}_{k+1} = \boldsymbol{\theta}_k + \Delta \boldsymbol{\theta}$ .

**Remark 1** (Relationship to the full Hessian.). *The exact Hessian of  $S$  is:*

$$H(\boldsymbol{\theta}) = \nabla^2 S = J^T J + Q, \quad Q := \sum_{i=1}^m r_i \nabla^2 r_i. \quad (16)$$

*The Gauss-Newton method drops the second-order correction  $Q$ , replacing  $H$  with the Gauss-Newton approximation  $J^T J$ . This is justified when  $\|\mathbf{r}\|$  is small (so  $Q \approx 0$ ) or when the model is approximately linear in  $\boldsymbol{\theta}$  (so  $\nabla^2 r_i \approx 0$ ). For the Chinchilla and repeated-data scaling laws,  $\hat{L}$  is linear in the scale coefficients  $A$  and  $B$ , so  $\nabla_{A,B}^2 r_i = 0$  exactly and  $Q_{A,B} = 0$ : the Gauss-Newton and full Newton curvatures coincide in the  $(A, B)$  sub-block regardless of residual magnitudes.*

**Remark 2** (Why  $J^T J$  controls identifiability.). When  $J^T J$  is well conditioned, the normal equations (15) have a unique, numerically stable solution. When two columns of  $J$  are nearly proportional,  $J^T J$  becomes nearly singular:

$$\lambda_{\min}(J^T J) \rightarrow 0 \implies \|(J^T J)^{-1}\| \rightarrow \infty, \quad (17)$$

and the step  $\Delta\theta$  becomes unbounded in the direction of the near-null eigenvector. Under i.i.d. noise with variance  $\sigma^2$ , one has

$$\text{Cov}(\hat{\theta}) = \sigma^2 (J^T J)^{-1} \quad (18)$$

in the linear least-squares case (Lemma 1), and the same expression approximates the large-sample covariance for nonlinear least squares (Remark 3); thus the parameter variances along the near-null direction scale as  $\sigma^2/\lambda_{\min}(J^T J)$ . This is the statistical manifestation of the ill-conditioning: any parameter combination aligned with the sloppy direction of  $J^T J$  is effectively unconstrained by the data. The remainder of Section 3 shows that, on each single collinear ray  $D = k_\ell N$ , the scale-coefficient columns of  $J$  are nearly proportional whenever  $\varepsilon \ll 1$  (the law-specific exponent gap of Definition 3; e.g.,  $|\alpha - \beta|$  for Chinchilla), driving  $\lambda_{\min}(J^T J) = \Theta(\varepsilon^2)$  and hence  $\kappa(J^T J) = \Theta(\varepsilon^{-2})$ . With  $K > 1$  rays, the bound applies ray-by-ray; the design escapes ill-conditioning only when the TPP diversity  $V_K \geq \tau_K$  in (5) (Proposition 2). For  $K = 2$ , this requires a sufficient endpoint spread  $R = k_K/k_1$  (Eq. (95) and Table 9).

## B.2 Appendix - Covariance under homoscedastic i.i.d. noise

**Lemma 1** (Parameter covariance in linear least squares). For any  $\mathbf{M} \in \mathbb{R}^{m \times p}$  of full column rank and  $\theta^* \in \mathbb{R}^p$ , suppose

$$L_i = (\mathbf{M}\theta^*)_i + \epsilon_i, \quad i = 1, \dots, m,$$

where  $\{\epsilon_i\}_{i=1}^m$  are i.i.d. with mean zero and variance  $\sigma^2$ . Let  $\hat{\theta}$  minimize  $\sum_{i=1}^m (L_i - (\mathbf{M}\theta)_i)^2$ , and let  $J \in \mathbb{R}^{m \times p}$  be the Jacobian of the residuals  $r_i(\theta) := L_i - (\mathbf{M}\theta)_i$  with respect to  $\theta$  (holding  $\mathbf{M}$  fixed). Then  $J = -\mathbf{M}$  and

$$\text{Cov}(\hat{\theta}) = \sigma^2 (J^T J)^{-1}. \quad (19)$$

*Proof.* Differentiating  $r_i(\theta) = L_i - \sum_{j=1}^p M_{ij} \theta_j$  gives  $\partial r_i / \partial \theta_j = -M_{ij}$ , hence  $J = -\mathbf{M}$  and  $J^T J = \mathbf{M}^T \mathbf{M}$ . The normal equations yield  $\mathbf{M}^T \mathbf{M} \hat{\theta} = \mathbf{M}^T \mathbf{L}$  with  $\mathbf{L} := (L_1, \dots, L_m)^T$ , so

$$\hat{\theta} = (\mathbf{M}^T \mathbf{M})^{-1} \mathbf{M}^T \mathbf{L}.$$

Substituting  $\mathbf{L} = \mathbf{M}\theta^* + \epsilon$  with  $\epsilon := (\epsilon_1, \dots, \epsilon_m)^T$ :

$$\hat{\theta} - \theta^* = (\mathbf{M}^T \mathbf{M})^{-1} \mathbf{M}^T \epsilon.$$

Because  $\mathbb{E}[\epsilon] = \mathbf{0}$ , also  $\mathbb{E}[\hat{\theta}] = \theta^*$ . Because  $\text{Cov}(\epsilon) = \sigma^2 I_m$ ,

$$\begin{aligned} \text{Cov}(\hat{\theta}) &= (\mathbf{M}^T \mathbf{M})^{-1} \mathbf{M}^T (\sigma^2 I_m) \mathbf{M} (\mathbf{M}^T \mathbf{M})^{-1} \\ &= \sigma^2 (\mathbf{M}^T \mathbf{M})^{-1} = \sigma^2 (J^T J)^{-1}. \end{aligned} \quad \square$$

**Remark 3** (Nonlinear least squares). Lemma 1 applies directly when the predictor  $\hat{L}(N_i, D_i; \theta)$  is affine in  $\theta$  on the design (e.g., fitting  $(A, B, E)$  in (1) with  $(\alpha, \beta)$  held fixed). For general nonlinear  $\hat{L}$ , the same matrix  $\sigma^2 (J^T J)^{-1}$  with  $J_{ij} = \partial r_i / \partial \theta_j$  evaluated at the true parameter is the standard large-sample approximation to  $\text{Cov}(\hat{\theta})$  under regularity conditions for nonlinear least squares (Bates and Watts, 1988).

## B.3 Appendix - Proof of Proposition 1 (Full-Matrix Conditioning)

**Proposition** (Full-matrix conditioning - full statement; restated from Proposition 1). Let  $J \in \mathbb{R}^{m \times p}$  be the Jacobian of the residuals with columns  $\mathbf{j}_1, \dots, \mathbf{j}_p \in \mathbb{R}^m$  (i.e.,  $J = [\mathbf{j}_1 \mid \dots \mid \mathbf{j}_p]$ ), so that  $J_{ij} = (\mathbf{j}_j)_i$ . Suppose that two columns, indexed by  $a, b \in \{1, \dots, p\}$  with  $a \neq b$ , satisfy the near-proportionality condition  $\mathbf{j}_b = c\mathbf{j}_a + \delta$  with  $c \neq 0$ ,  $\delta \in \mathbb{R}^m$ , and  $\|\delta\| = O(\varepsilon)$ , where  $\varepsilon > 0$  is the law-specific exponent gap. Define the  $m \times 2$  matrix formed by extracting these two columns from  $J$ :

$$J_1 := [\mathbf{j}_a \mid \mathbf{j}_b] \in \mathbb{R}^{m \times 2}, \quad \text{i.e., } (J_1)_{i1} = J_{ia}, \quad (J_1)_{i2} = J_{ib}, \quad (20)$$

Since  $J_1^T J_1$  is a  $2 \times 2$  real symmetric positive-semidefinite matrix (symmetry:  $(J_1^T J_1)^T = J_1^T J_1$ ; positive semidefiniteness:  $\mathbf{v}^T J_1^T J_1 \mathbf{v} = \|J_1 \mathbf{v}\|^2 \geq 0$  for all  $\mathbf{v} \in \mathbb{R}^2$ ), the spectral theorem guarantees that it possesses an orthonormal eigenbasis. Let  $\mathbf{w} \in \mathbb{R}^2$  be a unit eigenvector corresponding to its smallest eigenvalue:

$$(J_1^T J_1) \mathbf{w} = \lambda_{\min}(J_1^T J_1) \mathbf{w}, \quad \|\mathbf{w}\| = 1. \quad (21)$$

Construct the test vector  $\tilde{\mathbf{w}} \in \mathbb{R}^p$  by placing the entries of  $\mathbf{w}$  in positions  $a$  and  $b$  and zeros elsewhere:

$$\tilde{w}_j := \begin{cases} w_1 & \text{if } j = a, \\ w_2 & \text{if } j = b, \\ 0 & \text{otherwise.} \end{cases} \quad (22)$$

Then  $\|\tilde{\mathbf{w}}\| = \|\mathbf{w}\| = 1$  and:

$$\lambda_{\min}(J^T J) \leq \tilde{\mathbf{w}}^T (J^T J) \tilde{\mathbf{w}} = \lambda_{\min}(J_1^T J_1) = O(\varepsilon^2), \quad (23)$$

and consequently, under the global dominance assumption (Section 3.1),

$$\kappa(J^T J) = \Theta(\varepsilon^{-2}) \quad \text{with} \quad \lambda_{\max}(J^T J) = \Theta(1). \quad (3)$$

We proceed in three steps: (i) show that Proposition 1's assumption  $\mathbf{j}_b = c\mathbf{j}_a + \boldsymbol{\delta}$  forces  $\lambda_{\min}(J_1^T J_1) = O(\varepsilon^2)$ ; (ii) use the Rayleigh quotient to transfer this to the full  $p \times p$  Gram matrix; (iii) conclude the condition-number bound.

**Step 1:**  $\lambda_{\min}(J_1^T J_1) = O(\varepsilon^2)$ .

By the near proportionality assumption of Proposition 1,  $\mathbf{j}_b = c\mathbf{j}_a + \boldsymbol{\delta}$  with  $\|\boldsymbol{\delta}\| = O(\varepsilon)$ . The  $2 \times 2$  Gram matrix of  $J_1 = [\mathbf{j}_a \mid \mathbf{j}_b]$  is:

$$G := J_1^T J_1 = \begin{pmatrix} \|\mathbf{j}_a\|^2 & \mathbf{j}_a^T \mathbf{j}_b \\ \mathbf{j}_a^T \mathbf{j}_a & \|\mathbf{j}_b\|^2 \end{pmatrix}. \quad (24)$$

Substituting  $\mathbf{j}_b = c\mathbf{j}_a + \boldsymbol{\delta}$ :

$$\|\mathbf{j}_b\|^2 = c^2 \|\mathbf{j}_a\|^2 + 2c\mathbf{j}_a^T \boldsymbol{\delta} + \|\boldsymbol{\delta}\|^2, \quad (25)$$

$$\mathbf{j}_a^T \mathbf{j}_b = c\|\mathbf{j}_a\|^2 + \mathbf{j}_a^T \boldsymbol{\delta}. \quad (26)$$

Write  $s := \|\mathbf{j}_a\|^2 > 0$  and  $\eta := \mathbf{j}_a^T \boldsymbol{\delta}$  (so  $|\eta| \leq \|\mathbf{j}_a\| \|\boldsymbol{\delta}\| = O(\varepsilon)$  by Cauchy-Schwarz). Then:

$$G = \begin{pmatrix} s & cs + \eta \\ cs + \eta & c^2s + 2c\eta + \|\boldsymbol{\delta}\|^2 \end{pmatrix}.$$

The determinant is:

$$\begin{aligned} \det(G) &= s(c^2s + 2c\eta + \|\boldsymbol{\delta}\|^2) - (cs + \eta)^2 \\ &= sc^2s + 2sc\eta + s\|\boldsymbol{\delta}\|^2 - c^2s^2 - 2cs\eta - \eta^2 \\ &= s\|\boldsymbol{\delta}\|^2 - \eta^2. \end{aligned} \quad (27)$$

By the Cauchy-Schwarz inequality applied to  $\mathbf{j}_a$  and  $\boldsymbol{\delta}$ :  $\eta^2 = (\mathbf{j}_a^T \boldsymbol{\delta})^2 \leq \|\mathbf{j}_a\|^2 \|\boldsymbol{\delta}\|^2 = s\|\boldsymbol{\delta}\|^2$ , with equality if and only if  $\boldsymbol{\delta}$  is proportional to  $\mathbf{j}_a$  (which would make  $\mathbf{j}_b$  exactly proportional to  $\mathbf{j}_a$  and hence  $\det(G) = 0$ ). In general:

$$0 \leq \det(G) = s\|\boldsymbol{\delta}\|^2 - \eta^2 \leq s\|\boldsymbol{\delta}\|^2 = O(\varepsilon^2). \quad (28)$$

Since  $G$  is a  $2 \times 2$  positive semidefinite matrix with  $\text{tr}(G) = s + c^2s + O(\varepsilon) = \Theta(1)$ , its eigenvalues  $\lambda_+ \geq \lambda_- \geq 0$  satisfy  $\lambda_+ + \lambda_- = \text{tr}(G) = \Theta(1)$  and  $\lambda_+ \cdot \lambda_- = \det(G) = O(\varepsilon^2)$ . Therefore:

$$\lambda_-(G) = \frac{\det(G)}{\lambda_+(G)} = \frac{O(\varepsilon^2)}{\Theta(1)} = O(\varepsilon^2). \quad (29)$$

Let  $\mathbf{w} \in \mathbb{R}^2$  be a unit eigenvector of  $G$  corresponding to  $\lambda_- = \lambda_{\min}(G)$ , as defined in (21). Then:

$$\mathbf{w}^T G \mathbf{w} = \lambda_{\min}(G) = O(\varepsilon^2). \quad (30)$$

**Step 2: Rayleigh-quotient transfer to the full system.**

Partition  $J = [J_1 \mid J_2]$  where  $J_1 \in \mathbb{R}^{m \times 2}$  consists of columns  $a$  and  $b$ , and  $J_2 \in \mathbb{R}^{m \times (p-2)}$  contains all remaining columns. Construct the padded test vector  $\tilde{\mathbf{w}} \in \mathbb{R}^p$  as in the proposition statement ( $\tilde{w}_a = w_1$ ,  $\tilde{w}_b = w_2$ ,  $\tilde{w}_j = 0$  otherwise), so that  $\|\tilde{\mathbf{w}}\| = \|\mathbf{w}\| = 1$ .

The full Gram matrix has block structure:

$$J^T J = \begin{pmatrix} J_1^T J_1 & J_1^T J_2 \\ J_2^T J_1 & J_2^T J_2 \end{pmatrix}. \quad (31)$$

Evaluating the quadratic form at  $\tilde{\mathbf{w}}$ :

$$\begin{aligned}\tilde{\mathbf{w}}^T (J^T J) \tilde{\mathbf{w}} &= \begin{pmatrix} \mathbf{w} \\ \mathbf{0} \end{pmatrix}^T \begin{pmatrix} J_1^T J_1 & J_1^T J_2 \\ J_2^T J_1 & J_2^T J_2 \end{pmatrix} \begin{pmatrix} \mathbf{w} \\ \mathbf{0} \end{pmatrix} \\ &= \mathbf{w}^T (J_1^T J_1) \mathbf{w} + \underbrace{\mathbf{0}^T (J_2^T J_1) \mathbf{w}}_{=0} + \underbrace{\mathbf{w}^T (J_1^T J_2) \mathbf{0}}_{=0} + \underbrace{\mathbf{0}^T (J_2^T J_2) \mathbf{0}}_{=0} \\ &= \mathbf{w}^T (J_1^T J_1) \mathbf{w} = \lambda_{\min}(J_1^T J_1) = O(\varepsilon^2).\end{aligned}\quad (32)$$

By the Rayleigh-Ritz principle,  $\lambda_{\min}(M) = \min_{\|\mathbf{v}\|=1} \mathbf{v}^T M \mathbf{v}$ , so every unit  $\mathbf{v}$  satisfies  $\lambda_{\min}(M) \leq \mathbf{v}^T M \mathbf{v}$ :

$$\lambda_{\min}(J^T J) \leq \tilde{\mathbf{w}}^T (J^T J) \tilde{\mathbf{w}} = O(\varepsilon^2).\quad (33)$$

### Step 3: Condition-number bound.

For the upper bound on  $\lambda_{\max}$ , note that  $\lambda_{\max}(J^T J)$  is at least  $\lambda_{\max}(J_1^T J_1) \geq \text{tr}(G)/2 = \Theta(1)$  (since  $G$  has two eigenvalues summing to  $\text{tr}(G) = \Theta(1)$ , the larger is at least half the trace). More generally,  $\lambda_{\max}(J^T J) \leq \text{tr}(J^T J) = \|J\|_F^2 = \Theta(1)$  for any non-degenerate dataset (all columns of  $J$  have bounded norms). Therefore  $\lambda_{\max}(J^T J) = \Theta(1)$ , and:

$$\kappa(J^T J) = \frac{\lambda_{\max}(J^T J)}{\lambda_{\min}(J^T J)} \geq \frac{\Theta(1)}{O(\varepsilon^2)} = \Omega(\varepsilon^{-2}).\quad (34)$$

The matching upper bound  $\kappa(J^T J) = O(\varepsilon^{-2})$  follows from the global dominance assumption (Section 3.1): since  $(A, B)$  is the only source of small eigenvalues,  $\lambda_{\min}(J^T J) = \Theta(\varepsilon^2)$ , yielding  $\kappa(J^T J) = \Theta(\varepsilon^{-2})$ .  $\square$

## B.4 Appendix - Cauchy-Schwarz gap identity

**Lemma 2** (Cauchy-Schwarz gap identity). *Let  $\mathbf{f}, \mathbf{g} \in \mathbb{R}^m$  with  $g_i = c f_i h_i$  for a scalar  $c \neq 0$  and arbitrary  $h_i > 0$ . Define the power-law weights  $w_i := f_i^2 / \sum_j f_j^2$  and the weighted variance  $\sigma_w^2(h) := \sum_i w_i h_i^2 - (\sum_i w_i h_i)^2$ . Then:*

$$\det \begin{pmatrix} \mathbf{f}^T \mathbf{f} & \mathbf{f}^T \mathbf{g} \\ \mathbf{g}^T \mathbf{f} & \mathbf{g}^T \mathbf{g} \end{pmatrix} = c^2 \left( \sum_i f_i^2 \right)^2 \sigma_w^2(h).\quad (35)$$

*Proof.* Expand:  $\mathbf{f}^T \mathbf{g} = c \sum_i f_i^2 h_i$ ,  $\mathbf{g}^T \mathbf{g} = c^2 \sum_i f_i^2 h_i^2$ , so  $\det = (\sum_i f_i^2)(c^2 \sum_i f_i^2 h_i^2) - c^2 (\sum_i f_i^2 h_i)^2 = c^2 (\sum_i f_i^2)^2 [\sum_i w_i h_i^2 - (\sum_i w_i h_i)^2]$ .  $\square$

For  $h_i = N_i^\eta$  with  $|\eta|$  small, a Taylor expansion gives:

$$\sigma_w^2(N_i^\eta) = \eta^2 \sigma_w^2(\log N_i) + O(|\eta|^3),\quad (36)$$

For Chinchilla, take  $\eta = \alpha - \beta$  and  $\varepsilon := |\alpha - \beta|$  (Definition 3), so  $\eta^2 = \varepsilon^2$ . Thus the same bound applies to  $h_i = N_i^{\alpha - \beta}$ , yielding a non-asymptotic condition-number bound depending on  $\varepsilon$ , the sample size  $n$ , and the spread of  $\{N_i\}$ .

## B.5 Appendix - Chinchilla scaling law: detailed analysis

The Chinchilla parameter vector is  $\boldsymbol{\theta} = [A, B, E, \alpha, \beta]^T$  ( $p = 5$ ). The following analysis holds on a single collinear ray  $D_i = k_\ell N_i$  (i.e.,  $K = 1$  or a single fixed ratio  $k_\ell$  from the design); the scale-coefficient columns then satisfy:

$$\frac{\partial \hat{L}_i}{\partial B} = \underbrace{k_\ell^{-\beta}}_c N_i^{-\alpha} N_i^{\alpha - \beta},\quad (37)$$

with  $\varepsilon := |\alpha - \beta|$ . The corresponding residual Jacobian entries are  $J_{iA} = -\partial \hat{L}_i / \partial A$  and  $J_{iB} = -\partial \hat{L}_i / \partial B$ , but  $(J^T J)_{A,B}$  equals the Gram matrix of  $(\partial \hat{L} / \partial A, \partial \hat{L} / \partial B)$  because both columns pick up the same sign. The determinant of the  $(A, B)$  sub-block of  $J^T J$  satisfies:

$$\det \left( (J^T J)_{A,B} \right) = O(\varepsilon^2),\quad (38)$$

so  $\kappa((J^T J)_{A,B}) = \Theta(\varepsilon^{-2})$ . Applying Proposition 1 (under the  $(A, B)$ -dominance assumption of Section 3.1),  $\kappa(J^T J) = \Theta(\varepsilon^{-2})$  for the full  $5 \times 5$  system. For the empirical gap  $|\alpha - \beta| \approx 0.06$ , the condition number is on the order of  $10^2$ - $10^3$ .

**Explicit finite-sample bound.** This subsection provides the explicit finite-sample bound for the Chinchilla law (1) on a single collinear ray ( $K = 1$ ,  $D_i = k_\ell N_i$  for a fixed ratio  $k_\ell$ ).

Applying Lemma 2 with  $f_i = N_i^{-\alpha}$ ,  $c = k_\ell^{-\beta}$ , and  $h_i = N_i^{\alpha-\beta}$ , the sub-block determinant admits the exact factorisation:

$$\det\left((J^T J)_{A,B}\right) = k_\ell^{-2\beta} \Phi_2^2 \sigma_w^2(N_i^{\alpha-\beta}), \quad (39)$$

where  $\Phi_2 := \sum_{i=1}^n N_i^{-2\alpha}$  and the weights are  $w_i = N_i^{-2\alpha}/\Phi_2$ . Using the Taylor expansion (36):

$$\det\left((J^T J)_{A,B}\right) \approx k_\ell^{-2\beta} \Phi_2^2 \varepsilon^2 \sigma_w^2(\log N), \quad (40)$$

with  $\sigma_w^2(\log N) = \sum_i w_i (\log N_i)^2 - (\sum_i w_i \log N_i)^2$ . The condition number of the sub-block is therefore:

$$\kappa\left((J^T J)_{A,B}\right) \approx \frac{\text{tr}\left((J^T J)_{A,B}\right)^2}{k_\ell^{-2\beta} \Phi_2^2 \varepsilon^2 \sigma_w^2(\log N)}, \quad (41)$$

which makes the three sources of ill-conditioning explicit: (i) small exponent gap  $\varepsilon \rightarrow 0$ ; (ii) narrow model-size range, i.e. small  $\sigma_w^2(\log N)$  when the  $N_i$  are clustered; and (iii) finite sample effects through  $\Phi_2$  and the weights  $w_i$ , which concentrate on the *smallest* models and reduce the effective sample diversity. For the empirical gap  $|\alpha - \beta| \approx 0.06$ , equation (41) yields a condition number on the order of  $10^2$ - $10^3$ , rendering the system numerically ill-conditioned.  $\square$

## B.6 Appendix - Full Jacobian and tight conditioning

**Full Jacobian analysis.** The preceding argument concerns only the  $A$  and  $B$  columns. We now list the five model sensitivities  $\partial \hat{L}_i / \partial \theta_j$  on a single collinear ray  $D_i = k_\ell N_i$ ; by (10), the residual Jacobian  $J$  is obtained by negating each of these columns, so  $J^T J$  equals the Gram matrix of the sensitivities below. We claim the  $(E, \alpha, \beta)$  coordinates do not rescue the conditioning. The complete set of partial derivatives is:

$$\begin{aligned} \frac{\partial \hat{L}_i}{\partial A} &= N_i^{-\alpha}, & \frac{\partial \hat{L}_i}{\partial B} &= k_\ell^{-\beta} N_i^{-\beta}, \\ \frac{\partial \hat{L}_i}{\partial E} &= 1, & \frac{\partial \hat{L}_i}{\partial \alpha} &= -A N_i^{-\alpha} \log N_i, \\ \frac{\partial \hat{L}_i}{\partial \beta} &= -B k_\ell^{-\beta} N_i^{-\beta} (\log k_\ell + \log N_i). \end{aligned} \quad (42)$$

Observe that (writing  $\mathbf{j}_u$  for the  $m$ -vector with entries  $\partial \hat{L}_i / \partial u$ )  $\mathbf{j}_\alpha = -A \text{diag}(\log N_i) \mathbf{j}_A$  and  $\mathbf{j}_\beta = -B (\log k_\ell) \mathbf{j}_B - B \text{diag}(\log N_i) \mathbf{j}_B$ . Using  $\mathbf{j}_B \approx c \mathbf{j}_A + O(\varepsilon)$  (from (37)), both exponent columns lie approximately in the two-dimensional subspace  $\text{span}\{\mathbf{j}_A, \text{diag}(\log N_i) \mathbf{j}_A\}$ . In particular, if  $\mathbf{j}_B = c \mathbf{j}_A$  exactly, then  $\mathbf{j}_\beta - (Bc/A) \mathbf{j}_\alpha = -Bc(\log k_\ell) \mathbf{j}_A$ , so  $\mathbf{j}_\alpha$  and  $\mathbf{j}_\beta$  are *not* scalar multiples whenever  $\log k_\ell \neq 0$ ; more generally they share the same underlying column space as the scale-coefficient pair and therefore do not contribute an independent direction that overlaps the near-null space of  $(J^T J)_{A,B}$ . The  $E$ -column of sensitivities is  $\mathbf{1}$ , hence the  $E$ -column of  $J$  is  $-\mathbf{1}$ ; either way it is linearly independent of the power-law columns but likewise does not break the collinearity between the  $A/B$  pair.

By Proposition 1, the near-null eigenvector  $\mathbf{w}$  of  $(J^T J)_{A,B}$ , extended to  $\tilde{\mathbf{w}} \in \mathbb{R}^5$  with zeros in the  $(E, \alpha, \beta)$  coordinates matching (22), satisfies  $\tilde{\mathbf{w}}^T (J^T J) \tilde{\mathbf{w}} = O(\varepsilon^2)$ , hence  $\kappa(J^T J) = \Theta(\varepsilon^{-2})$  for the full  $5 \times 5$  system under the dominance assumption in Section 3.1.  $\square$

## B.7 Appendix - Repeated-data scaling law: detailed analysis

This subsection analyses the Jacobian of the repeated-data law on a single collinear ray ( $K = 1$ ,  $D_i = k_\ell N_i$ ). Muennighoff et al. (2025) retain the Chinchilla form but replace  $N$  and  $D$  with *effective* quantities  $N'$  and  $D'$  that decay under repetition:

$$L(N, D) = \frac{A}{N^\alpha} + \frac{B}{D'^\beta} + E, \quad (43)$$

with  $D' = U_D + U_D R_D^* (1 - e^{-R_D/R_D^*})$ ,  $U_D = \min\{D_C, D\}$ ,  $R_D = (D/U_D) - 1$ , and analogously  $N' = U_N + U_N R_N^* (1 - e^{-R_N/R_N^*})$ ,  $R_N = (N/U_N) - 1$ , with  $U_N$  Chinchilla-optimal for  $U_D$ . When  $R_D = R_N = 0$  (single epoch, no excess parameters),  $D' = D$  and  $N' = N$ , recovering Chinchilla exactly.

Under  $D_i = k_\ell N_i$ , both  $D'_i$  and  $N'_i$  become deterministic functions of  $N_i$ ; write  $D'_i = \phi(N_i)$  and  $N'_i = \psi(N_i)$ . The scale-coefficient sensitivities are  $\partial \hat{L}_i / \partial A = \psi(N_i)^{-\alpha}$  and  $\partial \hat{L}_i / \partial B = \phi(N_i)^{-\beta}$ , so Lemma 2 applies to the scale-coefficient pair with  $f_i = \psi(N_i)^{-\alpha}$ ,  $c = k_\ell^{-\beta}$ , and  $h_i = k_\ell^\beta \phi(N_i)^{-\beta} \psi(N_i)^\alpha$ , yielding

$\det((J^T J)_{A,B}) = c^2 \Phi_2^2 \sigma_w^2(h)$  with  $\Phi_2 = \sum_i \psi(N_i)^{-2\alpha}$  and  $w_i = \psi(N_i)^{-2\alpha}/\Phi_2$ . The conditioning of the  $(A, B)$  sub-block therefore depends on the variance of  $h_i$  across the ray, which differs sharply between two regimes.

**Unsaturated regime** ( $R_D = R_N = 0$ ). Here  $\phi(N) = k_\ell N$  and  $\psi(N) = N$ , so  $h_i = N_i^{\alpha-\beta}$ . The Taylor expansion  $\sigma_w^2(N_i^{\alpha-\beta}) \approx \varepsilon^2 \sigma_w^2(\log N_i)$  (with  $\varepsilon = |\alpha - \beta|$ ) gives  $\det((J^T J)_{A,B}) = O(\varepsilon^2)$ , so under the  $(A, B)$ -dominance assumption of Section 3.1,  $\kappa(J^T J) = \Theta(\varepsilon^{-2})$  for the full  $5 \times 5$  system - the law inherits Chinchilla's ill-conditioning verbatim.

**Saturated regime** ( $R_D, R_N \neq 0$ ). Once the ratio  $\phi(N_i)/\psi(N_i)$  varies systematically with  $N_i$ ,  $h_i$  ceases to be a pure power of  $N_i$ : the saturation curves of  $\phi$  and  $\psi$  inject an  $\varepsilon$ -independent contribution into  $\log h_i$ . Concretely,  $\sigma_w^2(h) = \Omega(1)$  as  $\varepsilon \rightarrow 0$ , so the Taylor expansion that produced the  $\varepsilon^2$  factor no longer applies. The scale-coefficient columns are no longer near-proportional,  $\det((J^T J)_{A,B}) = \Omega(1)$ , and the design is generically well-conditioned with  $\kappa(J^T J) = \Theta(1)$  - the saturation curvature itself breaks the degeneracy.

The repeated-data law therefore inherits the  $\Theta(\varepsilon^{-2})$  collinearity of Chinchilla *only* in the unsaturated regime. The  $(A, B)$  sub-block of  $Q$  is identically zero (as for Chinchilla) because  $\hat{L}$  is linear in  $A$  and  $B$ . Empirically, in our seed-paired comparisons the repeated-data law tracks the Chinchilla pattern (CO holdout  $R^2$  degrades and NC consistently wins), consistent with our multi-epoch fits sitting close to the unsaturated regime; we flag the saturated regime as a setting in which the formal guarantee does not apply.  $\square$

## B.8 Appendix - Kaplan scaling law: detailed analysis

This subsection expands on Section 3 for a single collinear ray ( $K = 1, D_i = k_\ell N_i$ ). The Kaplan law as fit in our experiments (matching the convention of, e.g., [Porian et al. \(2025\)](#)) takes the additive form

$$\hat{L}(N, D) = N_c^{\alpha_N} N^{-\alpha_N} + D_c^{\alpha_D} D^{-\alpha_D}, \quad (44)$$

with  $p = 4$  parameters  $\theta = [N_c, D_c, \alpha_N, \alpha_D]^T$ . The  $u^{\alpha_D}$  compositional form of [Kaplan et al. \(2020\)](#) is recovered by substituting  $\tilde{N}_c := N_c^{\alpha_N/\alpha_D}$ ,  $\tilde{D}_c := D_c^{\alpha_D}$ , and absorbing the outer exponent; the additive form is the parameterization under which identifiability is most directly comparable to Chinchilla, and the form fit by our optimizer (Appendix D.6).

**Explicit finite-sample bound.** Under  $D_i = k_\ell N_i$ , the scale-coefficient columns are  $\partial \hat{L}_i / \partial N_c = \alpha_N N_c^{\alpha_N-1} N_i^{-\alpha_N}$  and  $\partial \hat{L}_i / \partial D_c = \alpha_D D_c^{\alpha_D-1} k_\ell^{-\alpha_D} N_i^{-\alpha_D}$ . Lemma 2 applies with  $f_i = \alpha_N N_c^{\alpha_N-1} N_i^{-\alpha_N}$ ,  $c = (\alpha_D/\alpha_N)(D_c^{\alpha_D-1}/N_c^{\alpha_N-1})k_\ell^{-\alpha_D}$ , and  $h_i = N_i^\varepsilon$  with  $\varepsilon := \alpha_D - \alpha_N$  and  $\tilde{\varepsilon} := |\varepsilon|$ , giving  $\det((J^T J)_{N_c, D_c}) \approx c^2 \Phi_2^2 \varepsilon^2 \sigma_w^2(\log N)$  with  $\Phi_2 := \sum_i f_i^2/\alpha_N^2$  and weights  $w_i \propto f_i^2$ . The interpretation mirrors the Chinchilla case: ill-conditioning worsens when the model sizes  $\{N_i\}$  are clustered or the exponent gap  $|\alpha_D - \alpha_N|$  is small.

**Full Jacobian analysis.** Write  $\mathbf{j}_u$  for the sensitivity vector  $(\partial \hat{L}_i / \partial u)_i$ . We derive the two remaining columns,  $\mathbf{j}_{\alpha_N}$  and  $\mathbf{j}_{\alpha_D}$ . Differentiating (44) via  $N_c^{\alpha_N} = \exp(\alpha_N \log N_c)$  and the analogous identity for  $D_c^{\alpha_D}$ :

$$\frac{\partial \hat{L}}{\partial \alpha_N} = N_c^{\alpha_N} N^{-\alpha_N} (\log N_c - \log N), \quad (45)$$

$$\frac{\partial \hat{L}}{\partial \alpha_D} = D_c^{\alpha_D} D^{-\alpha_D} (\log D_c - \log D). \quad (46)$$

The  $\alpha_N$ -column (45) equals  $\mathbf{j}_{N_c}$  scaled element-wise by the observation-dependent factor  $(N_c/\alpha_N)(\log N_c - \log N_i)$ ; likewise the  $\alpha_D$ -column (46) equals  $\mathbf{j}_{D_c}$  scaled element-wise by  $(D_c/\alpha_D)(\log D_c - \log D_i)$ . Both therefore lie in the subspace spanned by the scale-coefficient columns and their log-modulated variants, rather than introducing genuinely new directions (cf. the Droppo-Elibol analysis in Appendix B.9).

Applying Proposition 1 with  $p = 4$ : the extended near-null vector  $\tilde{\mathbf{w}} \in \mathbb{R}^4$  padding  $\mathbf{w}$  with zeros in the  $(\alpha_N, \alpha_D)$  coordinates as in (22) satisfies  $\tilde{\mathbf{w}}^T (J^T J) \tilde{\mathbf{w}} = O(\varepsilon^2)$ , hence, under scale-coefficient dominance (Section 3.1),  $\kappa(J^T J) = \Theta(\varepsilon^{-2})$  for the full  $4 \times 4$  system.  $\square$

## B.9 Appendix - Droppo & Elibol scaling law: detailed analysis

We use the form fit in our experiments and recorded in Table 1,

$$\hat{L}(N, D) = [L_\infty^{1/\alpha} + N_c^{\alpha_N} N^{-\alpha_N} + D_c^{\alpha_D} D^{-\alpha_D}]^\alpha, \quad (47)$$

[Droppo and Elibol \(2021\)](#) motivate this compositional structure; we fit (47) as in Table 1, with  $p = 6$  parameters  $(L_\infty, N_c, D_c, \alpha_N, \alpha_D, \alpha)$ . Definition 3 writes  $\gamma_N = \alpha_N/\alpha$  and  $\gamma_D = \alpha_D/\alpha$ . Substituting  $D = k_\ell N$  (single collinear ray,  $K = 1$ ),

$$\hat{L}(N, k_\ell N) = \left[ L_\infty^{1/\alpha} + N^{-\alpha_N} \left( N_c^{\alpha_N} + D_c^{\alpha_D} k_\ell^{-\alpha_D} N^{\alpha_N - \alpha_D} \right) \right]^\alpha. \quad (48)$$

In particular, when  $\alpha_N = \alpha_D$  this reduces to  $[L_\infty^{1/\alpha} + C_{\text{total}} N^{-\alpha_N}]^\alpha$  with  $C_{\text{total}} = N_C^{\alpha_N} + D_C^{\alpha_D} k_\ell^{-\alpha_D}$ . When  $|\alpha_N - \alpha_D|$  is small, Taylor expanding  $N^{\alpha_N - \alpha_D}$  about  $\alpha_N = \alpha_D$  recovers the same  $O(\varepsilon)$  near-proportionality as in the Chinchilla case, with  $\varepsilon = |\alpha_N - \alpha_D|$  at leading order (and  $|\gamma_N - \gamma_D| = \varepsilon/\alpha$  in Definition 3 when  $\alpha = \Theta(1)$ ). The irreducible loss  $L_\infty$  remains independently identifiable.

**Explicit finite-sample bound.** After absorbing the shared chain-rule prefactor  $\alpha v_i^{\alpha-1}$ , Lemma 2 applies with  $f_i \propto \alpha_N N_C^{\alpha_N-1} N_i^{-\alpha_N}$ , the scalar  $\lambda = (\alpha_D/\alpha_N) (D_C^{\alpha_D-1}/N_C^{\alpha_N-1}) k_\ell^{-\alpha_D}$ , and  $h_i = N_i^\varepsilon$  with  $\varepsilon := \alpha_N - \alpha_D$  and  $\varepsilon := |\varepsilon|$ , yielding

$$\det\left((J^T J)_{N_C, D_C}\right) \approx \lambda^2 \Phi_2^2 \varepsilon^2 \sigma_w^2(\log N), \quad (49)$$

with weights  $w_i \propto f_i^2$ . As in the Chinchilla and Kaplan cases, ill-conditioning worsens when the training configurations are clustered in  $\log N$  or when  $|\alpha_N - \alpha_D|$  is small.

**Full Jacobian analysis.** Write  $\mathbf{j}_u$  for the sensitivity vector  $(\partial \hat{L}_i / \partial u)_i$ . We derive the four remaining columns  $\mathbf{j}_{L_\infty}$ ,  $\mathbf{j}_{\alpha_N}$ ,  $\mathbf{j}_{\alpha_D}$ , and  $\mathbf{j}_\alpha$ , and show they do not break the near-singularity. Recall  $\hat{L} = v^\alpha$  with

$$v = L_\infty^{1/\alpha} + N_C^{\alpha_N} N^{-\alpha_N} + D_C^{\alpha_D} D^{-\alpha_D}.$$

*Irreducible loss:* the chain rule gives  $\mathbf{j}_{L_\infty} = \alpha v^{\alpha-1} \partial v / \partial L_\infty = L_\infty^{1/\alpha-1} (v_i^{\alpha-1})_i$ , i.e. the constant scalar  $L_\infty^{1/\alpha-1}$  times the observation-dependent vector  $(v_i^{\alpha-1})_i$  - so  $\mathbf{j}_{L_\infty}$  is *not* a constant vector, and only the scalar  $\partial v / \partial L_\infty$  is  $i$ -independent. Linear independence with  $(\mathbf{j}_{N_C}, \mathbf{j}_{D_C})$  follows because  $v_i^{\alpha-1}$  depends on  $(N_i, D_i)$  through the sum  $L_\infty^{1/\alpha} + N_C^{\alpha_N} N_i^{-\alpha_N} + D_C^{\alpha_D} D_i^{-\alpha_D}$  raised to  $\alpha - 1$  and is therefore not a scalar multiple of  $N_i^{-\alpha_N}$  or  $D_i^{-\alpha_D}$ , so  $\mathbf{j}_{L_\infty}$  does not share the  $(N_C, D_C)$  near-collinearity.

*Exponent columns:*

$$\frac{\partial \hat{L}}{\partial \alpha_N} = \alpha v^{\alpha-1} N_C^{\alpha_N} N^{-\alpha_N} (\log N_C - \log N), \quad (50)$$

$$\frac{\partial \hat{L}}{\partial \alpha_D} = \alpha v^{\alpha-1} D_C^{\alpha_D} D^{-\alpha_D} (\log D_C - \log D), \quad (51)$$

$$\frac{\partial \hat{L}}{\partial \alpha} = v^\alpha \log v - \frac{1}{\alpha} v^{\alpha-1} L_\infty^{1/\alpha} \log L_\infty. \quad (52)$$

Equation (52) uses  $\partial v / \partial \alpha = -(1/\alpha^2) L_\infty^{1/\alpha} \log L_\infty$  because only the  $L_\infty^{1/\alpha}$  summand depends on  $\alpha$  when  $(\alpha_N, \alpha_D)$  are free. The  $\alpha_N$ -column (50) equals  $\mathbf{j}_{N_C}$  scaled element-wise by  $(N_C/\alpha_N)(\log N_C - \log N_i)$ ; likewise the  $\alpha_D$ -column (51) equals  $\mathbf{j}_{D_C}$  scaled element-wise by  $(D_C/\alpha_D)(\log D_C - \log D_i)$ . Both therefore lie in the subspace spanned by the scale-coefficient columns and their log-modulated variants, rather than introducing genuinely new directions. The  $\alpha$ -column (52) combines  $\log v$  with the  $L_\infty$  term and does not contribute an independent direction that overlaps the near-null space of  $(J^T J)_{N_C, D_C}$ .

Applying Proposition 1 with  $p = 6$ , extend the near-null  $\mathbf{w} \in \mathbb{R}^2$  for the  $(N_C, D_C)$  pair to  $\tilde{\mathbf{w}} \in \mathbb{R}^6$  by padding with zeros in the other four coordinates as in (22); then  $\tilde{\mathbf{w}}^T (J^T J) \tilde{\mathbf{w}} = O(\varepsilon^2)$ , hence, under scale-coefficient dominance (Section 3.1),  $\kappa(J^T J) = \Theta(\varepsilon^{-2})$  for the full  $6 \times 6$  system. The ill-conditioning arises exclusively from the model-capacity and data-size terms.  $\square$

## B.10 Appendix - Identified submodels on a single collinear ray ( $K = 1$ )

This subsection provides the formal statements supporting Section 3.1. Throughout, we fix  $K = 1$ , i.e. all training points share a single TPP ratio  $k_\ell$ , so  $D_i = k_\ell N_i$ . The reduced model  $L(N) = \psi N^{-\alpha} + E$  with  $\psi := A + B k_\ell^{-\alpha}$  (equation (2)) is defined in the main text. We next define the power sums  $\Phi_q$ , weights  $w_i$ , and  $\sigma_w^2(\log N)$  (Definitions 5, 6, and 7). Proposition 4 shows that the  $(\psi, \alpha)$  Gram block of the reduced Jacobian has determinant  $\psi^2 \Phi_2^2 \sigma_w^2(\log N)$  (via Lemma 2 in Appendix B.4), positive for any design with at least two distinct model sizes and independent of  $\varepsilon$ , and Corollary 2 records an  $\Theta(\varepsilon^{-2})$  condition-number gain relative to the full model.

Let  $N_1 < \dots < N_n$  be the distinct model sizes (as in the observation model, Section 3).

**Definition 5** (Power sums). For  $q > 0$ , the *power sums* are  $\Phi_q := \sum_{i=1}^n N_i^{-q\alpha}$ . In particular,  $\Phi_2 := \sum_{i=1}^n N_i^{-2\alpha}$ .

**Definition 6** (Weights). Given  $\Phi_2$  from Definition 5, the *weights* are  $w_i := N_i^{-2\alpha} / \Phi_2$  for  $i = 1, \dots, n$ .

**Definition 7** (Weighted log-variance). Given weights  $(w_i)$  from Definition 6, the *weighted log-variance* is  $\sigma_w^2(\log N) := \sum_{i=1}^n w_i (\log N_i)^2 - (\sum_{i=1}^n w_i \log N_i)^2$ .

**Proposition 4** (Identification of the reduced model). *The Gram determinant of the  $(\psi, \alpha)$  sub-block of  $J_{\text{red}}^T J_{\text{red}}$  is*

$$\det((J_{\text{red}}^T J_{\text{red}})_{\psi, \alpha}) = \psi^2 \Phi_2^2 \sigma_w^2(\log N), \quad (53)$$

where  $\sigma_w^2(\log N)$  is as in Definition 7. The determinant is **positive** for any design with at least two distinct model sizes and is **independent of the exponent gap**  $\varepsilon$ . The full  $3 \times 3$  matrix  $J_{\text{red}}^T J_{\text{red}}$  is non-singular.

**Corollary 2** (Condition-number improvement). *In the setting of Proposition 4,  $\kappa_{\text{full}}/\kappa_{\text{red}} = \Theta(\varepsilon^{-2})$ . For  $|\alpha - \beta| \approx 0.06$ , this is a factor of  $10^2 \cdot 10^3$ .*

### B.10.1 Identified submodels: proofs

*Proof of Proposition 4.* Apply Lemma 2 with  $f_i = N_i^{-\alpha}$  (the  $\psi$ -sensitivity  $\partial \hat{L}_i / \partial \psi$ ),  $g_i = c f_i h_i$  where  $c = -\psi$  and  $h_i = \log N_i$  (so that  $g_i = \partial \hat{L}_i / \partial \alpha$ ). The Gram determinant is  $c^2 (\sum f_i^2)^2 \sigma_w^2(h) = \psi^2 \Phi_2^2 \sigma_w^2(\log N)$ . No  $\varepsilon$  appears because the reduced model contains a single power-law term.  $\square$

*Proof of Corollary 2.* From equation (40), the sub-block determinant of the full model scales as  $\varepsilon^2 \sigma_w^2(\log N)$ , while from equation (53) the corresponding determinant of the reduced model is proportional to  $\sigma_w^2(\log N)$  alone. The  $\sigma_w^2(\log N)$  factors cancel in the ratio, leaving a factor of  $\varepsilon^{-2}$ .  $\square$

### B.11 Appendix - Proof of Corollary 1 (Confidence Interval Inflation)

**Corollary** (Confidence interval inflation (full statement)). *Under i.i.d. Gaussian noise with variance  $\sigma^2$  and a single collinear ray  $D = k_\ell N$  ( $K = 1$ ), the least-squares estimator  $\hat{A}$  in the full Chinchilla model (1) satisfies*

$$\text{Var}(\hat{A}) \geq \frac{\sigma^2 \Phi_2^{(2\varepsilon)}}{\Phi_2^2 \sigma_w^2(N_i^\varepsilon)}, \quad (54)$$

where  $\Phi_2^{(2\varepsilon)} := \sum_{i=1}^n N_i^{-2\beta}$  (equivalently  $\sum_i N_i^{-2\alpha+2\varepsilon}$  with  $\tilde{\varepsilon} := \alpha - \beta$  and  $|\tilde{\varepsilon}| = \varepsilon$  from Definition 3), and  $\sigma_w^2(N_i^\varepsilon)$  uses the same weights ( $w_i$ ) as  $\sigma_w^2(\log N)$  (Definitions 6-7), with equality when  $E$ ,  $\alpha$ , and  $\beta$  are known. To leading order in  $\varepsilon$ :

$$\text{Var}(\hat{A}) \geq \frac{\sigma^2}{\Phi_2 \varepsilon^2 \sigma_w^2(\log N)} (1 + O(\varepsilon)). \quad (55)$$

The corresponding variance of  $\hat{\psi}$  in the reduced model (2) satisfies

$$\text{Var}(\hat{\psi}) = \sigma^2 \frac{G_{\alpha\alpha}^{\text{eff}}}{(\Phi_2 - \Phi_1^2/n) G_{\alpha\alpha}^{\text{eff}} - (G_{\psi\alpha}^{\text{eff}})^2}, \quad (56)$$

where  $G^{\text{eff}}$  is the  $(\psi, \alpha)$  Schur complement after profiling  $E$  (see below for the explicit entries); all quantities are bounded and independent of  $\varepsilon$ . Combining (54)-(56) with Gaussian interval half-widths yields the simplified asymptotic ratio (4) recorded in Corollary 1.

We derive the variance bounds for  $\hat{A}$  (full model) and  $\hat{\psi}$  (reduced model) under i.i.d. Gaussian noise  $L_i = \hat{L}(N_i, D_i; \theta^*) + \epsilon_i$ ,  $\epsilon_i \sim \mathcal{N}(0, \sigma^2)$  with  $\mathbb{E}[\epsilon_i] = 0$ .

**Variance of  $\hat{A}$  in the full model.** Under Gaussian noise the covariance of the OLS estimator is  $\text{Cov}(\hat{\theta}) = \sigma^2 (J^T J)^{-1}$ , so  $\text{Var}(\hat{A}) = \sigma^2 [(J^T J)^{-1}]_{AA}$ .

Partition  $J^T J$  conformably as

$$J^T J = \begin{pmatrix} G_{AB} & G_{12} \\ G_{21} & G_{22} \end{pmatrix},$$

where  $G_{AB} := (J^T J)_{A,B} \in \mathbb{R}^{2 \times 2}$  is the  $(A, B)$  sub-block and  $G_{22}$  contains the remaining  $(E, \alpha, \beta)$  entries. By the Schur-complement formula for the inverse of a partitioned matrix:

$$[(J^T J)^{-1}]_{(A,B)} = (G_{AB} - G_{12} G_{22}^{-1} G_{21})^{-1}. \quad (57)$$

Since  $G_{12} G_{22}^{-1} G_{21}$  is positive semidefinite, the Schur complement satisfies  $S_{AB} := G_{AB} - G_{12} G_{22}^{-1} G_{21} \preceq G_{AB}$  (Löwner order), and therefore

$$[(J^T J)^{-1}]_{(A,B)} = S_{AB}^{-1} \succeq G_{AB}^{-1}. \quad (58)$$

In particular, the  $(1, 1)$  entry obeys  $[(J^T J)^{-1}]_{AA} \geq [G_{AB}^{-1}]_{AA}$ .

For the  $2 \times 2$  matrix  $G_{AB} = \begin{pmatrix} a & b \\ b & d \end{pmatrix}$  with  $a = \mathbf{j}_A^T \mathbf{j}_A = \Phi_2$ ,  $d = \mathbf{j}_B^T \mathbf{j}_B = k_\ell^{-2\beta} \Phi_2^{(2\varepsilon)}$ , and  $\det(G_{AB}) = k_\ell^{-2\beta} \Phi_2^2 \sigma_w^2(N_i^\varepsilon)$  (equation (39)):

$$[G_{AB}^{-1}]_{AA} = \frac{d}{\det(G_{AB})} = \frac{k_\ell^{-2\beta} \Phi_2^{(2\varepsilon)}}{k_\ell^{-2\beta} \Phi_2^2 \sigma_w^2(N_i^\varepsilon)} = \frac{\Phi_2^{(2\varepsilon)}}{\Phi_2^2 \sigma_w^2(N_i^\varepsilon)}. \quad (59)$$

Hence

$$\text{Var}(\hat{A}) = \sigma^2 [(J^T J)^{-1}]_{AA} \geq \sigma^2 [G_{AB}^{-1}]_{AA} = \frac{\sigma^2 \Phi_2^{(2\varepsilon)}}{\Phi_2^2 \sigma_w^2(N_i^\varepsilon)},$$

establishing (54).

To obtain the leading-order form (55), note that  $\Phi_2^{(2\varepsilon)} = \sum_i N_i^{-2\beta} = \Phi_2 + 2\varepsilon T_2 + O(\varepsilon^2)$  where  $T_2 = \sum_i N_i^{-2\alpha} \log N_i$ , so  $\Phi_2^{(2\varepsilon)}/\Phi_2 = 1 + O(\varepsilon)$ . Combined with the Taylor expansion  $\sigma_w^2(N_i^\varepsilon) = \varepsilon^2 \sigma_w^2(\log N_i) + O(|\varepsilon|^3)$  (equation (36)):

$$\frac{\Phi_2^{(2\varepsilon)}}{\Phi_2^2 \sigma_w^2(N_i^\varepsilon)} = \frac{1 + O(\varepsilon)}{\Phi_2 \varepsilon^2 \sigma_w^2(\log N)} = \frac{1}{\Phi_2 \varepsilon^2 \sigma_w^2(\log N)} (1 + O(\varepsilon)).$$

**Variance of  $\hat{\psi}$  in the reduced model.** The reduced model (2) has parameter vector  $\boldsymbol{\theta}_{\text{red}} = (\psi, \alpha, E)^T$  and Jacobian  $J_{\text{red}} \in \mathbb{R}^{n \times 3}$  with columns

$$\mathbf{j}_\psi = (N_i^{-\alpha})_{i=1}^n, \quad \mathbf{j}_\alpha = (-\psi N_i^{-\alpha} \log N_i)_{i=1}^n, \quad \mathbf{j}_E = \mathbf{1}_n. \quad (60)$$

Define  $\Phi_1 := \sum_i N_i^{-\alpha}$ ,  $T_1 := \sum_i N_i^{-\alpha} \log N_i$ ,  $U_2 := \sum_i N_i^{-2\alpha} (\log N_i)^2$ . The  $3 \times 3$  Gram matrix is

$$G_{\text{red}} = \begin{pmatrix} \Phi_2 & -\psi T_2 & \Phi_1 \\ -\psi T_2 & \psi^2 U_2 & -\psi T_1 \\ \Phi_1 & -\psi T_1 & n \end{pmatrix}.$$

Since  $\text{Var}(\hat{\psi}) = \sigma^2 [G_{\text{red}}^{-1}]_{\psi\psi}$ , we compute the  $(\psi, \alpha)$  Schur complement after profiling  $E$ :

$$\begin{aligned} G_{\psi\psi}^{\text{eff}} &= \Phi_2 - \Phi_1^2/n, \\ G_{\psi\alpha}^{\text{eff}} &= -\psi (T_2 - \Phi_1 T_1/n), \\ G_{\alpha\alpha}^{\text{eff}} &= \psi^2 (U_2 - T_1^2/n). \end{aligned}$$

The first entry  $G_{\psi\psi}^{\text{eff}}$  is the sample variance of  $\{N_i^{-\alpha}\}$  (times  $n$ ); the other entries are analogous centered moments. The profiled  $2 \times 2$  determinant is

$$\det(G^{\text{eff}}) = G_{\psi\psi}^{\text{eff}} G_{\alpha\alpha}^{\text{eff}} - (G_{\psi\alpha}^{\text{eff}})^2,$$

and

$$\text{Var}(\hat{\psi}) = \sigma^2 \frac{G_{\alpha\alpha}^{\text{eff}}}{\det(G^{\text{eff}})}. \quad (61)$$

No power of  $\varepsilon$  appears anywhere in  $G^{\text{eff}}$ : the entries depend only on  $\{N_i\}$ ,  $\alpha$ ,  $\psi$ , and  $n$ , all of which are  $O(1)$  with respect to the exponent gap. Hence  $\text{Var}(\hat{\psi})$  is bounded and  $\varepsilon$ -independent, confirming (56).

**Confidence-interval ratio.** Under Gaussianity, the 95% interval half-width for any scalar parameter  $\theta_j$  is  $1.96 \sqrt{\text{Var}(\hat{\theta}_j)}$ . Therefore:

$$\begin{aligned} \frac{\text{CI}_{0.95}(A)}{\text{CI}_{0.95}(\psi)} &\geq \sqrt{\frac{\text{Var}(\hat{A})}{\text{Var}(\hat{\psi})}} \\ &\geq \sqrt{\frac{\Phi_2^{(2\varepsilon)}}{\Phi_2^2 \sigma_w^2(N_i^\varepsilon)} \cdot \frac{\det(G^{\text{eff}})}{G_{\alpha\alpha}^{\text{eff}}}} \\ &= \frac{1}{\varepsilon} \sqrt{\frac{\Phi_2^{(2\varepsilon)}}{\Phi_2}} \cdot \underbrace{\sqrt{\frac{\det(G^{\text{eff}})}{\Phi_2 \sigma_w^2(\log N) G_{\alpha\alpha}^{\text{eff}}}}}_{\Theta(1)} \cdot (1 + O(\varepsilon)), \end{aligned}$$

where in the last step we used  $\sigma_w^2(N_i^\varepsilon) = \varepsilon^2 \sigma_w^2(\log N)(1 + O(\varepsilon))$  and  $\Phi_2^{(2\varepsilon)}/\Phi_2 = 1 + O(\varepsilon)$ . The  $\Theta(1)$  factor depends on the design  $\{N_i\}$  but *not* on  $\varepsilon$ ; for typical designs spanning 1-2 decades in  $N$ , it is  $O(1)$ .  $\square$

## B.12 Appendix - Proof of Proposition 2 (TPP diversity and full-matrix conditioning)

We give a self-contained proof. Throughout,  $\beta_{\text{eff}}$  denotes the law-specific data-size exponent (Table 8). For any  $K \geq 1$  distinct TPP ratios  $k_1 < \dots < k_K$ , let each ratio contribute  $n_\ell \geq 1$  observations at model sizes  $\{N_i\}$  (the same set for each ray, without loss of generality for the leading-order analysis). The training Jacobian is evaluated at the collinear design  $D_{i\ell} = k_\ell N_i$ .

**Step 1: Jacobian columns for the scale-coefficient pair.** For any of the four scaling laws in Definition 3, the two scale-coefficient columns of  $J$  on observation  $(N_i, k_\ell N_i)$  are (cf. Appendix B.5, eqn. (37) for Chinchilla; analogous expressions hold for the other three laws with the substitutions of Table 8):

$$(j_A)_{i\ell} = N_i^{-\alpha}, \quad (j_B)_{i\ell} = k_\ell^{-\beta_{\text{eff}}} N_i^{-\alpha} N_i^{\tilde{\varepsilon}}, \quad (62)$$

where  $\tilde{\varepsilon}$  is the *signed* native gap in each law (e.g.  $\alpha - \beta$  for Chinchilla and repeated-data,  $\alpha_N - \alpha_D$  for Kaplan,  $\gamma_N - \gamma_D$  for Droppo-Elibol), so  $|\tilde{\varepsilon}| = \varepsilon$  in Definition 3, and the displayed  $\alpha$  is the model-side exponent paired with  $\beta_{\text{eff}}$  as in Table 8.

**Step 2:  $(A, B)$  Gram sub-block.** Define  $\Phi_2 := \sum_{i=1}^n N_i^{-2\alpha}$  (Definition 5). The four entries of the  $2 \times 2$  Gram sub-block  $G_{A,B} = J_{A,B}^T J_{A,B}$  are obtained by summing over all  $m = nK$  observations. Working at leading order in  $\varepsilon$  (i.e.,  $N_i^{\tilde{\varepsilon}} = 1 + O(\varepsilon)$ ,  $N_i^{2\tilde{\varepsilon}} = 1 + O(\varepsilon)$ ):

$$(G_{A,B})_{11} = \sum_{\ell=1}^K \sum_{i=1}^n N_i^{-2\alpha} = K \Phi_2, \quad (63)$$

$$(G_{A,B})_{12} = \sum_{\ell=1}^K k_\ell^{-\beta_{\text{eff}}} \sum_{i=1}^n N_i^{-2\alpha} N_i^{\tilde{\varepsilon}} = \Phi_2 \sum_{\ell=1}^K k_\ell^{-\beta_{\text{eff}}} + O(\varepsilon), \quad (64)$$

$$(G_{A,B})_{22} = \sum_{\ell=1}^K k_\ell^{-2\beta_{\text{eff}}} \sum_{i=1}^n N_i^{-2\alpha} N_i^{2\tilde{\varepsilon}} = \Phi_2 \sum_{\ell=1}^K k_\ell^{-2\beta_{\text{eff}}} + O(\varepsilon). \quad (65)$$

Write  $S_1 := \sum_{\ell=1}^K k_\ell^{-\beta_{\text{eff}}}$  and  $S_2 := \sum_{\ell=1}^K k_\ell^{-2\beta_{\text{eff}}}$ . Then at leading order:

$$G_{A,B} = \Phi_2 \begin{pmatrix} K & S_1 \\ S_1 & S_2 \end{pmatrix} + O(\varepsilon). \quad (66)$$

**Step 3: Trace, determinant, and condition number.** From (66):

$$\text{tr}(G_{A,B}) = \Phi_2 (K + S_2) + O(\varepsilon), \quad (67)$$

$$\det(G_{A,B}) = \Phi_2^2 (K S_2 - S_1^2) + O(\varepsilon). \quad (68)$$

Note that  $K S_2 - S_1^2 = K^2 V_K$ , where  $V_K$  is the sample variance of  $\{k_\ell^{-\beta_{\text{eff}}}\}$  defined in the proposition statement (eqn. (5)):

$$V_K = \frac{1}{K} \sum_{\ell=1}^K k_\ell^{-2\beta_{\text{eff}}} - \left( \frac{1}{K} \sum_{\ell=1}^K k_\ell^{-\beta_{\text{eff}}} \right)^2 = \frac{K S_2 - S_1^2}{K^2}. \quad (69)$$

For a  $2 \times 2$  positive-semidefinite matrix with eigenvalues  $\lambda_+ \geq \lambda_- \geq 0$ ,  $\kappa = \lambda_+/\lambda_-$  and the identities  $\lambda_+ \cdot \lambda_- = \det$ ,  $\lambda_+ + \lambda_- = \text{tr}$  give  $\lambda_\pm = \frac{1}{2}(\text{tr} \pm \sqrt{\text{tr}^2 - 4 \det})$ , hence  $\kappa = \frac{\text{tr}^2}{2 \det} - 1 + \frac{\text{tr}^2}{2 \det} \sqrt{1 - 4 \det / \text{tr}^2}$ . At leading order, when  $\det \ll \text{tr}^2$  (the regime of interest),  $\sqrt{1 - 4 \det / \text{tr}^2} \approx 1 - 2 \det / \text{tr}^2$ , so  $\kappa \approx \text{tr}^2 / \det - 2 \approx \text{tr}^2 / \det$ . Therefore:

$$\kappa_{A,B} \approx \frac{\text{tr}(G_{A,B})^2}{\det(G_{A,B})} = \frac{\Phi_2^2 (K + S_2)^2}{\Phi_2^2 K^2 V_K} = \frac{(K + S_2)^2}{K^2 V_K}. \quad (70)$$

The factors of  $\Phi_2^2$  cancel exactly.

**Step 4: The biconditional.** For any  $\kappa_{\text{target}} > 0$ , from (70):

$$\kappa_{A,B} \leq \kappa_{\text{target}} \iff \frac{(K + S_2)^2}{K^2 V_K} \leq \kappa_{\text{target}} \iff V_K \geq \underbrace{\frac{(K + S_2)^2}{K^2 \kappa_{\text{target}}}}_{\tau_K}. \quad (71)$$

The second equivalence is valid because  $V_K \geq 0$ ,  $(K + S_2)^2 > 0$ , and  $\kappa_{\text{target}} > 0$ ; the inequality is reversed by dividing both sides by the positive quantity  $K^2 V_K \cdot \kappa_{\text{target}}^{-1}$  and rearranging. This establishes (5).

**Step 5: The three cases.**

**Case  $K = 1$ .** When  $K = 1$ , there is a single TPP ratio  $k_1$ , so  $S_1 = k_1^{-\beta_{\text{eff}}}$ ,  $S_2 = k_1^{-2\beta_{\text{eff}}}$ , and  $V_1 = k_1^{-2\beta_{\text{eff}}} - (k_1^{-\beta_{\text{eff}}})^2 = 0$ . The threshold satisfies  $\tau_1 = (1 + k_1^{-2\beta_{\text{eff}}})^2 / \kappa_{\text{target}} > 0$  for every  $\kappa_{\text{target}} > 0$ . Therefore  $V_1 = 0 < \tau_1$  and the condition (5) can never hold. Equivalently,  $\det(G_{A,B}) = O(\varepsilon^2)$  (the next-order term from  $N_i^\varepsilon \neq 1$ ; see eqns. (39)-(40)), confirming the ill-conditioning  $\kappa_{A,B} = \Theta(\varepsilon^{-2})$  established by Proposition 1.

**Case  $K = 2$ .** Set  $k_1 < k_2$  with ratio  $R := k_2/k_1$ . Then:

$$S_1 = k_1^{-\beta_{\text{eff}}}(1 + R^{-\beta_{\text{eff}}}), \quad S_2 = k_1^{-2\beta_{\text{eff}}}(1 + R^{-2\beta_{\text{eff}}}),$$

$$V_2 = \frac{1}{2}S_2 - \left(\frac{1}{2}S_1\right)^2 = \frac{1}{4}k_1^{-2\beta_{\text{eff}}}(1 - R^{-\beta_{\text{eff}}})^2.$$

Substituting into (71) and simplifying (dividing both sides by  $k_1^{-2\beta_{\text{eff}}}/4$  and rearranging): the condition  $V_2 \geq \tau_2$  reduces to  $R \geq R_{\min}$  where  $R_{\min}$  is determined by (95) (Appendix B.15).

**Case  $K > 2$ .** For  $K > 2$ , there is no single closed-form analog of Eq. (95): feasibility is determined directly by (71). Since  $V_K = \text{Var}(k_\ell^{-\beta_{\text{eff}}})$ , interior rays at fixed endpoints generally reduce this variance, while  $\tau_K$  changes with  $K$  through  $(K + S_2)^2/K^2$ . Hence the practical criterion is to evaluate  $V_K \geq \tau_K$  for the proposed set  $\{k_\ell\}_{\ell=1}^K$ . Since interior rays sit between the endpoint values of  $\{k_\ell^{-\beta_{\text{eff}}}\}$  and pull the sample toward its mean,  $V_K$  at fixed endpoint spread  $R = k_K/k_1$  is maximized by the two-ray configuration with mass at the endpoints; the threshold  $\tau_K$  tightens at a comparable rate via the  $K^2$  denominator, so  $K > 2$  generally requires  $R \geq R_{\min}$  - the additional rays serve residual diagnostics and robustness rather than relaxing the spread requirement (Appendix B.15).

**Step 6: Lifting to  $\kappa(J^T J)$ .** By Cauchy interlacing,  $\kappa_{A,B} \leq \kappa(J^T J)$ , so  $\kappa(J^T J) \leq \kappa_{\text{target}}$  implies  $\kappa_{A,B} \leq \kappa_{\text{target}}$  and hence  $V_K \geq \tau_K$  (the ‘‘only if’’ direction lifts immediately). Conversely, when  $V_K \geq \tau_K$  the sub-block is well-conditioned ( $\kappa_{A,B} \leq \kappa_{\text{target}}$ ), and by the global dominance assumption (Section 3.1), the remaining eigenvalues of  $J^T J$  are  $\Theta(1)$ . Therefore  $\lambda_{\min}(J^T J) = \lambda_{\min}(G_{A,B})(1 + O(\varepsilon))$  and  $\lambda_{\max}(J^T J) = \Theta(1)$ , giving  $\kappa(J^T J) = \kappa_{A,B}(1 + O(\varepsilon)) \leq \kappa_{\text{target}}$  at leading order (the ‘‘if’’ direction).  $\square$

### B.13 Appendix - Proof of Theorem 1 (Holdout prediction regimes)

**Scope.** Theorem 1 assumes a small  $\kappa_{\text{target}}$  so that  $\kappa(J^T J) \leq \kappa_{\text{target}}$  matches numerically well-conditioned NLS and faithful Gauss-Newton linearization. We treat Regime A via the  $K = 1$  collinear (CO) ray  $D_i = k_\ell N_i$  ( $V_K = 0$ , so (5) fails) versus dense non-collinear (NC)  $(N, D)$  coverage (all eigenvalues of  $J_T^T J_T$  are  $\Theta(1)$ ). We derive the RMSE ordering on a general holdout  $\mathcal{H}$  containing at least one off-manifold point, then establish Regime B ( $\kappa(J^T J) \leq \kappa_{\text{target}}$ , equivalently  $V_K \geq \tau_K$ ; Proposition 2). The Regime B bound extends to any  $K \geq 2$  collinear rays with sufficient TPP diversity (Appendix B.15).

**Setup and linearization.** Both designs fit the same scaling law  $\hat{L}(N, D; \theta)$  by nonlinear least squares (Sec. 3.1). Well-specified training losses satisfy  $L_i = \hat{L}(N_i, D_i; \theta^*) + \eta_i$  with  $\mathbb{E}[\eta_i] = 0$  and  $\text{Var}(\eta_i) = \sigma^2$ , i.i.d. across  $i$  (Propositions 1 and 2). Under Gauss-Newton linearization, the parameter estimation error from training set  $\mathcal{D}_T$  satisfies

$$\delta\theta = (J_T^T J_T)^{-1} J_T^T \boldsymbol{\eta} + O(\|\boldsymbol{\eta}\|^2), \quad (72)$$

where  $J_T$  is the training Jacobian and  $\boldsymbol{\eta} \sim \mathcal{N}(\mathbf{0}, \sigma^2 I)$ . The prediction error at test point  $(N', D')$  is, to first order:

$$\hat{L}(N', D'; \hat{\theta}) - L^*(N', D') \approx \mathbf{j}_{(N', D')}^T \delta\theta, \quad (73)$$

For any test set  $\mathcal{S} = \{(N'_i, D'_i)\}_{i=1}^{|\mathcal{S}|}$ , the leading-order unconditional expected squared prediction error is (Björck, 1996, §2.8.3, eq. (2.8.7), p. 118):

$$\mathbb{E}[(\hat{L}(N', D'; \hat{\theta}) - L^*(N', D'))^2] = \sigma^2 \mathbf{j}^T (J_T^T J_T)^{-1} \mathbf{j} + O(\sigma^4), \quad (74)$$

$$\mathbb{E}[\text{MSE}_{\mathcal{S}}] = \frac{\sigma^2}{|\mathcal{S}|} \sum_{i=1}^{|\mathcal{S}|} \mathbf{j}_i^T (J_T^T J_T)^{-1} \mathbf{j}_i. \quad (75)$$

where  $L^*(N', D') = \mathbb{E}[L | N', D']$  under the same homoscedastic model.

**Spectral decomposition of the CO Gram matrix.** By Proposition 1 and the perturbative analysis (Appendix B.6), the eigenvalues of  $J_T^T J_T$  under the collinear design are:

$$\lambda_1^{\text{CO}} = c^2 \Phi_2 \varepsilon^2 \sigma_w^2 (\log N) (1 + c^2)^{-1} + O(\varepsilon^3), \quad (76)$$

$$\lambda_j^{\text{CO}} = \Theta(1), \quad j = 2, \dots, p. \quad (77)$$

where  $c = k^{-\beta}$ . The  $\Phi_2$  (rather than  $\Phi_2^2$ ) factor follows from  $\lambda_- = \det(G_{A,B}) / \text{tr}(G_{A,B})$  with  $\det(G_{A,B}) = c^2 \Phi_2^2 \varepsilon^2 \sigma_w^2 (\log N)$  from Eq. (40) and  $\text{tr}(G_{A,B}) = \Phi_2(1 + c^2) + O(\varepsilon)$ , so that the single-design point parameter

variance  $\sigma^2/\lambda_1 = \Theta(\sigma^2/n)$  obeys the standard OLS rate (Lemma 1). The sloppy eigenvector at  $\varepsilon = 0$  is  $\mathbf{v}_1^{(0)} = (1 + k^{2\beta})^{-1/2} [1, -k^\beta, 0, \dots, 0]^T$  in the parameter basis. The predictive variance decomposes as:

$$\mathbf{j}^T (J_T^T J_T)^{-1} \mathbf{j} = \frac{(\mathbf{j}^T \mathbf{v}_1)^2}{\lambda_1} + \underbrace{\sum_{j=2}^p \frac{(\mathbf{j}^T \mathbf{v}_j)^2}{\lambda_j}}_{=: S_{\text{stiff}}(\mathbf{j}) = O(1)}. \quad (78)$$

**Sloppy projection and leverage.** For the Chinchilla law at test point  $(N', D')$  with  $k' = D'/N'$ , the projection onto the sloppy eigenvector is (Appendix B.5):

$$\mathbf{j}^T \mathbf{v}_1 \approx \frac{N'^{-\alpha}}{\sqrt{1 + k^{2\beta}}} [1 - (k/k')^\beta N'^\varepsilon]. \quad (79)$$

**Definition 8** (Sloppy leverage). For test set  $\mathcal{S} = \{(N'_i, D'_i)\}_{i=1}^{|\mathcal{S}|}$  evaluated against a model trained at TPP  $k$ , with  $\beta_{\text{eff}}$  as in Proposition 2:

$$\Lambda(\mathcal{S}) := \frac{1}{|\mathcal{S}| \Phi_2} \sum_{i=1}^{|\mathcal{S}|} N_i'^{-2\alpha} [1 - (k/k'_i)^{\beta_{\text{eff}}}]^2, \quad (80)$$

where  $k'_i = D'_i/N'_i$ .

Substituting (79) into (78) and summing over  $\mathcal{S}$ :

$$\mathbb{E}[\text{MSE}_{\mathcal{S}}^{\text{CO}}] = \sigma^2 \varepsilon^{-2} \Lambda(\mathcal{S}) G + \sigma^2 \bar{S}_{\text{stiff}}, \quad (81)$$

where  $G = \sigma_w^2 (\log N)^{-1} > 0$  depends only on the training design, and  $\bar{S}_{\text{stiff}} = |\mathcal{S}|^{-1} \sum_i S_{\text{stiff}}(\mathbf{j}_i) = O(1)$ . Indeed, with  $(1 + c^2)/(1 + k^{2\beta}) = c^2$  (since  $c^2 k^{2\beta} = 1$ ), the per-point sloppy contribution  $(\mathbf{j}^T \mathbf{v}_1)^2/\lambda_1 = N_i'^{-2\alpha} \Delta(k'_i, N'_i)^2 / [(1 + k^{2\beta}) \lambda_1]$  simplifies via Eq. (76) to  $N_i'^{-2\alpha} \Delta_i^2 / [\Phi_2 \varepsilon^2 \sigma_w^2 (\log N)]$ , and averaging over  $\mathcal{S}$  absorbs the  $1/\Phi_2$  into Definition 8 of  $\Lambda(\mathcal{S})$ , leaving  $G = \sigma_w^2 (\log N)^{-1}$ . With  $\Lambda(\mathcal{S}) = \Theta(1/\Phi_2) = \Theta(1/n)$ , the prefactor  $\sigma^2 \varepsilon^{-2} \Lambda(\mathcal{S}) G$  recovers the standard  $\Theta(\sigma^2/n)$  OLS rate inflated by the sloppy factor  $\varepsilon^{-2}$ .

**NC Gram matrix: all eigenvalues**  $\Theta(1)$ . Under a non-collinear design with dense two-dimensional coverage, the training set contains observations at multiple distinct TPP ratios satisfying  $V_K \geq \tau_K$ . The Jacobian columns for the scale coefficients are:  $(\mathbf{j}_A)_i = N_i^{-\alpha}$  and  $(\mathbf{j}_B)_i = D_i^{-\beta}$ . Under the collinear constraint  $D_i = k N_i$ , these satisfy the near-proportionality  $\mathbf{j}_B = k^{-\beta} \mathbf{j}_A + O(\varepsilon)$ . Under the NC design, observations sample diverse  $k'_i = D_i/N_i$ , so

$$\|\mathbf{j}_B - c \mathbf{j}_A\|^2 = \sum_i (D_i^{-\beta} - c N_i^{-\alpha})^2 \quad (82)$$

is  $\Theta(1)$  for any scalar  $c$ , since the ratio  $D_i^{-\beta}/N_i^{-\alpha}$  varies across training points. The near-proportionality condition in Proposition 1 fails, so Proposition 1 does not apply:  $\lambda_{\min}(J_T^T J_T) = \Theta(1)$ . The condition-number factor  $(1 - R^{-\beta})^{-2}$  replaces  $\varepsilon^{-2}$ ; for  $R \geq 5$  this is  $O(1)$ .

The predictive variance at any test point is therefore:

$$\mathbf{j}^T (J_T^T J_T)^{-1} \mathbf{j} = \sum_{j=1}^p \frac{(\mathbf{j}^T \mathbf{v}_j^{\text{NC}})^2}{\lambda_j^{\text{NC}}} = \frac{O(1)}{\Theta(1)} = O(1), \quad (83)$$

regardless of test geometry. Hence:

$$\mathbb{E}[\text{MSE}_{\mathcal{S}}^{\text{NC}}] = O(\sigma^2) \quad (84)$$

for any test set  $\mathcal{S}$ .

**General holdout RMSE ordering.** Let  $\mathcal{H}$  be a holdout set containing at least one point with  $k'_i \neq k$  (off-manifold). We first establish the strict ordering for  $\mathbb{E}[\text{MSE}_{\mathcal{H}}^{\text{X}}]$  defined in (75) (under holdout noise with the same variance  $\sigma^2$  as in the main text). Theorem 1 is stated for  $\mathbb{E}[\text{RMSE}_{\mathcal{H}}^{\text{X}}]$ ; under the Gauss–Newton linearization each summand  $(\hat{L}_i - L_i)^2$  in  $\text{MSE}_{\mathcal{H}}$  is a quadratic form in  $\boldsymbol{\eta} \sim \mathcal{N}(\mathbf{0}, \sigma^2 I)$  centered at  $\mathbf{0}$ , so  $\mathbb{E}[\text{RMSE}_{\mathcal{H}}^{\text{X}}] = \sqrt{\mathbb{E}[\text{MSE}_{\mathcal{H}}^{\text{X}}]} (1 + o(1))$  to leading order in  $\sigma$  and strict inequality on  $\mathbb{E}[\text{MSE}_{\mathcal{H}}^{\text{X}}]$  for each design  $\text{X} \in \{\text{CO}, \text{NC}\}$  therefore yields the same strict inequality on  $\mathbb{E}[\text{RMSE}_{\mathcal{H}}^{\text{X}}]$ . By (81), the CO expected MSE decomposes into a sloppy term and a stiff term:

$$\mathbb{E}[\text{MSE}_{\mathcal{H}}^{\text{CO}}] = \sigma^2 \varepsilon^{-2} \Lambda(\mathcal{H}) G + \sigma^2 \bar{S}_{\text{stiff}}. \quad (85)$$

Since at least one holdout point has  $k'_i \neq k$ ,  $[1 - (k/k'_i)^{\beta_{\text{eff}}}]^2 > 0$  for that point, so  $\Lambda(\mathcal{H}) > 0$  by Definition 8. The sloppy term therefore contributes a strictly positive  $\Theta(\sigma^2 \varepsilon^{-2})$  term, giving  $\mathbb{E}[\text{MSE}_{\mathcal{H}}^{\text{CO}}] \geq \Theta(\sigma^2 \varepsilon^{-2})$ .

Since  $\mathbb{E}[\text{MSE}_{\mathcal{H}}^{\text{NC}}] = O(\sigma^2)$  by (84), and  $\varepsilon^{-2} \gg 1$ :

$$\mathbb{E}[\text{MSE}_{\mathcal{H}}^{\text{NC}}] < \mathbb{E}[\text{MSE}_{\mathcal{H}}^{\text{CO}}], \quad \text{hence} \quad \mathbb{E}[\text{RMSE}_{\mathcal{H}}^{\text{NC}}] < \mathbb{E}[\text{RMSE}_{\mathcal{H}}^{\text{CO}}]. \quad (86)$$

Writing the holdout coefficient of determination as  $R_{\mathcal{H}}^2 = 1 - \text{MSE}_{\mathcal{H}}/\text{Var}(\mathcal{H})$  with  $\text{Var}(\mathcal{H})$  fixed across designs,  $\mathbb{E}[\text{MSE}_{\mathcal{H}}^{\text{NC}}] < \mathbb{E}[\text{MSE}_{\mathcal{H}}^{\text{CO}}]$  implies  $\mathbb{E}[R_{\mathcal{H}}^2]^{\text{NC}} > \mathbb{E}[R_{\mathcal{H}}^2]^{\text{CO}}$  at leading order (ignoring  $O(\sigma^4)$  ratio-of-expectations corrections).

**Misspecification extension.** Under model misspecification with design-independent bias  $B^2 > 0$ , the strict ordering of Theorem 1 is preserved. For  $K = 1$ , Proposition 2 gives  $V_1 = 0 < \tau_1$ , so (5) never holds; in the well-specified case  $B^2 = 0$ ,  $\mathbb{E}[\text{MSE}_{\mathcal{H}}^{\text{CO}}]/\mathbb{E}[\text{MSE}_{\mathcal{H}}^{\text{NC}}] = \Theta(\varepsilon^{-2})$ , and for  $B^2 > 0$  the same rate appears in the estimation-variance pieces in (89). The total expected-MSE ratio takes the form

$$\frac{\mathbb{E}[\text{MSE}_{\mathcal{H}}^{\text{CO}}]}{\mathbb{E}[\text{MSE}_{\mathcal{H}}^{\text{NC}}]} = \frac{B^2 + \Theta(\sigma^2 \varepsilon^{-2})}{B^2 + \Theta(\sigma^2)}, \quad (87)$$

which interpolates between  $\Theta(\varepsilon^{-2})$  when  $B^2 \ll \sigma^2$  and  $1 + o(1)$  when  $B^2 \gg \sigma^2 \varepsilon^{-2}$ . For  $K \geq 2$  still in Regime A ( $V_K < \tau_K$  in (5)), the ordering is preserved but the exact rate depends on how far  $V_K$  falls short of  $\tau_K$  (equivalently, at leading order, on  $\tau_K/V_K$  in the same sense as  $\kappa(J^T J)/\kappa_{\text{target}}$ ).

*Derivation.* Suppose the true data-generating process is  $L_i = f(N_i, D_i) + \eta_i$  where  $f$  does not lie in the model family  $\{\hat{L}(\cdot; \boldsymbol{\theta})\}$ . Let  $\boldsymbol{\theta}^*$  denote the pseudo-true parameters minimizing the population risk. The total MSE at a test point decomposes as:

$$\mathbb{E}[(\hat{L} - f)^2] = \underbrace{\mathbb{E}[(\hat{L}(\cdot; \boldsymbol{\theta}^*) - f)^2]}_{=: b^2 \text{ (approximation bias)}} + \underbrace{\sigma^2 \mathbf{j}^T (J_T^T J_T)^{-1} \mathbf{j}}_{\text{estimation variance}}, \quad (88)$$

where we assume that the cross-term  $\mathbb{E}[\delta \boldsymbol{\theta}^T \mathbf{j} (\hat{L}(\cdot; \boldsymbol{\theta}^*) - f)]$  vanishes to leading order under the Gauss-Newton linearization (since  $\mathbb{E}[\delta \boldsymbol{\theta}] = 0$  when  $\boldsymbol{\theta}^*$  is a critical point of the population risk restricted to the model family).

Averaging over a test set and writing  $B^2 = |\mathcal{S}|^{-1} \sum_i b_i^2$  for the mean squared approximation bias:

$$\mathbb{E}[\text{MSE}_{\mathcal{S}}^X] = B_{\mathcal{S}}^2 + \sigma^2 V_{\mathcal{S}}^X, \quad (89)$$

where  $V_{\mathcal{S}}^X$  is the mean predictive variance from (75) for design  $X$ .

For a general holdout  $\mathcal{H}$  with  $\Lambda(\mathcal{H}) > 0$ :  $V_{\mathcal{H}}^{\text{CO}} = \Theta(\varepsilon^{-2})$  and  $V_{\mathcal{H}}^{\text{NC}} = O(1)$  by (85) and (84). Therefore the ratio agrees with (87). This ratio is strictly greater than 1 for all  $B^2 \geq 0$  (since the numerator exceeds the denominator by  $\Theta(\sigma^2 \varepsilon^{-2}) - \Theta(\sigma^2) > 0$ ), so the strict ordering  $\mathbb{E}[\text{RMSE}_{\mathcal{H}}^{\text{NC}}] < \mathbb{E}[\text{RMSE}_{\mathcal{H}}^{\text{CO}}]$  is preserved under misspecification.

**Regime B: well-conditioned** ( $\kappa(J^T J) \leq \kappa_{\text{target}}$ ). When  $V_K \geq \tau_K$  (equivalently,  $\kappa(J^T J) \leq \kappa_{\text{target}}$ ) and observations are well-balanced across at least two TPP groups, the CO design satisfies the same non-proportionality condition (82) as the NC design: the training TPPs are sufficiently diverse that  $\|\mathbf{j}_B - c \mathbf{j}_A\| = \Theta(1)$  for all  $c$ . All eigenvalues of  $J_T^T J_T$  are then  $\Theta(1)$ , and (81) reduces to  $\mathbb{E}[\text{RMSE}_{\mathcal{H}}^{\text{CO}}] = O(\sigma)$  on any holdout, matching the NC scaling. Since  $\mathbb{E}[\text{RMSE}_{\mathcal{H}}^{\text{NC}}] = O(\sigma)$  by (84), the expected-RMSE ratio is:

$$\frac{\mathbb{E}[\text{RMSE}_{\mathcal{H}}^{\text{CO}}]}{\mathbb{E}[\text{RMSE}_{\mathcal{H}}^{\text{NC}}]} = \Theta(1), \quad (90)$$

with the  $\Theta(1)$  constant depending on the stiff-mode prefactors of each design.  $\square$

## B.14 Appendix - Proof of Proposition 3 (RMSE Invariance Under IsoFLOP Reparametrisation)

By Definition 4,  $C_i = 6 N_i D_i$  for each  $i \in \{1, \dots, n_{\mathcal{H}}\}$ . Substituting into the isoFLOP evaluation:

$$\frac{C_i}{6 N_i} = \frac{6 N_i D_i}{6 N_i} = D_i. \quad (91)$$

Therefore, for every holdout index  $i$ :

$$\hat{L}(N_i, C_i/(6N_i); \boldsymbol{\theta}) = \hat{L}(N_i, D_i; \boldsymbol{\theta}). \quad (92)$$

Each summand in the RMSE is identical under both parametrisations; hence the realized RMSE on  $\mathcal{H}$  coincides and  $\mathbb{E}[\text{RMSE}_{\mathcal{H}}]$  agrees under either evaluation map.  $\square$

## B.15 Appendix - General recipe for TPP line selection

We now generalize from the two-TPP rule-of-thumb to a recipe for selecting the number  $K$ , placement  $\{k_1, \dots, k_K\}$ , and per-ratio allocation  $\{n_1, \dots, n_K\}$  of TPP lines given three inputs:

- a target condition number  $\kappa_{\text{target}}$  (e.g.,  $10^2$ ),
- the expected exponent gap  $\varepsilon$  (e.g., 0.06 for Chinchilla),
- a total observation budget  $m$  (total number of  $(N, D)$  configurations).

**Law-specific exponent substitutions.** The formula below uses two law-specific quantities: the exponent gap  $\varepsilon$  and the effective data-size exponent  $\beta_{\text{eff}}$ . Table 8 gives the correct substitution for each of the four scaling laws.

Table 8: Exponent substitutions for each scaling law.  $\beta_{\text{eff}}$  is the data-size exponent governing the collinearity factor  $(1 - R^{-\beta_{\text{eff}}})^{-2}$  in (95); it is always the exponent on the token/data-count term of the collinear Jacobian pair.

Law	Collinear pair	$\varepsilon$	$\beta_{\text{eff}}$
Chinchilla	$(A, B)$	$ \alpha - \beta $	$\beta$
Repeated-data	$(A, B)$	$ \alpha - \beta $	$\beta$
Kaplan	$(N_c, D_c)$	$ \alpha_D - \alpha_N $	$\alpha_D$
Droppo-Elibol	$(N_C, D_C)$	$ \gamma_N - \gamma_D $	$\gamma_D$

**General diversity condition ( $K \geq 2$ ).** For  $K \geq 2$  rays with ratios  $k_1 < \dots < k_K$ , the leading-order Gram sub-block of the two scale-coefficient columns (Table 8; Chinchilla  $(A, B)$ , Kaplan  $(N_c, D_c)$ , etc.) satisfies  $\text{tr}(G_{A,B}) \approx \Phi_2(K + \sum_{\ell} k_{\ell}^{-2\beta_{\text{eff}}})$  and  $\det(G_{A,B}) \approx K^2 \Phi_2^2 V_K$ , where  $\Phi_2 := \sum_i N_i^{-2\alpha}$  with  $\alpha$  the model-side exponent in the Jacobian column paired with  $\beta_{\text{eff}}$  (Table 8; Chinchilla  $\alpha$ , Kaplan  $\alpha_N$ , Droppo-Elibol  $\gamma_N$ ) and the TPP diversity is

$$V_K := \frac{1}{K} \sum_{\ell} k_{\ell}^{-2\beta_{\text{eff}}} - \left( \frac{1}{K} \sum_{\ell} k_{\ell}^{-\beta_{\text{eff}}} \right)^2. \quad (93)$$

The condition number is therefore  $\kappa_{A,B} \approx \text{tr}^2 / \det = \Phi_2^2 (K + \sum_{\ell} k_{\ell}^{-2\beta_{\text{eff}}})^2 / (K^2 \Phi_2^2 V_K)$ ; the  $\Phi_2^2$  factors cancel. The condition  $\kappa_{A,B} \leq \kappa_{\text{target}}$  is therefore equivalent to

$$V_K \geq \tau_K := \frac{(K + \sum_{\ell} k_{\ell}^{-2\beta_{\text{eff}}})^2}{K^2 \kappa_{\text{target}}}. \quad (94)$$

For  $K = 2$  with  $k_2 = Rk_1$ ,  $V_2 = k_1^{-2\beta_{\text{eff}}} (1 - R^{-\beta_{\text{eff}}})^2 / 4$ , and (94) reduces to the explicit spread condition below.

**Step 1: determine minimum  $R$  (for  $K = 2$ ).** Under a two-TPP collinear design the collinearity factor is  $(1 - R^{-\beta_{\text{eff}}})^{-2}$ . We write  $\kappa_K$  for  $\kappa(J^T J)$  on a collinear training design with  $K \geq 1$  TPP ratios (Sec. 3.1; Proposition 2). For  $K \geq 2$ , well-conditioning is equivalent to  $V_K \geq \tau_K$  (94). The closed-form spread bound below uses the single-ray baseline  $\kappa_1 := \kappa_K|_{K=1}$  (when  $V_1 = 0$ ): at leading order in small  $\varepsilon$ , with  $\{N_i\}$  and the single-ray ratio  $k_{\ell}$  fixed,  $\kappa_1 = \Theta(\varepsilon^{-2})$  up to a design-dependent factor - evaluate  $\kappa_1$  from the fitted Jacobian (indicative magnitudes in Table 2).

To achieve  $\kappa_{A,B} \leq \kappa_{\text{target}}$ , the TPP spacing must satisfy:

$$R \geq \left( 1 - \varepsilon \sqrt{\kappa_1 / \kappa_{\text{target}}} \right)^{-1/\beta_{\text{eff}}}, \quad (95)$$

which is feasible iff  $\varepsilon \sqrt{\kappa_1 / \kappa_{\text{target}}} < 1$ ; when this fails,  $\kappa_{\text{target}}$  is unachievable at  $K = 2$  on the prevailing single-ray baseline and the practitioner must either widen the model-size grid (which reduces  $\kappa_1$  via  $\sigma_w^2(\log N)$ ) or move to  $K \geq 3$  with the additional rays placed near the endpoints rather than the interior (see (94); the bound below). Substituting the leading-order baseline  $\kappa_1 \approx c \varepsilon^{-2}$  with  $c \in [10, 30]$  for typical model-size spreads, (95) simplifies to  $R \geq (1 - \sqrt{c / \kappa_{\text{target}}})^{-1/\beta_{\text{eff}}}$ , which makes manifest that the two-TPP  $R_{\text{min}}$  depends on  $(\kappa_{\text{target}}, \beta_{\text{eff}})$  at leading order and not on  $\varepsilon$  - consistent with the  $\varepsilon$ -independence of the two-TPP collinearity factor  $(1 - R^{-\beta_{\text{eff}}})^{-2}$  at leading order once  $\kappa_1 \asymp \Theta(\varepsilon^{-2})$ .

For  $K > 2$  at the same endpoint spread  $R = k_K / k_1$ ,  $V_K$  generally *decreases* when interior rays are added: an interior  $k_{\ell}^{-\beta_{\text{eff}}}$  sits between the endpoint values and pulls the sample toward its mean, reducing variance. The threshold  $\tau_K$  tightens via the  $K^2$  denominator at a comparable rate, so the two effects largely cancel and  $K = 2$  with mass concentrated at the endpoints is near-optimal for conditioning at fixed total budget;  $K \geq 3$  is recommended for residual diagnostics or outlier robustness (Step 2), not to relax the spread requirement. Verify any specific  $K$ -ray design directly via (94).

Table 9: Minimum TPP ratio  $R_{\min} = k_K/k_1$  to achieve  $\kappa_{A,B} \leq \kappa_{\text{target}}$  under a two-TPP design. Use the law-specific  $\varepsilon$  and  $\beta_{\text{eff}}$  from Table 8.

$\varepsilon$	$\kappa_{\text{target}}$	$\beta = 0.40$	$\beta = 0.35$	$\beta = 0.28$
0.10	$10^2$	2.8	3.2	4.4
0.08	$10^2$	3.4	3.9	5.5
0.06	$10^2$	4.2	4.7	7.1
0.06	$10^1$	7.2	8.5	15
0.04	$10^2$	5.8	6.8	11
0.03	$10^2$	7.0	7.8	14

**Sensitivity to exponent values and noise.** The threshold  $R_{\min}$  depends on  $\varepsilon$  and  $\beta$  but *not* on the noise level  $\sigma^2$ . The condition number  $\kappa$  is a property of the Jacobian  $J^T J$ , which is determined by the design and the functional form—not by the residual variance. Noise affects *parameter variance* ( $\text{Var}(\hat{\theta}) \propto \sigma^2 (J^T J)^{-1}$ ) but not the design threshold for a given  $\kappa_{\text{target}}$ . To achieve a target *coefficient precision* (e.g., a desired width of the confidence interval for  $A$  or  $B$ ), one must increase the number of observations  $m$  when noise is high; the required  $R$  stays the same.

Sensitivity to exponents is moderate: *smaller*  $\beta_{\text{eff}}$  increases  $R_{\min}$  ( $R^{-\beta_{\text{eff}}}$  decays more slowly, so more TPP spread is needed). The lookup table (Table 9) varies both  $\varepsilon$  and  $\beta$  because  $\kappa_1$  in (95) retains design-dependent prefactors beyond the leading  $\Theta(\varepsilon^{-2})$  rate. At fixed  $(\kappa_{\text{target}}, \beta_{\text{eff}})$ , substituting  $\kappa_1 \approx c\varepsilon^{-2}$  into (95) removes explicit  $\varepsilon$  dependence at first order (lines above), while finite spreads and  $\sigma_w^2(\log N)$  move the numerical entries. For Chinchilla-like priors ( $\varepsilon \in [0.04, 0.08]$ ,  $\beta \in [0.28, 0.40]$ ),  $R_{\min}$  ranges from  $\approx 3$  to  $\approx 11$  for  $\kappa_{\text{target}} = 10^2$ . When priors are very uncertain, use the most conservative combination (smallest  $\varepsilon$ , smallest  $\beta$ ) from the table.

**Sensitivity to prior exponent errors.** Underestimating  $\varepsilon$  (guessing a larger exponent gap than the truth) is the risky direction: the design then yields  $\kappa_{A,B}$  above the target. From Table 9, a 30% underestimate of  $\varepsilon$  (e.g., guessing 0.06 when true is 0.04) increases  $R_{\min}$  by  $\approx 45\%$  (from 4.7 to 6.8 for  $\beta_{\text{eff}} = 0.35$ ). Underestimating  $\beta_{\text{eff}}$  has a smaller effect (the  $R^{-\beta_{\text{eff}}}$  term is less sensitive). We recommend adding a 20-50% margin to  $R_{\min}$  when priors are rough, or using the most conservative table entry.

**Adaptive adjustment of  $R$ .** We recommend an adaptive scheme when the design is built sequentially: (1) use conservative priors  $(\varepsilon, \beta)$  to choose initial  $R$ ; (2) after fitting on the first batch, obtain updated  $(\hat{\alpha}, \hat{\beta})$ ; (3) recompute  $R_{\min}$  from Table 9 using the fitted exponents; (4) if  $\kappa_{A,B}$  still exceeds  $\kappa_{\text{target}}$ , add augmentation runs at a second TPP ratio  $k'$  satisfying the updated  $R_{\min}$  (or increase the spread of existing TPP lines if the design is not yet fixed). This refines the design as exponent estimates sharpen, avoiding both over-investment (overly large  $R$  when priors were pessimistic) and under-design (insufficient  $R$  when priors were optimistic).

**Simple rule.** Given rough priors  $\alpha_0, \beta_0$  and target  $\kappa_{\text{target}}$ :

1. Set  $\varepsilon = |\alpha_0 - \beta_0|$ ; if unknown, use  $\varepsilon = 0.05$  (typical for Chinchilla-like laws).
2. Look up  $R_{\min}$  in Table 9 for the column closest to  $\beta_0$ ; interpolate linearly if needed.
3. Round up:  $R \geq \lceil R_{\min} \rceil$  (e.g.,  $R_{\min} = 4.7 \Rightarrow R \geq 5$ ).

When  $\varepsilon$  or  $\beta$  falls between table rows, use the *more conservative* (larger)  $R_{\min}$ .

**Step 2: decide  $K$  (number of TPP lines).** Two TPP lines ( $K = 2$ ) are sufficient for identifiability (the degeneracy is one-dimensional). Additional lines  $K > 2$  at the same endpoint spread provide no first-order improvement in conditioning (Step 1 above), but offer two practical benefits: (a) they enable *lack-of-fit* tests (degrees of freedom for model diagnostics), and (b) they reduce sensitivity to outlier runs at any single ratio. A useful rule:

- $K = 2$ : minimum for identifiability;
- $K = 3$ : recommended when the budget permits, to enable residual diagnostics;
- $K \geq 4$ : useful for meta-analytic settings or when the functional form is uncertain.

**Step 3: place the TPP ratios.** For  $K = 2$ , place  $k_1$  and  $k_2$  as far apart as feasible (subject to  $R \geq R_{\min}$  from Step 1); endpoint placement maximizes  $V_K$  at fixed support. For  $K \geq 3$ ,  $V_K$  is maximized by collapsing the additional rays onto the endpoints (since interior values pull the sample toward its mean), so the conditioning-optimal  $K \geq 3$  placement reduces effectively to the  $K = 2$  endpoint design. When intermediate ratios are desired for diagnostic value (lack-of-fit, residual checks across TPP), a log-uniform grid over  $[k_1, k_K]$  is a natural choice:

$$k_j = k_1 R^{(j-1)/(K-1)}, \quad j = 1, \dots, K, \quad (96)$$

at the cost of a modest reduction in  $V_K$  relative to the endpoint-only design; verify the resulting  $V_K \geq \tau_K$  via (94).

**Step 4: allocate runs across ratios.** Given a total budget of  $m$  observations split into  $K$  groups of  $m_j$  observations each ( $\sum_j m_j = m$ ), the D-optimal allocation for the scale-coefficient sub-block is approximately *balanced*:  $m_j \approx m/K$ . The intuition is that the sloppy direction receives information from the *contrast* between TPP groups, and this contrast is maximized when each group has equal weight. When the groups have different model-size ranges, slight rebalancing toward the group with smaller spread is beneficial.

Within each TPP group, the model sizes should span as wide a range as possible and be approximately log-uniformly spaced:

$$N_{j,\ell} = N_{\min} (N_{\max}/N_{\min})^{(\ell-1)/(m_j-1)}, \quad \ell = 1, \dots, m_j. \quad (97)$$

**Step 5: verify conditioning.** Before committing to expensive large-scale runs, compute the *expected* Jacobian  $J$  at a plausible parameter vector  $\theta_0$  (e.g., from a published fit) and evaluate the condition number  $\kappa$  of the  $2 \times 2$  Gram block for the law’s scale-coefficient pair (Table 8; Chinchilla’s  $\kappa_{A,B}$ , Kaplan ( $N_c, D_c$ ) block, etc.) for the proposed design. If it exceeds  $\kappa_{\text{target}}$ , increase  $R$  (TPP spread) or widen the model-size grid (raising  $\sigma_w^2(\log N)$  and thereby reducing  $\kappa_1$ ) and repeat. Replicating runs at fixed  $(N, D)$  does not change  $\kappa_{A,B}$  at leading order - replication scales  $J^T J$  uniformly and leaves the condition number invariant; it improves coefficient *precision* ( $\text{Var}(\hat{\theta}) \propto \sigma^2(J^T J)^{-1}$ ) but not identifiability.

**Worked example.** Target  $\kappa_{\text{target}} = 10^2$ , Chinchilla ( $\varepsilon = 0.06, \beta = 0.35, p = 5$ ).

1.  $R_{\min} \approx 5$  (from the table above).
2.  $K = 2$  (minimum budget).
3.  $k_1 = 20$  (Chinchilla baseline),  $k_2 = 100$  ( $R = 5$ ).
4. Budget  $n = 20$  runs:  $n_1 = n_2 = 10$ .
5. Model sizes  $N \in [10^7, 10^9]$ , log-uniformly spaced within each group.
6. Expected  $\kappa_{A,B} \approx 50$ -well within the target.

With  $K = 3$  and the same budget ( $n_j \approx 7$  each), placing  $k_3 = 45$  (geometric mean) provides a lack-of-fit check at the cost of a modest conditioning loss ( $\kappa_{A,B} \approx 60$  vs. 50 at  $K = 2$ ), consistent with the interior-ray  $V_K$  reduction discussed above.

## B.16 Appendix - Interaction-term scaling laws

The four laws analyzed in the main text are *additive* in the  $N$ - and  $D$ -contributions. Adding an explicit  $N$ - $D$  interaction  $F N^{-\gamma_N} D^{-\gamma_D}$  (as in Farseer (Li et al., 2025a)) does not alleviate the degeneracy: under  $D = k_\ell N$  the interaction column becomes a third near-proportional power of  $N$ , so the  $(A, B, F)$  sub-block has *two* near-zero eigenvalues and the problem is strictly worse. We derive this formally below.

**Representative model.** Consider a Chinchilla-style law augmented with a multiplicative interaction (with  $p = 8$  parameters  $\theta = [A, B, F, E, \alpha, \beta, \gamma_N, \gamma_D]^T$  or fewer if some exponents are tied):

$$\hat{L}(N, D) = A N^{-\alpha} + B D^{-\beta} + F N^{-\gamma_N} D^{-\gamma_D} + E, \quad (98)$$

$$\mathbf{j}_{A,i} = -N_i^{-\alpha}, \quad (99)$$

$$\mathbf{j}_{B,i} = -k_\ell^{-\beta} N_i^{-\beta} = -k_\ell^{-\beta} N_i^{-\alpha} N_i^{\varepsilon_1}, \quad (100)$$

$$\mathbf{j}_{F,i} = -k_\ell^{-\gamma_D} N_i^{-(\gamma_N + \gamma_D)} = -k_\ell^{-\gamma_D} N_i^{-\alpha} N_i^{\varepsilon_2}. \quad (101)$$

The interaction coefficient  $F$  and its associated exponents  $(\gamma_N, \gamma_D)$  introduce a third “capacity  $\times$  data” channel. We use residual Jacobian columns  $J_{i\theta} = -\partial \hat{L}_i / \partial \theta$  as in (10). Substituting  $D_i = k_\ell N_i$ , the three scale-coefficient columns are the last three rows of (98), where  $\varepsilon_1 = \alpha - \beta$  and  $\varepsilon_2 = \alpha - (\gamma_N + \gamma_D)$ . All three columns share the base function  $N_i^{-\alpha}$ , differing only by perturbations  $N_i^{\varepsilon_1}$  and  $N_i^{\varepsilon_2}$ .

**Near-proportionality of the Jacobian columns.** Writing  $N_i^{\varepsilon_j} = 1 + \varepsilon_j \log N_i + O(\varepsilon_j^2)$  for small  $|\varepsilon_j|$ , we obtain  $\mathbf{j}_B = c_1 \mathbf{j}_A + \delta_1$  and  $\mathbf{j}_F = c_2 \mathbf{j}_A + \delta_2$ , where  $c_1 = k_\ell^{-\beta}$ ,  $c_2 = k_\ell^{-\gamma_D}$ , and

$$\delta_{1,i} = c_1 N_i^{-\alpha} (N_i^{\varepsilon_1} - 1) = O(\varepsilon_1), \quad \delta_{2,i} = c_2 N_i^{-\alpha} (N_i^{\varepsilon_2} - 1) = O(\varepsilon_2). \quad (102)$$

Thus  $\|\delta_1\| = O(\varepsilon_1)$  and  $\|\delta_2\| = O(\varepsilon_2)$  - the same near-proportionality structure as the additive case (Section B.5), but now with *three* columns all proportional to  $\mathbf{j}_A$  up to  $O(\max\{|\varepsilon_1|, |\varepsilon_2|\})$  perturbations. Under  $D = k_\ell N$ , the interaction column  $\mathbf{j}_F$  is therefore nearly proportional to both  $\mathbf{j}_A$  and  $\mathbf{j}_B$ , generalizing the additive degeneracy to coupled laws.

**3 × 3 sub-block analysis.** The Gram matrix of the  $(A, B, F)$  sub-block has entries:

$$G_{jk} = \sum_{i=1}^n \mathbf{j}_{j,i} \mathbf{j}_{k,i}, \quad j, k \in \{A, B, F\}. \quad (103)$$

Write  $\mathbf{j}_B = c_1 \mathbf{j}_A \circ \mathbf{h}_1$  and  $\mathbf{j}_F = c_2 \mathbf{j}_A \circ \mathbf{h}_2$  where  $\circ$  denotes element-wise product,  $h_{1,i} = N_i^{\varepsilon_1}$ ,  $h_{2,i} = N_i^{\varepsilon_2}$ ,  $c_1 = k_\ell^{-\beta}$ ,  $c_2 = k_\ell^{-\gamma D}$ . When  $\varepsilon_1, \varepsilon_2 \rightarrow 0$ ,  $\mathbf{h}_1, \mathbf{h}_2 \rightarrow \mathbf{1}$  and the three columns become proportional, giving  $\text{rank}(G) = 1$ . More precisely:

$$\det(G_{A,B,F}) = O(\varepsilon_1^2 \varepsilon_2^2) + O(\varepsilon_1^2 (\varepsilon_1 - \varepsilon_2)^2), \quad (104)$$

$$\varepsilon_{\text{gap}} := \min(|\alpha - \beta|, |\alpha - (\gamma_N + \gamma_D)|, |(\gamma_N + \gamma_D) - \beta|). \quad (105)$$

The  $3 \times 3$  Gram determinant is controlled by the *pairwise* and *triple* volume elements among the three nearly-proportional vectors. The two smallest eigenvalues of  $G_{A,B,F}$  are  $O(\varepsilon_{\text{gap}}^2)$  at leading order.

**Condition number.** The  $3 \times 3$  block inherits the Gram-determinant scaling (104); combining with eigenvalue trace-determinant relations for positive semidefinite matrices (as in the proof of Proposition 1) shows that, under the usual block-dominance assumption for the scale coefficients,  $\kappa(J^T J)$  grows at least as  $\Omega(\varepsilon_{\text{gap}}^{-2})$  for  $\varepsilon_{\text{gap}}$  from (105), and can be *larger* than the pure  $(A, B)$  Chinchilla rate when multiple exponent gaps are small. Thus the problem is *worse* than the additive case: the interaction term introduces a *second* sloppy direction (the null space of the  $3 \times 3$  sub-block is two-dimensional when all three exponent gaps vanish), requiring two additional constraints (e.g., two distinct TPP ratios and a third quantity) for full identifiability.

**Implications.** Adding interaction terms does not cure collinearity - it exacerbates it. Under  $D = k_\ell N$ , the interaction coefficient  $F$  is confounded with both  $A$  and  $B$ : the data cannot distinguish whether a given loss level comes from model capacity, data volume, or their interaction. The design-of-experiments prescription is unchanged: diverse TPP ratios are essential, and with an interaction term even more diversity may be needed ( $K \geq 3$  TPP ratios to resolve the two-dimensional degeneracy).

## C Appendix - experimental setup

### C.1 Appendix - Transformer architecture

All models use the HuggingFace LlamaForCausalLM implementation with RoPE positional embeddings, RMSNorm, and SwiGLU activations.

### C.2 Appendix - Architecture configurations

Table 10: Model architecture configurations. All models use the LLaMA architecture with rotary position embeddings (RoPE), SwiGLU activation, RMSNorm, no bias terms, a context length of 256, and vocabulary size of 100,277 (cl100k\_base).

Params	$n_{\text{layers}}$	$d_{\text{model}}$	$d_{\text{ff}}$	$n_{\text{heads}}$	$d_{\text{head}}$
5,035,656	24	24	96	12	2
10,070,160	12	48	192	1	48
14,411,456	24	64	256	32	2
19,400,928	1	96	384	1	96
22,796,832	24	96	384	24	4
28,819,840	12	128	512	4	32
32,498,720	1	160	640	16	10
35,368,160	8	160	640	4	40
40,277,184	3	192	768	12	16
47,949,888	16	192	768	1	192
55,538,432	4	256	1024	32	8
63,931,136	12	256	1024	32	8
68,127,488	16	256	1024	32	8
76,520,192	24	256	1024	1	256

Model sizes were specified as target parameter counts and mapped to concrete architectures via nearest-neighbor matching on a grid of transformer hyperparameters (layer count, hidden dimension, head count), with

$d_{\text{ff}} = 4 \times d_{\text{model}}$ . Because the grid is discrete, realized parameter counts differ slightly from targets; the 14 configurations span  $N \in [5.04, 76.5] \text{M}$  ( $N_{\text{max}}/N_{\text{min}} \approx 15.2$ ). Table 10 reports the exact parameter counts as verified from trained checkpoints. Following Hoffmann et al. (2022),  $N$  includes all trainable parameters (embedding and unembedding layers included). An earlier version of the architecture-search procedure produced configurations with odd per-head dimension  $d_{\text{head}} = d_{\text{model}}/n_{\text{heads}}$ , which crashed at training time because rotary positional encoding’s `rotate_half` operation requires  $d_{\text{head}}$  to be even. The search was patched to filter to head counts producing even  $d_{\text{head}}$ , which is why  $n_{\text{heads}}$  varies across architectures in Table 10.

**Architecture heterogeneity, embeddings, and the role of  $C \approx 6ND$ .** The grid spans  $n_{\text{layers}} \in \{1, 3, 4, 8, 12, 16, 24\}$ , deliberately wider than a constant-shape sweep so that the fits are not informed only by smooth depth-vs-width co-variation; the four scaling laws under study are functions of  $(N, D)$  only and are agnostic to the internal architectural decomposition. Two configurations are shallow (19.4M and 32.5M, both single-layer); for these the `cl100k_base` vocabulary ( $V = 100,277$ ) makes the input/output embedding contribution  $2Vd_{\text{model}}$  dominate  $N$  (e.g.  $2 \cdot 100,277 \cdot 96 \approx 19.3\text{M}$  of the 19.4M total), so the Kaplan FLOPs approximation  $C \approx 6ND$  - calibrated for deep, embedding-light transformers - is loose. Two consequences, neither of which compromises the formal results:

- *Conditioning and CI inflation* (Proposition 1, Corollary 1, Theorem 1) are statements about the Jacobian geometry of the regression problem  $\hat{L}(N, D; \theta)$  as a function of the empirical pairs  $(N_i, D_i, L_i)$ . They do not assume that the underlying loss is a smooth power law, that depth is held fixed, or that any specific FLOPs identity holds; the Hoffmann/Chinchilla convention of taking  $N$  as *all* trainable parameters is preserved end-to-end. Architectural heterogeneity and any resulting departures of the empirical  $L_i$  from a clean power-law surface are absorbed by the misspecification extension (Eq. (87)), which preserves the CO/NC ordering under a shared design-independent approximation-bias floor.
- *IsoFLOP visualization* uses  $C_i := 6N_iD_i$  (Definition 4) purely as a relabelling: Proposition 3 and its proof in Appendix B.14 show that  $\hat{L}(N_i, C_i/(6N_i); \theta) = \hat{L}(N_i, D_i; \theta)$  as an algebraic identity - any constant or model-dependent rescaling of the FLOPs/token coefficient leaves the holdout RMSE unchanged. Embedding dominance therefore shifts where shallow points sit on the  $C$ -axis but does not affect any reported metric.

The shallow rows survive in the grid because dropping them would collapse the  $(N, D)$  design at the small- $N$  end and weaken the TPP-coverage contrast that the formal analysis targets; treating them as standard  $(N, D, L)$  observations under the Hoffmann convention is consistent with how prior fits handle the same regime. Figure 2 shows the empirical  $n_{\text{layers}}$  distribution across all 1,933 trained models: the bulk of the runs sit at  $n_{\text{layers}} \geq 4$  where  $C \approx 6ND$  is well-calibrated, and the embedding-dominated single-layer configurations contribute only a small minority of points, so any  $C \approx 6ND$  mismatch is concentrated in a sparse tail rather than driving the aggregate fit.

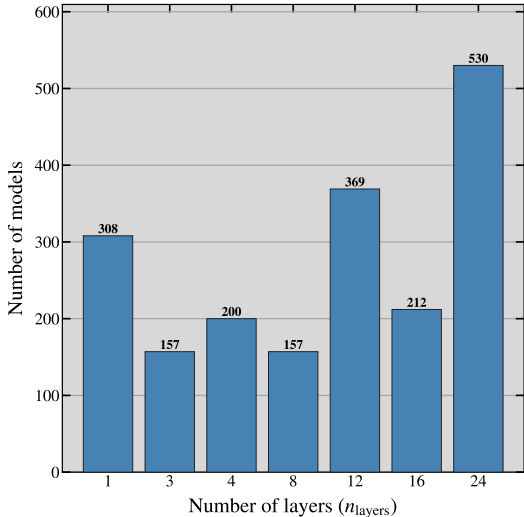


Figure 2:  $n_{\text{layers}}$  distribution, across 1933 trained models.

### C.3 Appendix - Hyperparameter selection

Table 11 summarizes the training hyperparameters shared across all experimental runs.

Table 11: Training hyper-parameters shared across all runs.

Hyperparameter	Value
Optimizer	AdamW ( $\beta_1=0.9, \beta_2=0.999, \epsilon=10^{-8}$ )
Gradient clipping	1.0
Weight decay	0.1
Batch size	96 per GPU
Max sequence length	256
Epochs	3
Warmup	Linear, first 3% of steps (start factor 0.01)
LR schedule	Cosine annealing to 10% of peak LR
Seed	42

### C.3.1 Learning rate

We selected  $\eta = 3 \times 10^{-4}$  for Wikipedia and RedPajama,  $\eta = 1 \times 10^{-3}$  for peS2o, Cosmopedia, and C4.

### C.4 Appendix - Loss extraction

We record the converged training loss as the mean of the final 100 batch losses per epoch, to account for batch-to-batch noise.

### C.5 Appendix - Dataset selection

We evaluate scaling law fits across five datasets spanning distinct data domains: Cosmopedia (Ben Allal et al., 2024) (synthetic educational text), Wikipedia (Foundation) (encyclopedic articles), peS2o (Soldaini and Lo, 2023) (academic papers and abstracts), RedPajama-V2 (Weber et al., 2024) (filtered web text), and C4 (Raffel et al., 2020) (web text).

#### C.5.1 Train/evaluation splits

Natural language corpora often exhibit systematic ordering biases; Wikipedia sorts by page creation date, peS2o groups abstracts before full papers, and RedPajama clusters by WARC file origin. A naive sequential (left/right) split therefore produces train and evaluation sets with different underlying distributions. *All five text corpora used in this paper (C4, Wikipedia, peS2o, RedPajama, and Cosmopedia) are split by the same procedure: we randomly permute all document indices with a fixed seed and take contiguous slices, guaranteeing zero overlap while eliminating ordering artifacts. No corpus uses a sequential / left-right / chronological split, and no corpus is treated as a special case. Table 12 confirms this approach.*

Table 12: Symmetric KL divergence and cosine similarity between train and validation  $n$ -gram distributions ( $n = 1, \dots, 3$ ). Both train and validation distributions have 600M tokens, drawn from the random-permutation split described above; the same split procedure is applied to every corpus, including Cosmopedia.

Dataset	Metric	$n = 1$	$n = 2$	$n = 3$
Wikipedia	Sym. KL	0.0006	0.4446	3.3681
	Cosine	0.999998	0.999952	0.999543
RedPajama	Sym. KL	0.0016	0.5904	4.1139
	Cosine	0.999965	0.997919	0.947550
Cosmopedia	Sym. KL	0.0002	0.2852	2.1356
	Cosine	1.000000	0.999994	0.999933
peS2o	Sym. KL	0.0007	0.4211	3.2188
	Cosine	0.999998	0.999977	0.999717
C4	Sym. KL	0.0013	0.8733	5.2464
	Cosine	0.999998	0.999953	0.998718

### C.5.2 Pre-processing

Our training data was pre-tokenized with `cl100k_base` (tiktoken), truncated or padded to 256 tokens if an article did not reach 256.

## C.6 Appendix - Training conditions and hardware

All pre-training used the NCSA DeltaAI GH200 partition (Access Allocation CIS230318) with four GH200 GPUs per node via PyTorch Distributed Data Parallel, totaling approximately 3,624 GPU-hours (151 GPU-days) across five primary corpora, BF16, and large-TPP settings. Scaling-law fitting, seed-variance analysis (Tables 3-4, Appendix E-F), and visualization used a dual-socket AMD EPYC 9755 node (256 cores, 512 threads, 1.5 TB RAM) with 230 parallel workers (~5 wall-clock hours). The exhaustive subset enumeration (Table 6, 22 independent seeds) used 480 workers on the same hardware (~24 wall-clock hours, ~65 min per seed). Total storage footprint is approximately 2.2 TB (1.5 TB model checkpoints and training metrics, 0.5 TB pre-tokenized datasets, 0.2 TB analysis artifacts and redundancy). Full-project compute was higher than the final reported runs because we also executed pilot and failed sweeps; those additional costs will be disclosed in the NeurIPS compute-reporting form. All training uses `worldsize=4` (PyTorch DDP); the LR schedule length depends on `worldsize` through the `DistributedSampler` batch count, so reproducing identical checkpoints requires exactly 4 GPUs. Training is bitwise reproducible within a fixed CUDA driver version (verified by repeated runs on NVIDIA driver 590.48). Slight cross-driver numerical drift of  $O(10^{-3})$  in the training loss over three epochs has been observed following a cluster driver update; we flag it as a minor reproducibility issue. The 30-seed CIs in Tables 3 and 4 are computed over L-BFGS-B optimizer restarts on *fixed* training data (Appendix C.8), so they quantify curve-fitting variance rather than absorbing a systematic shift in the data-generating process. A common driver-induced shift in the training losses, however, does not compromise our conclusions for two reasons. (i) All reported metrics are *paired* CO-vs-NC comparisons on the *same* pre-trained loss table per seed and dataset (Tables 3, 4; Appendix C.8); a uniform shift  $\Delta L$  in the underlying losses adds the same offset to the fitted irreducible-loss/intercept terms in both CO and NC fits, so the head-to-head difference  $\text{RMSE}_{\mathcal{H}}^{\text{NC}} - \text{RMSE}_{\mathcal{H}}^{\text{CO}}$  and the full-precision and BF16 win-rate summaries (97.3% and 98.7%, respectively) are first-order invariant to  $\Delta L$ . (ii) The drift magnitude  $O(10^{-3})$  is two-to-three orders of magnitude smaller than both the seed-to-seed L-BFGS-B spread on CO ( $53 \times$  CI inflation under our  $\epsilon$ ; Corollary 1) and the absolute NC-vs-CO RMSE gaps reported in Tables 3 and 5, so even if the shift propagated unevenly between designs the residual contamination of the win-rate would be well below the gap being estimated.

## C.7 Appendix - L-BFGS-B optimizer bounds

All scaling laws are fit via multi-start L-BFGS-B with a differential-evolution global fallback. Parameter bounds are identical across all designs, datasets, and random seeds. For the Kaplan law,  $N_c, D_c \in [10^3, 10^{14}]$  and  $\alpha_N, \alpha_D \in [0.01, 2.0]$ . For the Chinchilla law,  $E \in [0, 10]$ ,  $A, B \in [10^{-2}, 10^{10}]$ , and  $\alpha, \beta \in [0.01, 2.0]$ . For the Droppo-Elibol law,  $L_\infty \in [10^{-6}, 0.99 \cdot \min(L)]$ ,  $N_C, D_C \in [10^3, 10^{14}]$ , and  $\alpha_N, \alpha_D, \alpha \in [0.01, 2.0]$ . For the Repeated-Data law  $A, B \in [10^{-2}, 10^{12}]$ ,  $\alpha, \beta \in [0.01, 2.0]$ ,  $E \in [0, 10]$ , and the half-life parameters  $R_D^*, R_N^* \in [0.1, 50.0]$ ; the Repeated-data law is fit by Huber loss with  $\delta = 0.5$ , while the other three laws use squared-error loss.

**Active lower bound on  $R_N^*$ .** In the Repeated-Data fit (Tables 43 and 48), the parameter-side half-life  $R_N^*$  frequently terminates at exactly 0.1, the lower bound declared above. This is expected and not a fitting failure: our experimental grid fixes  $N$  per run and only  $D$  is repeated (epochs 1, 2, 3), so the data carries strong signal about the data-side half-life  $R_D^*$  but is essentially uninformative about  $R_N^*$ , whose objective contribution becomes flat at small values. The L-BFGS-B optimizer therefore drifts to the lower bound; the bound itself is the documented value 0.1 and applies uniformly across all designs, datasets, and seeds. The reported  $R^2$  on holdout is unaffected because the loss surface is flat in  $R_N^*$  at that point. Reporting the boundary-hitting fits as-is (rather than censoring or post-processing them) is what allows the diagnostic to be visible in the tables.

## C.8 Appendix - Confidence intervals and variability bands

Throughout the paper we characterize optimizer-induced variability by re-fitting each scaling law  $N_{\text{seeds}} = 30$  times per (dataset, law, epoch mode, design, coverage step) configuration, varying only the optimizer seed that controls the L-BFGS-B random-restart sequence and the differential-evolution polish. The training data and holdout splits are held fixed across seeds, so the resulting  $R^2$  distribution isolates optimizer-induced variance from data-induced variance.

**The Importance of seed-to-seed variance.** This choice is the empirical counterpart of Corollary 1. The corollary predicts that under collinearity parameter CIs inflate as  $\Theta(\epsilon^{-1})$ ; that parameter-space uncertainty propagates to prediction uncertainty on holdout, manifesting as wide seed-to-seed spread in holdout  $R^2$ . A single CO seed can fit a particular holdout well by luck; the Gauss-Newton step along the sloppy ( $A, B$ ) direction happens to land near the truth on that draw. The formal analysis predicts, and what the seed-to-seed CI measures,

is that this spread is systematically larger for CO than for NC. The CI gap between designs in Tables 3, 5 is the predicted parameter-CI inflation made empirical, observed one layer downstream in prediction error rather than in  $A$  directly.

**Coverage-fraction plots.** The central marker is the *median*  $R^2$  across the 30 seeds; error bars span the 5th-95th percentile of that distribution. These are empirical percentile bands of the per-seed  $R^2$  values, not Gaussian confidence intervals on the mean.

**Summary tables (e.g. Tables 3, 5).** Reported  $R^2$  *Mean* is the grand mean of the per-combo seed means; reported  $R^2$  *Median* is the median of those combo means; reported  $R^2$  *Std* is their across-combo standard deviation. The 95% CI is an optimizer-noise interval centered on  $R^2$  *Mean* with half-width

$$\Delta = 1.96 \cdot \frac{\overline{\sigma_{\text{seed}}}}{\sqrt{N_{\text{seeds}}}},$$

where  $\overline{\sigma_{\text{seed}}}$  is the average within-combo seed-to-seed standard deviation. RMSE columns follow the same convention. The CI quantifies how tightly seed-to-seed optimizer noise pins down a typical combo’s mean and is independent of the Median column.

**Subset analysis (Table 6).** For the budget-matched subset enumeration we use 22 optimizer seeds rather than 30 due to compute restrictions; reported NC win rates are accompanied by Wilson 95% binomial CIs over enumerated subsets.

## D Appendix - detailed results

### D.1 Appendix - Collinear and non-collinear experimental grid definitions

Figures 3 and 4 visualize the collinear and non-collinear experimental setup, as a grid. Red cells are holdout models; blue cells are training models. Each dataset comprises 324 runs (120 collinear training + 42 collinear holdout + 120 non-collinear training + 42 non-collinear holdout). Four of the five corpora completed all runs; C4 has 321 (3 collinear holdout jobs crashed).

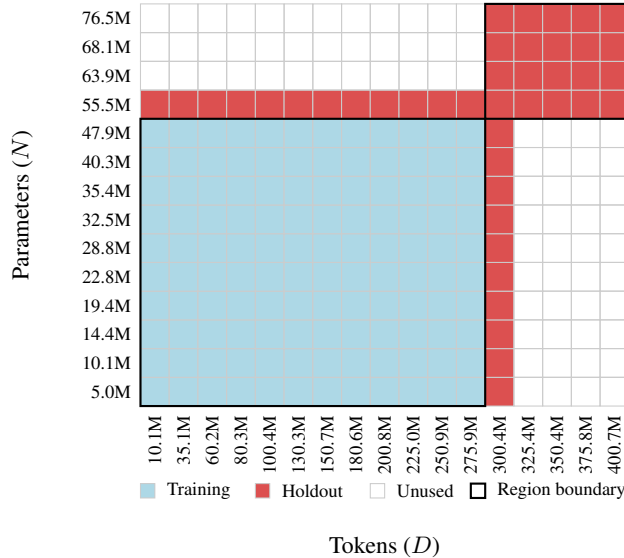


Figure 3: Token-parameter point (TPP) grid used in our experimental design. Each cell represents a unique  $(N, D)$  training configuration. The holdout set (red) forms an L-shaped boundary along the largest parameter count in the training region ( $N = 55.5\text{M}$ ) and at  $D = 300.4\text{M}$  tokens, plus the  $4 \times 5$  extrapolation block at the largest token and parameter counts. White cells denote configurations not included in either set. The bordered lower-left region contains the 120 in-distribution training configurations.

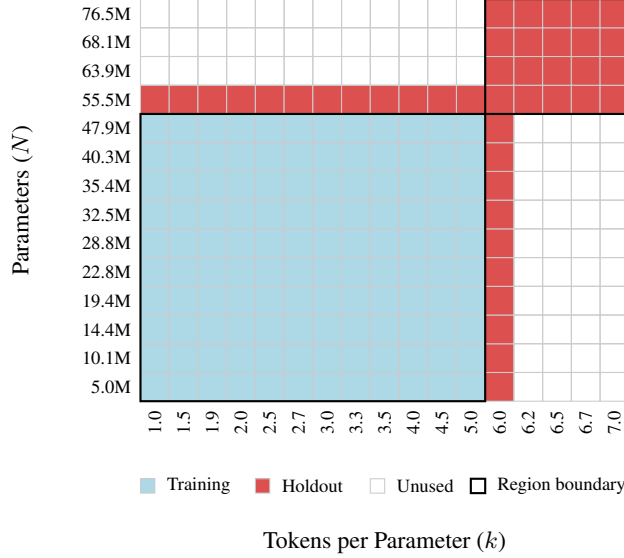


Figure 4: Token-parameter point (TPP) grid for the collinear (CO) experimental design. Each cell represents a unique  $(N, k)$  configuration where the token count is  $D = k \cdot N$ . The holdout set (red) forms an L-shaped boundary at the largest in-distribution parameter count ( $N = 55.5\text{M}$ ) and at  $k = 6$ , plus the  $4 \times 5$  extrapolation block. White cells denote configurations not included in either set. The bordered lower-left region contains the 120 in-distribution training configurations.

## D.2 Appendix - Table 3 holdout breakdown

The full metrics breakdown shows collinear and non-collinear holdout results for the main experiments below, and winrates broken down.

Table 13:  $R^2$  and RMSE summary across training designs with different seed-to-seed optimizer setup. 95% CI: confidence interval on the mean. Best per split in **bold**.

Split	Design	$R^2$				RMSE			
		Mean	95% CI	Median	Std	Mean	95% CI	Median	Std
Train ( $\mathcal{D}$ )	CO	<b>0.9848</b>	<b>[0.985, 0.985]</b>	<b>0.9850</b>	<b>0.0047</b>	<b>0.1737</b>	<b>[0.173, 0.174]</b>	<b>0.1616</b>	<b>0.0430</b>
	NC	0.9526	[0.952, 0.953]	0.9542	0.0172	0.2023	[0.202, 0.203]	0.1869	0.0443
Holdout ( $\mathcal{H}$ )	CO	0.8370	[0.832, 0.842]	0.8811	0.1129	0.2373	[0.233, 0.241]	0.2163	0.1229
	NC	<b>0.9319</b>	<b>[0.930, 0.934]</b>	<b>0.9392</b>	<b>0.0269</b>	<b>0.1561</b>	<b>[0.154, 0.158]</b>	<b>0.1242</b>	<b>0.0599</b>
Holdout ( $\mathcal{H}_{\text{col}}$ )	CO	0.9113	[0.907, 0.915]	0.9336	0.0514	0.1885	[0.185, 0.192]	0.1645	0.0903
	NC	<b>0.9437</b>	<b>[0.942, 0.945]</b>	<b>0.9439</b>	<b>0.0182</b>	<b>0.1560</b>	<b>[0.154, 0.158]</b>	<b>0.1182</b>	<b>0.0631</b>
Holdout ( $\mathcal{H}_{\text{nc}}$ )	CO	0.6984	[0.688, 0.708]	0.7490	0.2730	0.2757	[0.271, 0.281]	0.2445	0.1516
	NC	<b>0.9092</b>	<b>[0.907, 0.911]</b>	<b>0.9297</b>	<b>0.0492</b>	<b>0.1560</b>	<b>[0.154, 0.158]</b>	<b>0.1275</b>	<b>0.0569</b>

Table 14: Win rate breakdown by holdout split definition.

Holdout Split	NC Wins	CO Wins	Total	NC %
$\mathcal{H}$	1,460	40	1,500	97.3%
$\mathcal{H}_{\text{col}}$	1082	418	1,500	72.1%
$\mathcal{H}_{\text{nc}}$	1480	20	1,500	98.7%
$\mathcal{H} / \text{C4}$	279	21	300	93.0%
$\mathcal{H} / \text{Cosmopedia}$	284	16	300	94.7%
$\mathcal{H} / \text{peS2o}$	298	2	300	99.3%
$\mathcal{H} / \text{RedPajama}$	300	0	300	100.0%
$\mathcal{H} / \text{Wikipedia}$	299	1	300	99.7%
$\mathcal{H}_{\text{col}} / \text{C4}$	252	48	300	84.0%
$\mathcal{H}_{\text{col}} / \text{Cosmopedia}$	239	61	300	79.7%
$\mathcal{H}_{\text{col}} / \text{peS2o}$	295	5	300	98.3%
$\mathcal{H}_{\text{col}} / \text{RedPajama}$	151	149	300	50.3%
$\mathcal{H}_{\text{col}} / \text{Wikipedia}$	145	155	300	48.3%
$\mathcal{H}_{\text{nc}} / \text{C4}$	292	8	300	97.3%
$\mathcal{H}_{\text{nc}} / \text{Cosmopedia}$	289	11	300	96.3%
$\mathcal{H}_{\text{nc}} / \text{peS2o}$	299	1	300	99.7%
$\mathcal{H}_{\text{nc}} / \text{RedPajama}$	300	0	300	100.0%
$\mathcal{H}_{\text{nc}} / \text{Wikipedia}$	300	0	300	100.0%

### D.3 Appendix - Experimental setup for empirical validation of Theorem 1

We formalize the empirical protocol used to test Theorem 1’s Regime A prediction at matched training cardinality. The protocol is instantiated independently for each scaling law  $\mathcal{L} \in \{\text{Chinchilla, Kaplan, Droppo–Elibol}\}$  (Definition 3), each training corpus, and each training checkpoint mode  $\mu \in \{\text{first, second, final}\}$ . Throughout this section we reuse the symbols  $(N, D, L, \mathcal{D}, K, k_1, \dots, k_K, \mathcal{H}, \theta)$  from Definition 1 without redefinition; the quantities introduced below are the new objects specific to subset enumeration.

**Definition 9** (Available TPP ratios). For each corpus and mode  $\mu$ , let  $\mathbf{k}^{\text{all}} = (k_1 < \dots < k_{12})$  denote the ordered set of 12 TPP ratios at which the collinear training pool  $\mathcal{D}_{\text{train}}^{\text{CO}}$  (Definition 1) was collected (so  $K = 12$  for the full pool). Each ratio  $k_\ell$  indexes a ray  $\{(N, k_\ell N) : N \in \mathcal{N}\}$  in the  $(N, D)$  plane, where  $\mathcal{N} = \{N_1, \dots, N_n\}$  is the shared set of model sizes of Definition 1.

**Definition 10** (Collinear (CO) subset design). Given any non-empty index set  $S \subseteq \{1, \dots, 12\}$ , the induced *collinear subset design* is the union of training runs on the selected rays:

$$\text{CO}(S) := \{(N_i, D_i, L_i) \in \mathcal{D}_{\text{train}}^{\text{CO}} : D_i/N_i = k_\ell \text{ for some } \ell \in S\}, \quad (106)$$

with cardinality  $n_S := |\text{CO}(S)|$  and effective ray count  $K_S := |S|$  (the design’s  $K$  in the sense of Definition 1). Enumeration over all non-empty  $S$  yields  $2^{12} - 1 = 4,095$  CO subset designs per (corpus, mode) pair.

**Definition 11** (Bounding-box non-collinear (NC) design). Let  $\mathcal{D}_{\text{train}}^{\text{NC}}$  be the non-collinear training pool covering the rectangular grid  $\mathcal{N}_{\text{NC}} \times \mathcal{D}_{\text{NC}}$ , with  $M_N := |\mathcal{N}_{\text{NC}}|$  rows and  $M_D := |\mathcal{D}_{\text{NC}}|$  columns. Index the grid cells  $(i, j) \in \{0, \dots, M_N - 1\} \times \{0, \dots, M_D - 1\}$ . Given a target cardinality  $n^* \in \mathbb{N}$  and target TPP ratios  $\mathbf{k}_S = \{k_\ell : \ell \in S\}$  from a CO subset  $S$ , the *bounding-box NC design*  $\text{NC}_{\square}(n^*, \mathbf{k}_S)$  is constructed by the following deterministic algorithm (seeded by  $\text{hash}(\text{corpus}, \mu, S)$ ):

- Centre.** Initialise a  $2 \times 2$  bounding box  $[i_{\text{lo}}, i_{\text{hi}}] \times [j_{\text{lo}}, j_{\text{hi}}]$  centered on  $(\lfloor M_N/2 \rfloor, \lfloor M_D/2 \rfloor)$  (with a random  $\pm 1$  offset when  $M_N$  or  $M_D$  is even).
- Initial absorption.** Include all training runs whose  $(N, D)$  falls inside the initial bounding box. If  $|\text{NC}_{\square}| > n^*$ , subsample to exactly  $n^*$  using the priority rule below.
- Adaptive growth.** While  $|\text{NC}_{\square}| < n^*$  and the box has not spanned the full grid:
  - Enumerate the two candidate expansions: expand the  $N$ -dimension by one row on both edges, or expand the  $D$ -dimension by one column on both edges.
  - Score each candidate by  $(s_1, s_2, \xi)$ , where  $s_1$  counts newly-covered CO-target TPP bins,  $s_2$  counts newly-covered non-target TPP bins (induced by the  $(N, D)$  combinations on the boundary), and  $\xi \sim \text{Uniform}[0, 1]$ .
  - Select the candidate maximizing  $(s_1, s_2, \xi)$  lexicographically. If the resulting ring fits within  $n^* - |\text{NC}_{\square}|$  slots, absorb it entirely; otherwise absorb a priority subsample and terminate.

4. **Priority subsample rule.** When a ring must be trimmed to  $r$  training points, partition its runs by TPP bin into three priority buckets: (a) runs at a target TPP not yet covered, (b) runs at a non-target TPP not yet covered, (c) runs at an already-covered TPP. Shuffle each bucket with the seeded RNG and take the first  $r$  from their concatenation.

By construction,  $|\text{NC}_\square(n^*, \mathbf{k}_S)| = n^*$  whenever the NC grid has enough runs, and  $\text{NC}_\square$  is a connected rectangular region of  $\mathcal{N}_{\text{NC}} \times \mathcal{D}_{\text{NC}}$ .

**Definition 12** (Paired comparison). For any scaling law  $\mathcal{L}$ , corpus  $\mathcal{D}$ , mode  $\mu$ , and CO subset  $S$ , let  $n^* = n_S$  (Definition 10). Define:

$$\begin{aligned} \text{CO}(S) &— \text{training set from the selected rays.} \\ \text{NC}_\square(n^*, \mathbf{k}_S) &— \text{budget-matched bounding-box NC training set.} \\ \hat{\boldsymbol{\theta}}^{\text{CO}}, \hat{\boldsymbol{\theta}}^{\text{NC}} &— \text{least-squares fits of } \mathcal{L} \text{ on each design.} \end{aligned}$$

Both fits use the same optimization protocol and evaluate on the same unified holdout  $\mathcal{H}$  (Definition 1). The *paired comparison* is the tuple

$$\mathcal{C}(\mathcal{L}, \mathcal{D}, \mu, S) := (\text{RMSE}_{\mathcal{H}}^{\text{CO}}, \text{RMSE}_{\mathcal{H}}^{\text{NC}}, \hat{\boldsymbol{\theta}}^{\text{CO}}, \hat{\boldsymbol{\theta}}^{\text{NC}}), \quad (107)$$

with  $\text{RMSE}_{\mathcal{H}}^{\text{CO}}$  and  $\text{RMSE}_{\mathcal{H}}^{\text{NC}}$  as in Theorem 1. The set of all paired comparisons is

$$\begin{aligned} \mathcal{P} = \{ \mathcal{C}(\mathcal{L}, \mathcal{D}, \mu, S) : \mathcal{L} \in \{\text{Ch.}, \text{Ka.}, \text{DE}\}, \\ \mathcal{D} \in \{\text{C4}, \dots, \text{Wiki}\}, \\ \mu \in \{\text{1st}, \text{2nd}, \text{3rd}\}, \\ S \subseteq \{1, \dots, 12\} \}, \end{aligned} \quad (108)$$

with  $|\mathcal{P}| = 3 \cdot 5 \cdot 3 \cdot 4095 = 184,275$ .

**Note on the budget match.**  $\text{NC}_\square(n^*, \mathbf{k}_S)$  contains exactly  $n^*$  training points *by construction*, matching  $\text{CO}(S)$  precisely. Any observed RMSE advantage of  $\text{NC}_\square$  over CO therefore cannot arise from a training-data size difference; it must come from the *geometric* difference between ray-based and 2D designs — the object of Proposition 1 and Theorem 1.

**Definition 13** (NC win rate and Regime A NC win rate). For any collection  $\mathcal{P}' \subseteq \mathcal{P}$ , the *NC win rate* on  $\mathcal{P}'$  is

$$\text{WR}(\mathcal{P}') := \frac{1}{|\mathcal{P}'|} \sum_{\mathcal{C} \in \mathcal{P}'} \mathbf{1} \left\{ \text{RMSE}_{\mathcal{H}}^{\text{NC}}(\mathcal{C}) < \text{RMSE}_{\mathcal{H}}^{\text{CO}}(\mathcal{C}) \right\}, \quad (109)$$

where  $\mathbf{1}\{\cdot\}$  is the standard indicator (1 if the inequality holds, 0 otherwise) and ties are broken in favor of CO (negligible at our sample sizes).

Given a scaling law  $\mathcal{L}$ , mode  $\mu$ , and **target condition number**  $\kappa^* > 0$  (in the sense of  $\kappa_{\text{target}}$  from Proposition 2), the *predicted Regime A set* at  $\kappa^*$  is

$$\mathcal{P}_{\mathcal{L}, \mu}^A(\kappa^*) := \{ \mathcal{C}(\mathcal{L}, \mathcal{D}, \mu, S) \in \mathcal{P} : V_{K_S}(\cdot; \beta_{\text{eff}}^{\mathcal{L}}) < \tau_{K_S}(S; \beta_{\text{eff}}^{\mathcal{L}}, \kappa^*) \}, \quad (110)$$

where  $V_K(\cdot; \beta)$ ,  $\tau_K(\cdot; \beta, \kappa^*)$ , and  $\beta_{\text{eff}}^{\mathcal{L}}$  are exactly the quantities of Proposition 2 and Definition 3, evaluated on the rays selected by  $S$  (so  $K_S = |S|$ ). We use the **literature value** of  $\beta_{\text{eff}}^{\mathcal{L}}$  (Table 8) so that regime classification can be performed *a priori* without fitting. The *Regime A NC win rate* at target  $\kappa^*$  is

$$\text{WR}_A(\mathcal{L}, \mu; \kappa^*) := \text{WR}(\mathcal{P}_{\mathcal{L}, \mu}^A(\kappa^*)). \quad (111)$$

**Definition 14** (Measured condition numbers). For a paired comparison  $\mathcal{C}$  with fitted parameters  $\hat{\boldsymbol{\theta}}^{\text{CO}}, \hat{\boldsymbol{\theta}}^{\text{NC}}$ , let  $J^{\text{CO}}$  (resp.  $J^{\text{NC}}$ ) denote the residual Jacobian of Section 3.1 for  $\mathcal{L}$ , evaluated at  $\hat{\boldsymbol{\theta}}^{\text{CO}}$  on  $\text{CO}(S)$  (resp. at  $\hat{\boldsymbol{\theta}}^{\text{NC}}$  on  $\text{NC}_\square$ ). We report two condition-number diagnostics, both extending  $\kappa_{A,B}$  and  $\kappa(J^T J)$  from Section 3.1 with a design superscript:

$$\kappa_{A,B}^{\text{design}} := \kappa \left( [(J^{\text{design}})^{\top} J^{\text{design}}]_{A,B} \right), \quad (2 \times 2 \text{ sub-block on the } (A, B) \text{ pair}), \quad (112)$$

$$\kappa_{\text{full}}^{\text{design}} := \kappa((J^{\text{design}})^{\top} J^{\text{design}}), \quad (\text{full } p \times p \text{ matrix}), \quad (113)$$

for  $\text{design} \in \{\text{CO}, \text{NC}\}$ . The  $2 \times 2$  block is the quantity Proposition 1 bounds under the global dominance assumption of Section 3.1. The full-matrix  $\kappa$  is scale-sensitive (columns differ in magnitude by up to 20 orders, e.g.,  $A \sim 10^6$  vs  $\alpha \sim 10^{-1}$ ) but its *rank* across paired comparisons remains informative.

#### D.4 Appendix - BF16 results

Tables 5, 16, 17 report summary statistics and pairwise win rates for the BF16 mixed-precision experiments described in Section 4. These runs use the same 14 model sizes  $N$ , the same 12 NC dataset sizes  $D$ , and the same 12 collinear training TPP ratios  $\mathcal{K}_{\text{train}}$  as the FP32 main experiment, but are restricted to a single corpus (Wikipedia) due to compute. They are not to be confused with the preliminary high-TPP (BigTPP) experiment of Appendix D.7, which uses the disjoint set  $\mathcal{K}_{\text{big}} = \{10, 11, 12, 13, 14, 15\}$  in FP32.

Table 15:  $R^2$  and RMSE summary for BF16 across training designs with seed-to-seed optimizer variance (30 seeds). 95% CI: confidence interval on the mean. Best per split in **bold**.

Split	Design	$R^2$				RMSE			
		Mean	95% CI	Median	Std	Mean	95% CI	Median	Std
Train ( $\mathcal{D}$ )	CO	0.9896	[0.990, 0.990]	0.9916	0.0029	0.1854	[0.185, 0.185]	0.1606	0.0353
	NC	<b>0.9907</b>	<b>[0.991, 0.991]</b>	<b>0.9915</b>	<b>0.0020</b>	<b>0.1457</b>	<b>[0.145, 0.146]</b>	<b>0.1428</b>	<b>0.0171</b>
Holdout ( $\mathcal{H}$ )	CO	0.9412	[0.940, 0.942]	0.9473	0.0172	0.2546	[0.252, 0.257]	0.2402	0.0396
	NC	<b>0.9657</b>	<b>[0.965, 0.967]</b>	<b>0.9663</b>	<b>0.0068</b>	<b>0.1949</b>	<b>[0.192, 0.198]</b>	<b>0.1921</b>	<b>0.0203</b>
Holdout( $\mathcal{H}_{\text{col}}$ )	CO	0.9650	[0.964, 0.966]	0.9693	0.0089	0.2194	[0.218, 0.221]	0.2063	0.0279
	NC	<b>0.9734</b>	<b>[0.973, 0.974]</b>	<b>0.9741</b>	<b>0.0037</b>	<b>0.1919</b>	<b>[0.190, 0.194]</b>	<b>0.1897</b>	<b>0.0136</b>
Holdout( $\mathcal{H}_{\text{nc}}$ )	CO	0.9153	[0.913, 0.917]	0.9190	0.0254	0.2753	[0.272, 0.279]	0.2673	0.0477
	NC	<b>0.9568</b>	<b>[0.956, 0.958]</b>	<b>0.9582</b>	<b>0.0106</b>	<b>0.1964</b>	<b>[0.193, 0.199]</b>	<b>0.1906</b>	<b>0.0266</b>

Table 16: Win rate breakdown (NC vs. CO design) on holdout for BF16 with seed-paired comparisons. Overall NC win rate: 98.7% (296/300). 95% CI: [96.6%, 99.5%].

	Law	Epoch
Chinchilla	97.8%	first 100.0%
Droppo-Elibol	97.8%	second 96.7%
Kaplan	100.0%	final 98.9%
Repeated-Data	100.0%	

Table 17: Win rate breakdown by holdout split definition for bf16.

Holdout Split	NC Wins	CO Wins	Total	NC %
$\mathcal{H}$	296	4	300	98.7%
$\mathcal{H}_{\text{col}}$	222	78	300	74.0%
$\mathcal{H}_{\text{nc}}$	299	1	300	99.7%

The following tables expand on the summary in Section 4 and Table 13. We evaluate Chinchilla, repeated-data (Muennighoff et al., 2025), Kaplan, and Droppo & Elibol, on Wikipedia articles only, due to compute restrictions.

#### D.5 Appendix - TPP convergence fraction detailed setup

We construct an incremental coverage analysis to measure how scaling law fit quality evolves as the experimental design space is progressively expanded. This analysis reuses the runs from our main experiment rather than conducting independent trials, so the results should be interpreted as a post-hoc decomposition of existing data rather than a controlled ablation. For the collinear (CO) design, we sort the 12 designed TPP levels in ascending order and add them one at a time: step 1 trains on runs from only the lowest TPP, step 2 adds the second-lowest, and so on until all 12 levels are included. Each TPP level contributes  $120/12 = 10$  training-eligible runs (one per training model size after the L-shaped holdout removal), growing the training set from 10 to 120 runs across 12 steps. For the non-collinear (NC) design, we expand coverage by pinching inward from the extremes of the  $D$  range: step 1 includes runs at both the smallest and largest  $D$ , step 2 adds the second-smallest and second-largest, and so on, adding two  $D$  levels per step. This pairing ensures that even the earliest step spans the full  $D$  range. At each step, all four scaling laws are fit on the current subset and evaluated against fixed holdout sets, so

changes in  $R^2$  reflect only the effect of broader coverage. The TPP bins are scaled to match the epoch mode under evaluation ( $\times 1$  for first-epoch,  $\times 2$  for second-epoch,  $\times 3$  for final-epoch), aligning the groupings with the effective tokens-per-parameter that each fitter sees.

A coverage fraction of 1.0 means all 12 TPP levels (for CO) or all 12  $D$  levels (for NC) are included in the training set - this is the same configuration used in the main results tables, and the  $R^2$  values at full coverage correspond exactly to those reported there. The CO and NC coverage fractions are not directly comparable: they traverse different axes of the design space using non-corresponding sets of values. Furthermore, the observed  $R^2$  trajectory may depend not only on the number of levels included but also on their spacing; our designed TPP values (1.0, 1.5, 1.9, 2.0, 2.5, 2.7, 3.0, 3.3, 3.5, 4.0, 4.5, 5.0) are unevenly distributed, with denser coverage at the low end, so a different spacing (e.g., uniformly from 1 to 5) could yield a different convergence profile. The primary takeaway is qualitative - that collinear designs require substantially more coverage to approach their asymptotic  $R^2$ , while non-collinear designs converge rapidly with minimal coverage - rather than a precise quantitative comparison between the two trajectories.

## D.6 Appendix - Optimizer seed protocol

All scaling-law parameters are estimated via nonlinear least squares (L-BFGS-B with differential evolution polish) using multiple random restarts seeded by a deterministic sequence. The `seed` column in released parquet files and CSVs stores the seed *index*; the actual RNG seed passed to the optimizer is computed from this index as described below. All model pre-training uses a fixed seed of 42 for weight initialization and data shuffling; the seeds documented here govern only the scaling-law curve fitting. We use a multitude of random hashing functions for optimizer seed starts.

**Tables 3-4 and convergence-fraction plots.** Both the full-coverage analysis (Tables 3-4) and the seed-variance convergence fraction plots are produced by identical seed logic: 30 optimizer seeds at 100 random restarts each, base seed  $b = 0$ , stride 1:

$$s_i = i, \quad i \in \{0, 1, 2, \dots, 29\}.$$

Each seed index  $i$  is passed directly as the RNG seed to the optimizer. The full-coverage stage fits all four scaling laws  $\times$  five datasets  $\times$  three epoch modes  $\times$  two designs at each seed, producing 1,500 paired comparisons (Table 4). The seed-variance stage fits the same configurations at each incremental coverage step, recording the distribution of holdout  $R^2$  across the 30 seeds at every step.

**Tables 5-16 (BF16 replication).** The BF16 analysis uses 30 optimizer seeds at 100 random restarts each, base seed  $b = 0$ , stride 137:

$$s_i = 137 \cdot i, \quad i \in \{0, 1, 2, \dots, 29\},$$

yielding the sequence  $\{0, 137, 274, 411, \dots, 3,973\}$ . The wider stride avoids accidental overlap with the main analysis seeds; the results are statistically equivalent to any other choice of 30 independent seeds.

**Table 6 (subset enumeration).** The budget-matched subset enumeration uses 22 independent global seeds  $g \in \{0, 1, \dots, 21\}$ , each with 300 random restarts per fit. The actual optimizer seed for global seed  $g$  is:

$$s_g = 42 + 100,003 \cdot g.$$

Table 18 lists all 22 values. The NC bounding-box construction uses a separate deterministic seed derived via BLAKE2b hash of the dataset name, epoch mode, and subset mask, XORed with  $g \cdot 0x9E3779B1$  (a 32-bit golden-ratio constant ensuring uniform dispersion). The holdout subsample seed is intentionally *not* varied across  $g$ : it is fixed at  $7,777 + \text{hash}(\text{dataset}, \text{mode}) \bmod 10^5$  so that the holdout composition remains constant across all 22 runs.

**Preliminary Large TPP Seeds.** Our preliminary large TPP results use the same stride as in our BF16 results, using a stride of 137.

Table 18: Fit seeds for each of the 22 subset-enumeration runs ( $s_g = 42 + 100,003 \cdot g$ ).

$g$	$s_g$	$g$	$s_g$	$g$	$s_g$
0	42	8	800,066	16	1,600,090
1	100,045	9	900,069	17	1,700,093
2	200,048	10	1,000,072	18	1,800,096
3	300,051	11	1,100,075	19	1,900,099
4	400,054	12	1,200,078	20	2,000,102
5	500,057	13	1,300,081	21	2,100,105
6	600,060	14	1,400,084		
7	700,063	15	1,500,087		

Table 19: Seed protocol summary. Index  $i$  ranges over optimizer seeds within a stage;  $g$  ranges over independent subset-enumeration runs.

Stage	Count	Restarts	Tables/Figures	RNG seed
Full coverage	30	100	3, 4	$i$
Seed variance	30	100	Convergence plots	$i$
BF16 replication	30	100	5, 16	137 $i$
Subset enumeration	22	300	6	42 + 100,003 $g$
BigTPP prelim	30	100	20	137 $i$

## D.7 Appendix - Preliminary large TPP experiment

To check whether the NC advantage persists at higher TPP, we ran a single-corpus preliminary experiment on Wikipedia. Due to compute restrictions, the grid is smaller in size and available fits; we use Wikipedia and fit Chinchilla to this experiment exclusively.

**Training grid.** Both designs share ten model sizes

$$N \in \{5.04, 10.07, 14.41, 19.40, 22.80, 28.82, 32.50, 35.37, 40.28, 47.95\}M.$$

CO sweeps  $k \in \mathcal{K}_{\text{big}} := \{10, 11, 12, 13, 14, 15\}$ . NC sweeps  $D \in \{100, 225, 400, 550, 700, 825\}$ .

**Holdout.** Four out-of-grid sizes  $N_{\text{holdout}} \in \{54.57, 60.88, 64.04, 70.36\}M$ , all above the training maximum. For holdout model size 55M, the holdout model used TPP values 10, 11, 12, 13, 14, 15, 16, 18, 20. For non-collinear, 55M models used  $D \in \{100, 225, 400, 550, 700, 825, 900, 1100, 1400\}$ . At the three largest holdout sizes,  $\mathcal{H}_{\text{col}}$  only includes TPP  $\in \{16, 18, 20\}$  and  $\mathcal{H}_{\text{nc}}$  additionally includes  $D \in \{900, 1100, 1400\}M$ .

**Fitting.** Chinchilla, 30 seeds (stride 137, matching Appendix D.4), 100 restarts with differential evolution polish. We report seed-paired NC win rate (Table 20) with Wilson 95% CI. A full BigTPP replication is left to future work.

Table 20: Preliminary BigTPP NC win rate (Chinchilla, first epoch). Compute-limited preliminary experiment; not a full result conclusion.

Law	NC Wins	Total	NC % [95% CI]
Chinchilla	19	30	63.3% [45.5%, 78.1%]

## D.8 Appendix - Three-panel plots of scaling law fitted parameters

Figures 5-25 continue the three-panel plots from Section 4. The BF16 additional runs did not undergo the same increasing coverage fraction, as seen in Section 4.

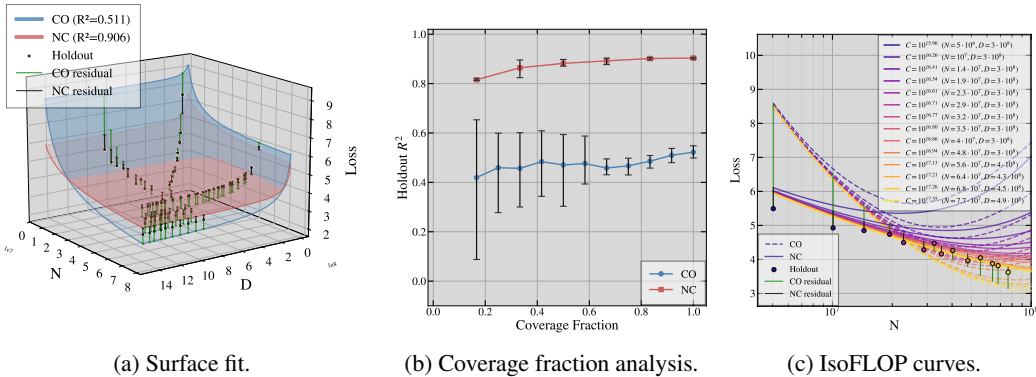


Figure 5: Kaplan law on RedPajama, first epoch.

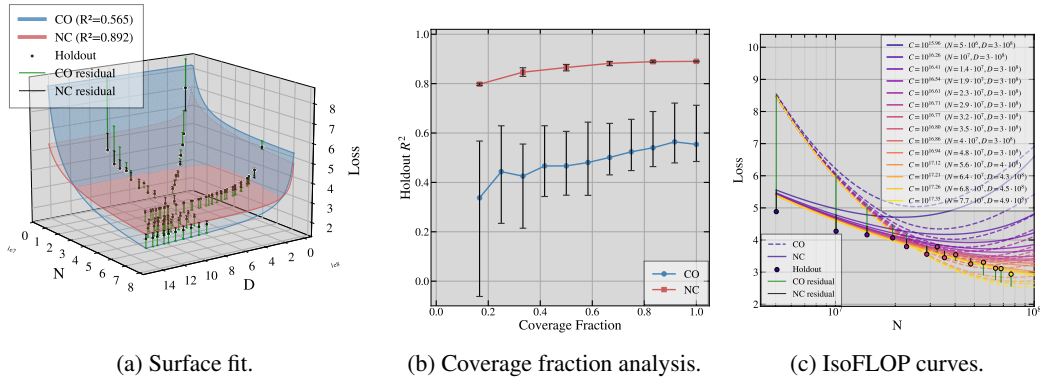


Figure 6: Kaplan law on Wikipedia, first epoch.

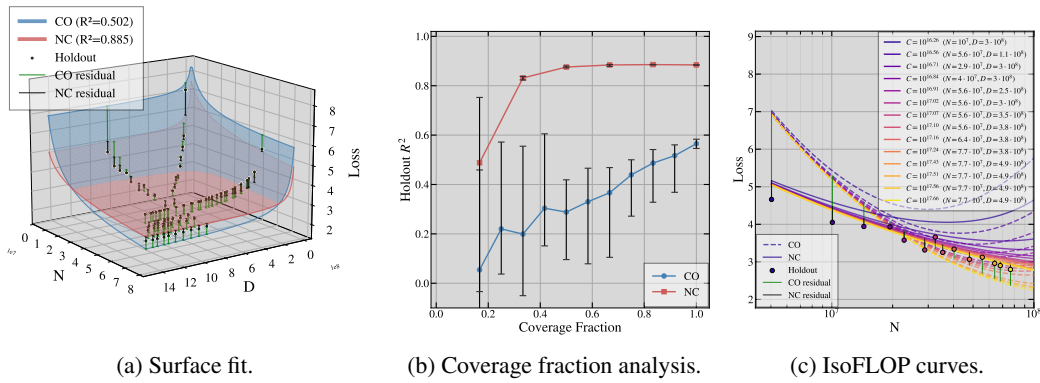


Figure 7: Kaplan law on Wikipedia, second epoch.

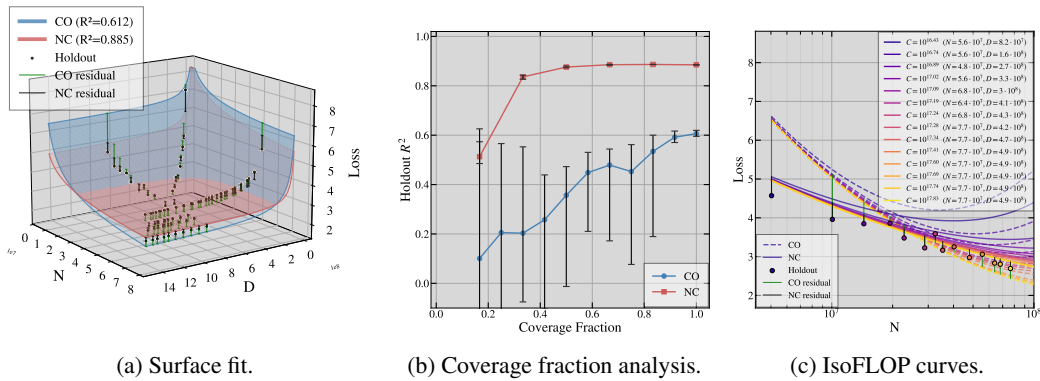


Figure 8: Kaplan law on Wikipedia, final epoch.

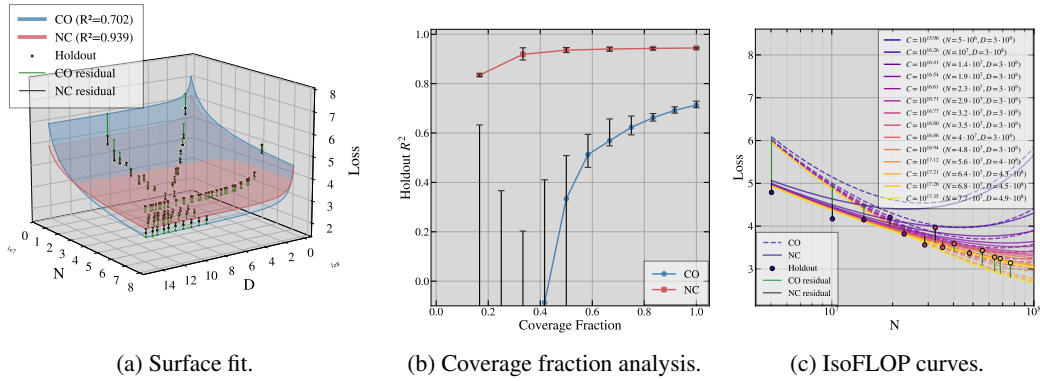


Figure 9: Kaplan law on peS2o, first epoch.

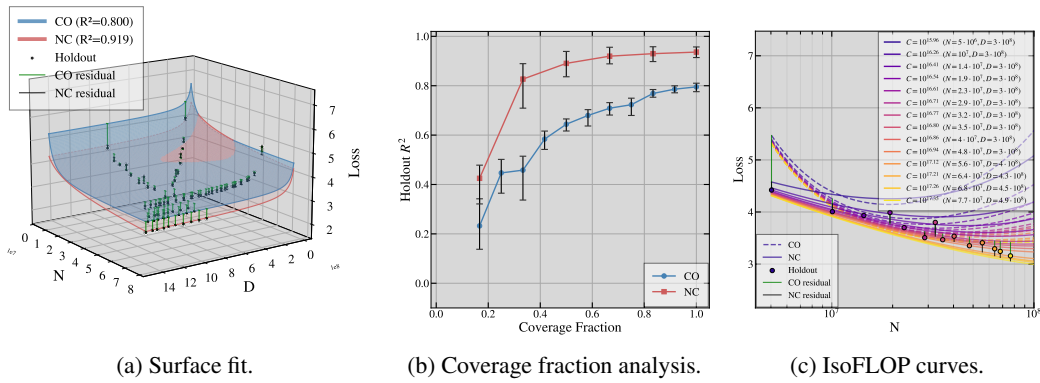


Figure 10: Chinchilla law on C4, first epoch.

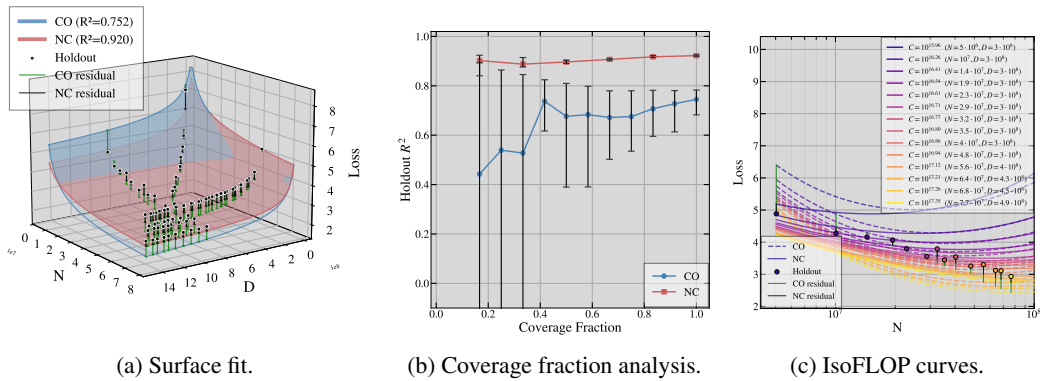


Figure 11: Droppo-Elibol law on Wikipedia, first epoch.

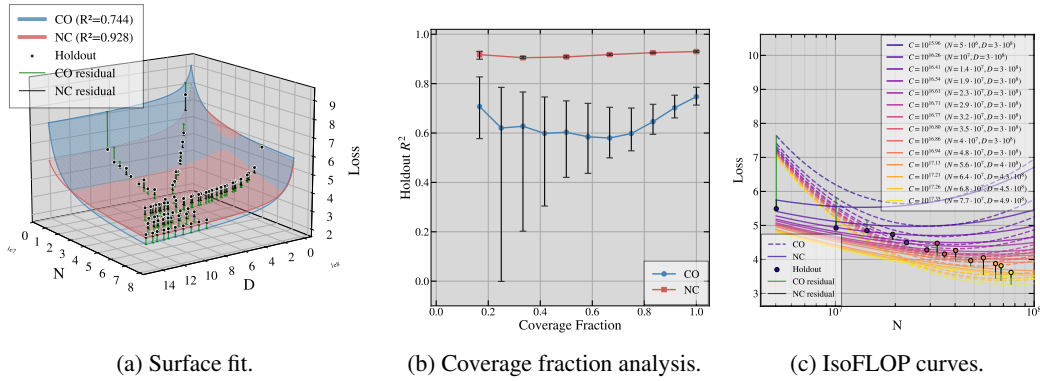


Figure 12: Droppo-Elilibol law on RedPajama, first epoch.

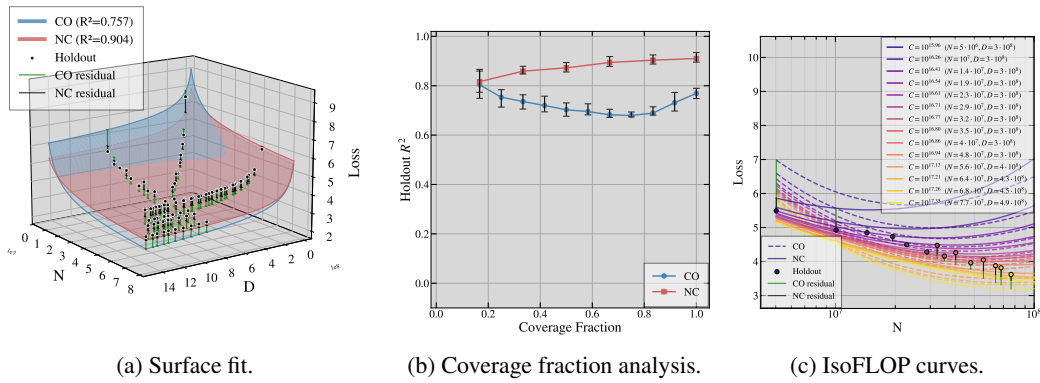


Figure 13: Chinchilla law on RedPajama, first epoch.

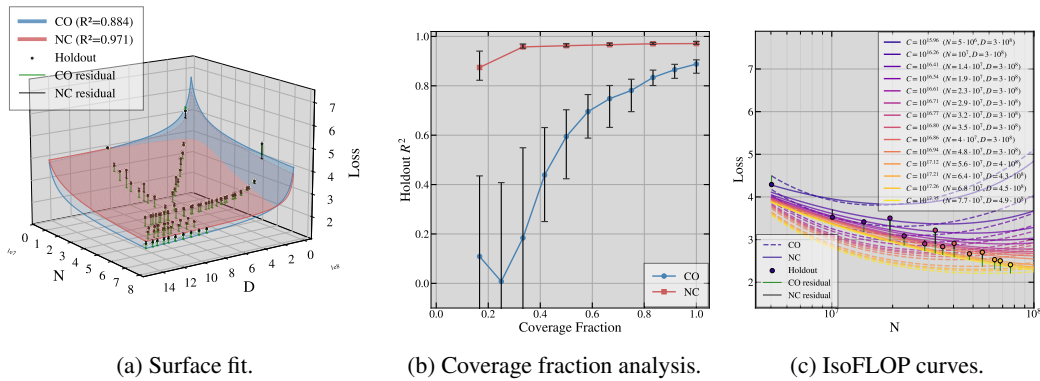


Figure 14: Droppo-Elilibol law on Cosmopedia, first epoch.

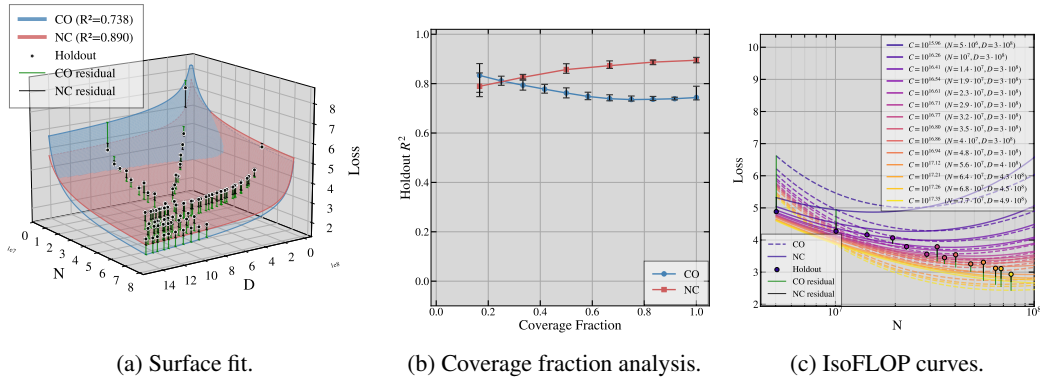


Figure 15: Chinchilla law on Wikipedia, first epoch.

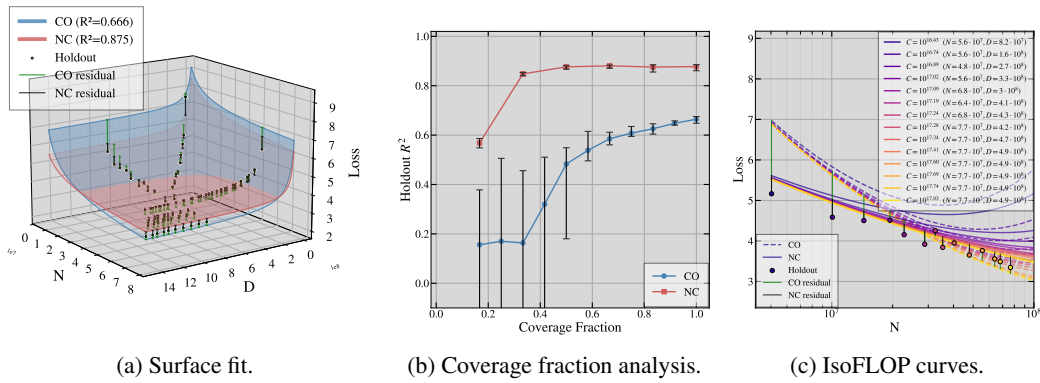


Figure 16: Kaplan law on RedPajama, final epoch.

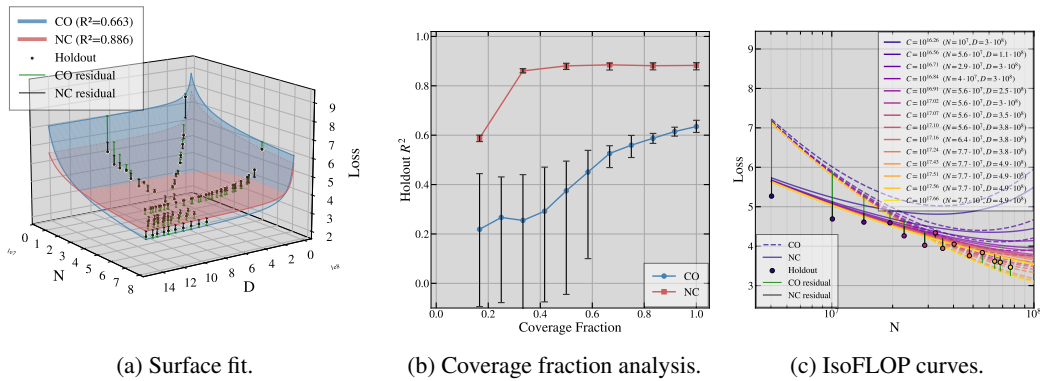


Figure 17: Kaplan law on RedPajama, second epoch.

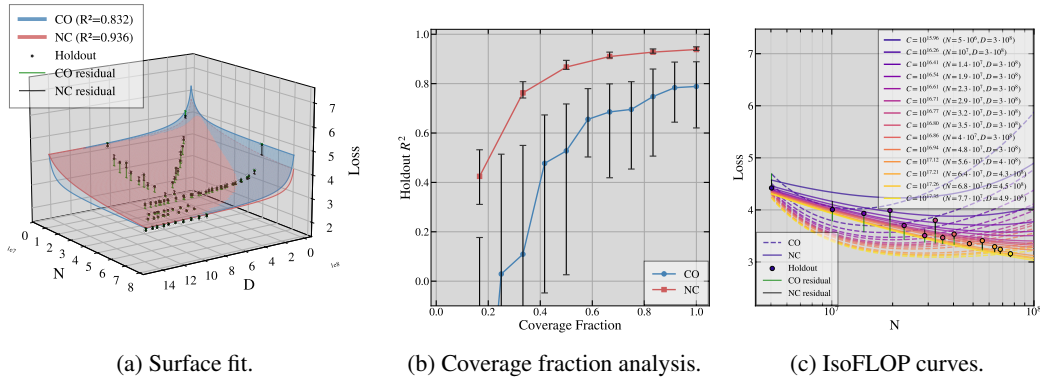


Figure 18: Droppo-Elibol law on C4, first epoch.

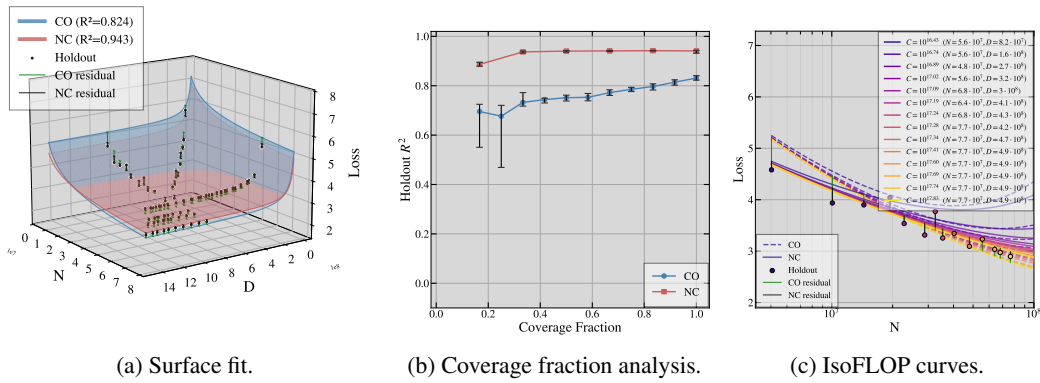


Figure 19: Kaplan law on peS2o, final epoch.

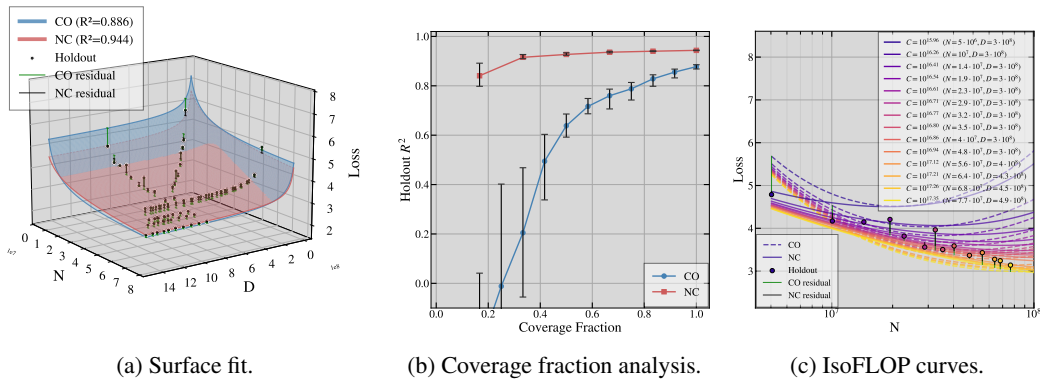
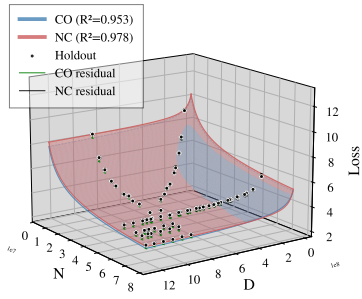
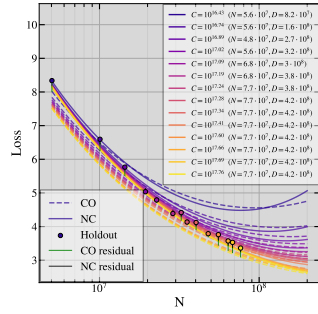


Figure 20: Droppo-Elibol law on peS2o, first epoch.

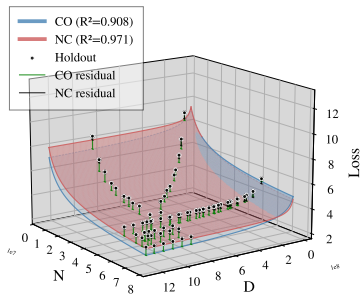


(a) Surface fit.

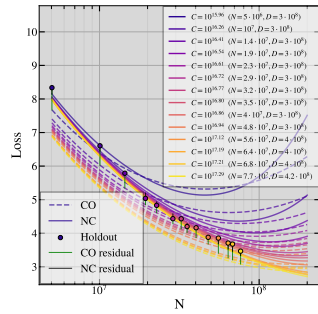


(b) IsoFLOP curves.

Figure 21: Chinchilla law on Wikipedia BF16, final epoch.

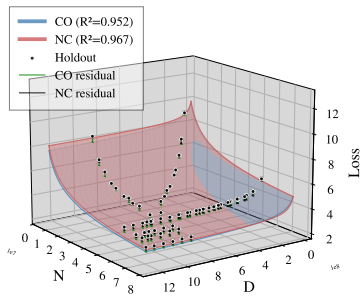


(a) Surface fit.

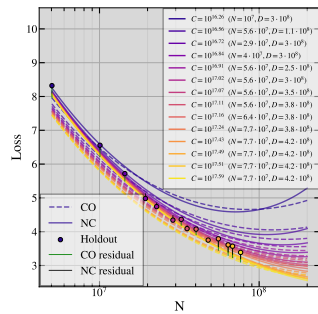


(b) IsoFLOP curves.

Figure 22: Chinchilla law on Wikipedia BF16, first epoch.

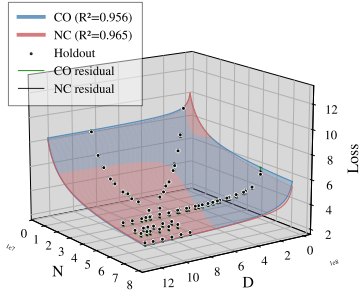


(a) Surface fit.

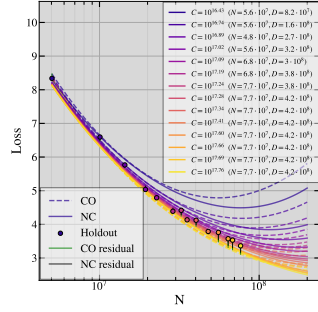


(b) IsoFLOP curves.

Figure 23: Chinchilla law on Wikipedia BF16, second epoch.

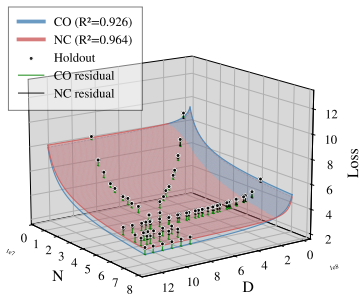


(a) Surface fit.

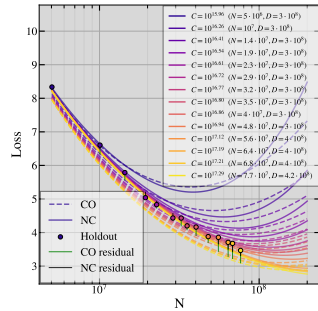


(b) IsoFLOP curves.

Figure 24: Droppo-Elibol law on Wikipedia BF16, final epoch.



(a) Surface fit.



(b) IsoFLOP curves.

Figure 25: Droppo-Elibol law on Wikipedia BF16, first epoch.

## E Appendix - Dataset, scaling-law, epoch extended breakdown

The following appendix material shows the full breakdown of our experimental fits at full coverage, disaggregating Table 3. At full coverage, seed-to-seed variance is small for both designs; the CI inflation predicted by Corollary 1 is most visible at lower coverage levels (see convergence plots in previous three-panel plots). The CI annotation on each cell is the half-width of the 95% confidence interval on the mean - i.e., the interval is the reported value  $\pm$  CI.

Table 21: C4 - Holdout ( $\mathcal{H}$ ). Mean across 30 seeds; CI = 95% CI on the mean.

Epoch	Law	Design	$R^2$ Train	$R^2 \mathcal{H}$	RMSE Train	RMSE $\mathcal{H}$
-	Repeated-data	Collinear	$0.9781 \pm 0.000$	$0.8183 \pm 0.000$	$0.1644 \pm 0.000$	$0.1844 \pm 0.000$
		Non-Collinear	$0.9361 \pm 0.000$	<b><math>0.9570 \pm 0.000</math></b>	$0.1778 \pm 0.000$	$0.0897 \pm 0.000$
	Chinchilla	Collinear	$0.9788 \pm 0.000$	$0.9158 \pm 0.014$	$0.1243 \pm 0.001$	$0.1091 \pm 0.009$
		Non-Collinear	$0.9354 \pm 0.000$	<b><math>0.9520 \pm 0.001</math></b>	$0.1387 \pm 0.000$	$0.0842 \pm 0.001$
Final	Droppo-Elibol	Collinear	$0.9805 \pm 0.000$	$0.9403 \pm 0.003$	$0.1192 \pm 0.000$	$0.0939 \pm 0.002$
		Non-Collinear	$0.9395 \pm 0.000$	<b><math>0.9544 \pm 0.001</math></b>	$0.1343 \pm 0.000$	$0.0822 \pm 0.000$
	Kaplan	Collinear	$0.9802 \pm 0.000$	<b><math>0.9412 \pm 0.001</math></b>	$0.1203 \pm 0.000$	$0.0933 \pm 0.001$
		Non-Collinear	$0.9271 \pm 0.001$	$0.9385 \pm 0.003$	$0.1473 \pm 0.001$	$0.0953 \pm 0.002$
	Chinchilla	Collinear	$0.9825 \pm 0.000$	$0.7953 \pm 0.004$	$0.1808 \pm 0.000$	$0.2135 \pm 0.002$
		Non-Collinear	$0.9328 \pm 0.000$	<b><math>0.9362 \pm 0.006</math></b>	$0.2236 \pm 0.000$	$0.1184 \pm 0.005$
First	Droppo-Elibol	Collinear	$0.9818 \pm 0.001$	$0.7886 \pm 0.029$	$0.1845 \pm 0.003$	$0.2135 \pm 0.014$
		Non-Collinear	$0.9463 \pm 0.000$	<b><math>0.9382 \pm 0.002</math></b>	$0.1999 \pm 0.000$	$0.1172 \pm 0.002$
	Kaplan	Collinear	$0.9674 \pm 0.000$	$0.7838 \pm 0.004$	$0.2468 \pm 0.000$	$0.2194 \pm 0.002$
		Non-Collinear	$0.9356 \pm 0.001$	<b><math>0.9398 \pm 0.001</math></b>	$0.2189 \pm 0.002$	$0.1158 \pm 0.001$
	Chinchilla	Collinear	$0.9799 \pm 0.000$	$0.8857 \pm 0.013$	$0.1345 \pm 0.001$	$0.1303 \pm 0.007$
		Non-Collinear	$0.9380 \pm 0.000$	<b><math>0.9472 \pm 0.002</math></b>	$0.1486 \pm 0.000$	$0.0893 \pm 0.001$
Second	Droppo-Elibol	Collinear	$0.9808 \pm 0.000$	$0.9282 \pm 0.004$	$0.1316 \pm 0.000$	$0.1040 \pm 0.003$
		Non-Collinear	$0.9432 \pm 0.000$	<b><math>0.9525 \pm 0.001</math></b>	$0.1422 \pm 0.000$	$0.0848 \pm 0.001$
	Kaplan	Collinear	$0.9795 \pm 0.000$	$0.9296 \pm 0.001$	$0.1361 \pm 0.000$	$0.1032 \pm 0.001$
		Non-Collinear	$0.9301 \pm 0.001$	<b><math>0.9395 \pm 0.002</math></b>	$0.1579 \pm 0.001$	$0.0956 \pm 0.002$

Table 22: C4 - Holdout-CO ( $\mathcal{H}_{\text{col}}$ ). Mean across 30 seeds; CI = 95% CI on the mean.

Epoch	Law	Design	$R^2$ Train	$R^2 \mathcal{H}_{\text{col}}$	RMSE Train	RMSE $\mathcal{H}_{\text{col}}$
-	Repeated-data	Collinear	$0.9781 \pm 0.000$	$0.8571 \pm 0.000$	$0.1644 \pm 0.000$	$0.1642 \pm 0.000$
		Non-Collinear	$0.9361 \pm 0.000$	<b><math>0.9590 \pm 0.000</math></b>	$0.1778 \pm 0.000$	$0.0880 \pm 0.000$
	Chinchilla	Collinear	$0.9788 \pm 0.000$	$0.9334 \pm 0.014$	$0.1243 \pm 0.001$	$0.0980 \pm 0.009$
		Non-Collinear	$0.9354 \pm 0.000$	<b><math>0.9595 \pm 0.001</math></b>	$0.1387 \pm 0.000$	$0.0788 \pm 0.001$
Final	Droppo-Elibol	Collinear	$0.9805 \pm 0.000$	$0.9510 \pm 0.002$	$0.1192 \pm 0.000$	$0.0866 \pm 0.002$
		Non-Collinear	$0.9395 \pm 0.000$	<b><math>0.9631 \pm 0.001</math></b>	$0.1343 \pm 0.000$	$0.0753 \pm 0.001$
	Kaplan	Collinear	$0.9802 \pm 0.000$	<b><math>0.9554 \pm 0.001</math></b>	$0.1203 \pm 0.000$	$0.0827 \pm 0.001$
		Non-Collinear	$0.9271 \pm 0.001$	$0.9456 \pm 0.003$	$0.1473 \pm 0.001$	$0.0912 \pm 0.002$
	Chinchilla	Collinear	$0.9825 \pm 0.000$	$0.8575 \pm 0.003$	$0.1808 \pm 0.000$	$0.1783 \pm 0.002$
		Non-Collinear	$0.9328 \pm 0.000$	<b><math>0.9402 \pm 0.006</math></b>	$0.2236 \pm 0.000$	$0.1142 \pm 0.006$
First	Droppo-Elibol	Collinear	$0.9818 \pm 0.001$	$0.8680 \pm 0.013$	$0.1845 \pm 0.003$	$0.1701 \pm 0.008$
		Non-Collinear	$0.9463 \pm 0.000$	<b><math>0.9398 \pm 0.002</math></b>	$0.1999 \pm 0.000$	$0.1158 \pm 0.002$
	Kaplan	Collinear	$0.9674 \pm 0.000$	$0.8397 \pm 0.004$	$0.2468 \pm 0.000$	$0.1891 \pm 0.002$
		Non-Collinear	$0.9356 \pm 0.001$	<b><math>0.9493 \pm 0.001</math></b>	$0.2189 \pm 0.002$	$0.1064 \pm 0.001$
	Chinchilla	Collinear	$0.9799 \pm 0.000$	$0.9023 \pm 0.012$	$0.1345 \pm 0.001$	$0.1193 \pm 0.007$
		Non-Collinear	$0.9380 \pm 0.000$	<b><math>0.9480 \pm 0.002</math></b>	$0.1486 \pm 0.000$	$0.0881 \pm 0.001$
Second	Droppo-Elibol	Collinear	$0.9808 \pm 0.000$	$0.9343 \pm 0.003$	$0.1316 \pm 0.000$	$0.0990 \pm 0.002$
		Non-Collinear	$0.9432 \pm 0.000$	<b><math>0.9542 \pm 0.001</math></b>	$0.1422 \pm 0.000$	$0.0828 \pm 0.001$
	Kaplan	Collinear	$0.9795 \pm 0.000$	$0.9398 \pm 0.001$	$0.1361 \pm 0.000$	$0.0949 \pm 0.001$
		Non-Collinear	$0.9301 \pm 0.001$	<b><math>0.9417 \pm 0.002</math></b>	$0.1579 \pm 0.001$	$0.0933 \pm 0.002$

Table 23: C4 - Holdout-NC ( $\mathcal{H}_{nc}$ ). Mean across 30 seeds; CI = 95% CI on the mean.

Epoch	Law	Design	$R^2$ Train	$R^2 \mathcal{H}_{nc}$	RMSE Train	RMSE $\mathcal{H}_{nc}$
-	Repeated-data	Collinear	$0.9781 \pm 0.000$	$0.7753 \pm 0.000$	$0.1644 \pm 0.000$	$0.2039 \pm 0.000$
		Non-Collinear	$0.9361 \pm 0.000$	<b><math>0.9547 \pm 0.000</math></b>	$0.1778 \pm 0.000$	$0.0915 \pm 0.000$
	Chinchilla	Collinear	$0.9788 \pm 0.000$	$0.8952 \pm 0.016$	$0.1243 \pm 0.001$	$0.1198 \pm 0.008$
		Non-Collinear	$0.9354 \pm 0.000$	<b><math>0.9433 \pm 0.001</math></b>	$0.1387 \pm 0.000$	$0.0897 \pm 0.001$
Final	Droppo-Elibol	Collinear	$0.9805 \pm 0.000$	$0.9277 \pm 0.003$	$0.1192 \pm 0.000$	$0.1011 \pm 0.002$
		Non-Collinear	$0.9395 \pm 0.000$	<b><math>0.9441 \pm 0.001</math></b>	$0.1343 \pm 0.000$	$0.0890 \pm 0.000$
	Kaplan	Collinear	$0.9802 \pm 0.000$	$0.9244 \pm 0.002$	$0.1203 \pm 0.000$	$0.1035 \pm 0.001$
		Non-Collinear	$0.9271 \pm 0.001$	<b><math>0.9301 \pm 0.003</math></b>	$0.1473 \pm 0.001$	$0.0994 \pm 0.002$
	Chinchilla	Collinear	$0.9825 \pm 0.000$	$0.7276 \pm 0.004$	$0.1808 \pm 0.000$	$0.2459 \pm 0.002$
		Non-Collinear	$0.9328 \pm 0.000$	<b><math>0.9317 \pm 0.005</math></b>	$0.2236 \pm 0.000$	$0.1226 \pm 0.004$
First	Droppo-Elibol	Collinear	$0.9818 \pm 0.001$	$0.7023 \pm 0.048$	$0.1845 \pm 0.003$	$0.2516 \pm 0.019$
		Non-Collinear	$0.9463 \pm 0.000$	<b><math>0.9364 \pm 0.002</math></b>	$0.1999 \pm 0.000$	$0.1187 \pm 0.002$
	Kaplan	Collinear	$0.9674 \pm 0.000$	$0.7231 \pm 0.005$	$0.2468 \pm 0.000$	$0.2480 \pm 0.002$
		Non-Collinear	$0.9356 \pm 0.001$	<b><math>0.9294 \pm 0.001</math></b>	$0.2189 \pm 0.002$	$0.1252 \pm 0.001$
	Chinchilla	Collinear	$0.9799 \pm 0.000$	$0.8677 \pm 0.013$	$0.1345 \pm 0.001$	$0.1411 \pm 0.006$
		Non-Collinear	$0.9380 \pm 0.000$	<b><math>0.9462 \pm 0.001</math></b>	$0.1486 \pm 0.000$	$0.0906 \pm 0.001$
Second	Droppo-Elibol	Collinear	$0.9808 \pm 0.000$	$0.9216 \pm 0.005$	$0.1316 \pm 0.000$	$0.1092 \pm 0.003$
		Non-Collinear	$0.9432 \pm 0.000$	<b><math>0.9505 \pm 0.001</math></b>	$0.1422 \pm 0.000$	$0.0870 \pm 0.001$
	Kaplan	Collinear	$0.9795 \pm 0.000$	$0.9185 \pm 0.002$	$0.1361 \pm 0.000$	$0.1116 \pm 0.001$
		Non-Collinear	$0.9301 \pm 0.001$	<b><math>0.9368 \pm 0.003</math></b>	$0.1579 \pm 0.001$	$0.0981 \pm 0.002$

Table 24: Cosmopedia - Holdout ( $\mathcal{H}$ ). Mean across 30 seeds; CI = 95% CI on the mean.

Epoch	Law	Design	$R^2$ Train	$R^2 \mathcal{H}$	RMSE Train	RMSE $\mathcal{H}$
-	Repeated-data	Collinear	$0.9841 \pm 0.000$	$0.9496 \pm 0.000$	$0.1805 \pm 0.000$	$0.1333 \pm 0.000$
		Non-Collinear	$0.9656 \pm 0.000$	<b><math>0.9684 \pm 0.000</math></b>	$0.1862 \pm 0.000$	$0.1056 \pm 0.000$
	Chinchilla	Collinear	$0.9857 \pm 0.000$	$0.9450 \pm 0.005$	$0.1401 \pm 0.001$	$0.1225 \pm 0.005$
		Non-Collinear	$0.9502 \pm 0.000$	<b><math>0.9580 \pm 0.003</math></b>	$0.1807 \pm 0.000$	$0.1073 \pm 0.004$
Final	Droppo-Elibol	Collinear	$0.9861 \pm 0.000$	$0.9581 \pm 0.001$	$0.1382 \pm 0.000$	$0.1076 \pm 0.002$
		Non-Collinear	$0.9545 \pm 0.000$	<b><math>0.9624 \pm 0.001</math></b>	$0.1728 \pm 0.000$	$0.1020 \pm 0.002$
	Kaplan	Collinear	$0.9847 \pm 0.000$	$0.9428 \pm 0.000$	$0.1446 \pm 0.000$	$0.1259 \pm 0.000$
		Non-Collinear	$0.9500 \pm 0.000$	<b><math>0.9558 \pm 0.001</math></b>	$0.1811 \pm 0.000$	$0.1105 \pm 0.001$
	Chinchilla	Collinear	$0.9858 \pm 0.000$	$0.8959 \pm 0.003$	$0.2020 \pm 0.000$	$0.2115 \pm 0.003$
		Non-Collinear	$0.9741 \pm 0.000$	<b><math>0.9626 \pm 0.003</math></b>	$0.1947 \pm 0.001$	$0.1260 \pm 0.005$
First	Droppo-Elibol	Collinear	$0.9858 \pm 0.000$	$0.8880 \pm 0.009$	$0.2023 \pm 0.001$	$0.2185 \pm 0.008$
		Non-Collinear	$0.9826 \pm 0.000$	<b><math>0.9711 \pm 0.001</math></b>	$0.1598 \pm 0.000$	$0.1114 \pm 0.003$
	Kaplan	Collinear	$0.9814 \pm 0.000$	$0.7448 \pm 0.015$	$0.2313 \pm 0.001$	$0.3306 \pm 0.009$
		Non-Collinear	$0.9704 \pm 0.000$	<b><math>0.9661 \pm 0.001</math></b>	$0.2083 \pm 0.000$	$0.1207 \pm 0.001$
	Chinchilla	Collinear	$0.9867 \pm 0.000$	$0.9504 \pm 0.002$	$0.1464 \pm 0.001$	$0.1214 \pm 0.003$
		Non-Collinear	$0.9574 \pm 0.000$	<b><math>0.9573 \pm 0.006</math></b>	$0.1812 \pm 0.001$	$0.1114 \pm 0.006$
Second	Droppo-Elibol	Collinear	$0.9869 \pm 0.000$	$0.9562 \pm 0.003$	$0.1451 \pm 0.001$	$0.1138 \pm 0.003$
		Non-Collinear	$0.9615 \pm 0.000$	<b><math>0.9676 \pm 0.001</math></b>	$0.1722 \pm 0.000$	$0.0981 \pm 0.002$
	Kaplan	Collinear	$0.9846 \pm 0.000$	$0.9284 \pm 0.001$	$0.1575 \pm 0.000$	$0.1461 \pm 0.001$
		Non-Collinear	$0.9569 \pm 0.000$	<b><math>0.9618 \pm 0.001</math></b>	$0.1822 \pm 0.000$	$0.1066 \pm 0.001$

Table 25: Cosmopedia - Holdout-CO ( $\mathcal{H}_{col}$ ). Mean across 30 seeds; CI = 95% CI on the mean.

Epoch	Law	Design	$R^2$ Train	$R^2 \mathcal{H}_{col}$	RMSE Train	RMSE $\mathcal{H}_{col}$
-	Repeated-data	Collinear	$0.9841 \pm 0.000$	$0.9646 \pm 0.000$	$0.1805 \pm 0.000$	$0.1137 \pm 0.000$
		Non-Collinear	$0.9656 \pm 0.000$	<b><math>0.9719 \pm 0.000</math></b>	$0.1862 \pm 0.000$	$0.1014 \pm 0.000$
	Chinchilla	Collinear	$0.9857 \pm 0.000$	$0.9573 \pm 0.004$	$0.1401 \pm 0.001$	$0.1119 \pm 0.005$
		Non-Collinear	$0.9502 \pm 0.000$	<b><math>0.9618 \pm 0.003</math></b>	$0.1807 \pm 0.000$	$0.1060 \pm 0.004$
Final	Droppo-Elibol	Collinear	$0.9861 \pm 0.000$	$0.9651 \pm 0.001$	$0.1382 \pm 0.000$	$0.1019 \pm 0.001$
		Non-Collinear	$0.9545 \pm 0.000$	<b><math>0.9658 \pm 0.001</math></b>	$0.1728 \pm 0.000$	$0.1007 \pm 0.002$
	Kaplan	Collinear	$0.9847 \pm 0.000$	<b><math>0.9593 \pm 0.000</math></b>	$0.1446 \pm 0.000$	$0.1100 \pm 0.000$
		Non-Collinear	$0.9500 \pm 0.000$	$0.9578 \pm 0.001$	$0.1811 \pm 0.000$	$0.1121 \pm 0.001$
	Chinchilla	Collinear	$0.9858 \pm 0.000$	$0.9100 \pm 0.003$	$0.2020 \pm 0.000$	$0.1980 \pm 0.004$
		Non-Collinear	$0.9741 \pm 0.000$	<b><math>0.9693 \pm 0.003</math></b>	$0.1947 \pm 0.001$	$0.1145 \pm 0.006$
First	Droppo-Elibol	Collinear	$0.9858 \pm 0.000$	$0.9041 \pm 0.008$	$0.2023 \pm 0.001$	$0.2034 \pm 0.008$
		Non-Collinear	$0.9826 \pm 0.000$	<b><math>0.9736 \pm 0.001</math></b>	$0.1598 \pm 0.000$	$0.1070 \pm 0.003$
	Kaplan	Collinear	$0.9814 \pm 0.000$	$0.8048 \pm 0.014$	$0.2313 \pm 0.001$	$0.2909 \pm 0.009$
		Non-Collinear	$0.9704 \pm 0.000$	<b><math>0.9681 \pm 0.001</math></b>	$0.2083 \pm 0.000$	$0.1179 \pm 0.001$
	Chinchilla	Collinear	$0.9867 \pm 0.000$	<b><math>0.9612 \pm 0.002</math></b>	$0.1464 \pm 0.001$	$0.1093 \pm 0.003$
		Non-Collinear	$0.9574 \pm 0.000$	$0.9590 \pm 0.006$	$0.1812 \pm 0.001$	$0.1110 \pm 0.007$
Second	Droppo-Elibol	Collinear	$0.9869 \pm 0.000$	$0.9650 \pm 0.001$	$0.1451 \pm 0.001$	$0.1039 \pm 0.002$
		Non-Collinear	$0.9615 \pm 0.000$	<b><math>0.9695 \pm 0.001</math></b>	$0.1722 \pm 0.000$	$0.0968 \pm 0.002$
	Kaplan	Collinear	$0.9846 \pm 0.000$	$0.9483 \pm 0.001$	$0.1575 \pm 0.000$	$0.1264 \pm 0.001$
		Non-Collinear	$0.9569 \pm 0.000$	<b><math>0.9621 \pm 0.001</math></b>	$0.1822 \pm 0.000$	$0.1081 \pm 0.001$

Table 26: Cosmopedia - Holdout-NC ( $\mathcal{H}_{nc}$ ). Mean across 30 seeds; CI = 95% CI on the mean.

Epoch	Law	Design	$R^2$ Train	$R^2 \mathcal{H}_{nc}$	RMSE Train	RMSE $\mathcal{H}_{nc}$
-	Repeated-data	Collinear	$0.9841 \pm 0.000$	$0.9335 \pm 0.000$	$0.1805 \pm 0.000$	$0.1504 \pm 0.000$
		Non-Collinear	$0.9656 \pm 0.000$	<b><math>0.9646 \pm 0.000</math></b>	$0.1862 \pm 0.000$	$0.1097 \pm 0.000$
	Chinchilla	Collinear	$0.9857 \pm 0.000$	$0.9308 \pm 0.006$	$0.1401 \pm 0.001$	$0.1323 \pm 0.005$
		Non-Collinear	$0.9502 \pm 0.000$	<b><math>0.9536 \pm 0.004</math></b>	$0.1807 \pm 0.000$	$0.1085 \pm 0.004$
Final	Droppo-Elibol	Collinear	$0.9861 \pm 0.000$	$0.9500 \pm 0.002$	$0.1382 \pm 0.000$	$0.1131 \pm 0.002$
		Non-Collinear	$0.9545 \pm 0.000$	<b><math>0.9583 \pm 0.001</math></b>	$0.1728 \pm 0.000$	$0.1033 \pm 0.002$
	Kaplan	Collinear	$0.9847 \pm 0.000$	$0.9235 \pm 0.000$	$0.1446 \pm 0.000$	$0.1400 \pm 0.000$
		Non-Collinear	$0.9500 \pm 0.000$	<b><math>0.9536 \pm 0.001</math></b>	$0.1811 \pm 0.000$	$0.1090 \pm 0.001$
	Chinchilla	Collinear	$0.9858 \pm 0.000$	$0.8814 \pm 0.002$	$0.2020 \pm 0.000$	$0.2241 \pm 0.002$
		Non-Collinear	$0.9741 \pm 0.000$	<b><math>0.9556 \pm 0.003</math></b>	$0.1947 \pm 0.001$	$0.1365 \pm 0.005$
First	Droppo-Elibol	Collinear	$0.9858 \pm 0.000$	$0.8713 \pm 0.013$	$0.2023 \pm 0.001$	$0.2317 \pm 0.011$
		Non-Collinear	$0.9826 \pm 0.000$	<b><math>0.9684 \pm 0.001</math></b>	$0.1598 \pm 0.000$	$0.1155 \pm 0.002$
	Kaplan	Collinear	$0.9814 \pm 0.000$	$0.6829 \pm 0.016$	$0.2313 \pm 0.001$	$0.3660 \pm 0.008$
		Non-Collinear	$0.9704 \pm 0.000$	<b><math>0.9641 \pm 0.001</math></b>	$0.2083 \pm 0.000$	$0.1234 \pm 0.001$
	Chinchilla	Collinear	$0.9867 \pm 0.000$	$0.9388 \pm 0.003$	$0.1464 \pm 0.001$	$0.1323 \pm 0.003$
		Non-Collinear	$0.9574 \pm 0.000$	<b><math>0.9555 \pm 0.006</math></b>	$0.1812 \pm 0.001$	$0.1117 \pm 0.006$
Second	Droppo-Elibol	Collinear	$0.9869 \pm 0.000$	$0.9468 \pm 0.005$	$0.1451 \pm 0.001$	$0.1228 \pm 0.005$
		Non-Collinear	$0.9615 \pm 0.000$	<b><math>0.9656 \pm 0.001</math></b>	$0.1722 \pm 0.000$	$0.0993 \pm 0.002$
	Kaplan	Collinear	$0.9846 \pm 0.000$	$0.9070 \pm 0.001$	$0.1575 \pm 0.000$	$0.1634 \pm 0.001$
		Non-Collinear	$0.9569 \pm 0.000$	<b><math>0.9615 \pm 0.001</math></b>	$0.1822 \pm 0.000$	$0.1051 \pm 0.001$

Table 27: peS2o - Holdout ( $\mathcal{H}$ ). Mean across 30 seeds; CI = 95% CI on the mean.

Epoch	Law	Design	$R^2$ Train	$R^2 \mathcal{H}$	RMSE Train	RMSE $\mathcal{H}$
-	Repeated-data	Collinear	$0.9862 \pm 0.000$	$0.9232 \pm 0.000$	$0.1588 \pm 0.000$	$0.1545 \pm 0.000$
		Non-Collinear	$0.9616 \pm 0.000$	<b><math>0.9464 \pm 0.000</math></b>	$0.1836 \pm 0.000$	$0.1290 \pm 0.000$
	Chinchilla	Collinear	$0.9829 \pm 0.000$	$0.9055 \pm 0.002$	$0.1463 \pm 0.000$	$0.1446 \pm 0.002$
		Non-Collinear	$0.9367 \pm 0.000$	<b><math>0.9421 \pm 0.002</math></b>	$0.1833 \pm 0.000$	$0.1132 \pm 0.002$
Final	Droppo-Elibol	Collinear	$0.9833 \pm 0.000$	$0.9081 \pm 0.004$	$0.1447 \pm 0.000$	$0.1425 \pm 0.003$
		Non-Collinear	$0.9426 \pm 0.000$	<b><math>0.9520 \pm 0.001</math></b>	$0.1744 \pm 0.001$	$0.1031 \pm 0.001$
	Kaplan	Collinear	$0.9810 \pm 0.000$	$0.8310 \pm 0.002$	$0.1543 \pm 0.000$	$0.1935 \pm 0.001$
		Non-Collinear	$0.9354 \pm 0.000$	<b><math>0.9409 \pm 0.002</math></b>	$0.1851 \pm 0.001$	$0.1143 \pm 0.002$
	Chinchilla	Collinear	$0.9887 \pm 0.000$	$0.8821 \pm 0.004$	$0.1674 \pm 0.000$	$0.2192 \pm 0.003$
		Non-Collinear	$0.9734 \pm 0.000$	<b><math>0.9272 \pm 0.006</math></b>	$0.1873 \pm 0.001$	$0.1711 \pm 0.007$
First	Droppo-Elibol	Collinear	$0.9887 \pm 0.000$	$0.8776 \pm 0.002$	$0.1675 \pm 0.000$	$0.2234 \pm 0.002$
		Non-Collinear	$0.9810 \pm 0.000$	<b><math>0.9435 \pm 0.000</math></b>	$0.1586 \pm 0.000$	$0.1517 \pm 0.001$
	Kaplan	Collinear	$0.9845 \pm 0.000$	$0.7131 \pm 0.004$	$0.1963 \pm 0.000$	$0.3420 \pm 0.002$
		Non-Collinear	$0.9676 \pm 0.000$	<b><math>0.9444 \pm 0.001</math></b>	$0.2068 \pm 0.001$	$0.1506 \pm 0.001$
	Chinchilla	Collinear	$0.9863 \pm 0.000$	$0.9108 \pm 0.003$	$0.1408 \pm 0.000$	$0.1483 \pm 0.002$
		Non-Collinear	$0.9484 \pm 0.000$	<b><math>0.9389 \pm 0.004</math></b>	$0.1822 \pm 0.001$	$0.1223 \pm 0.004$
Second	Droppo-Elibol	Collinear	$0.9864 \pm 0.000$	$0.9105 \pm 0.004$	$0.1404 \pm 0.000$	$0.1484 \pm 0.003$
		Non-Collinear	$0.9546 \pm 0.000$	<b><math>0.9534 \pm 0.001</math></b>	$0.1709 \pm 0.000$	$0.1072 \pm 0.001$
	Kaplan	Collinear	$0.9834 \pm 0.000$	$0.8129 \pm 0.002$	$0.1553 \pm 0.000$	$0.2150 \pm 0.001$
		Non-Collinear	$0.9455 \pm 0.000$	<b><math>0.9457 \pm 0.001</math></b>	$0.1872 \pm 0.001$	$0.1158 \pm 0.001$

Table 28: peS2o - Holdout-CO ( $\mathcal{H}_{col}$ ). Mean across 30 seeds; CI = 95% CI on the mean.

Epoch	Law	Design	$R^2$ Train	$R^2 \mathcal{H}_{col}$	RMSE Train	RMSE $\mathcal{H}_{col}$
-	Repeated-data	Collinear	$0.9862 \pm 0.000$	$0.9495 \pm 0.000$	$0.1588 \pm 0.000$	$0.1312 \pm 0.000$
		Non-Collinear	$0.9616 \pm 0.000$	<b><math>0.9513 \pm 0.000</math></b>	$0.1836 \pm 0.000$	$0.1290 \pm 0.000$
	Chinchilla	Collinear	$0.9829 \pm 0.000$	$0.9370 \pm 0.003$	$0.1463 \pm 0.000$	$0.1263 \pm 0.003$
		Non-Collinear	$0.9367 \pm 0.000$	<b><math>0.9538 \pm 0.002</math></b>	$0.1833 \pm 0.000$	$0.1082 \pm 0.002$
Final	Droppo-Elibol	Collinear	$0.9833 \pm 0.000$	$0.9302 \pm 0.003$	$0.1447 \pm 0.000$	$0.1330 \pm 0.003$
		Non-Collinear	$0.9426 \pm 0.000$	<b><math>0.9620 \pm 0.001</math></b>	$0.1744 \pm 0.001$	$0.0983 \pm 0.001$
	Kaplan	Collinear	$0.9810 \pm 0.000$	$0.8872 \pm 0.002$	$0.1543 \pm 0.000$	$0.1694 \pm 0.001$
		Non-Collinear	$0.9354 \pm 0.000$	<b><math>0.9526 \pm 0.002</math></b>	$0.1851 \pm 0.001$	$0.1097 \pm 0.002$
	Chinchilla	Collinear	$0.9887 \pm 0.000$	$0.9107 \pm 0.004$	$0.1674 \pm 0.000$	$0.1979 \pm 0.004$
		Non-Collinear	$0.9734 \pm 0.000$	<b><math>0.9314 \pm 0.006</math></b>	$0.1873 \pm 0.001$	$0.1726 \pm 0.007$
First	Droppo-Elibol	Collinear	$0.9887 \pm 0.000$	$0.9077 \pm 0.006$	$0.1675 \pm 0.000$	$0.2009 \pm 0.006$
		Non-Collinear	$0.9810 \pm 0.000$	<b><math>0.9451 \pm 0.000</math></b>	$0.1586 \pm 0.000$	$0.1555 \pm 0.001$
	Kaplan	Collinear	$0.9845 \pm 0.000$	$0.7955 \pm 0.003$	$0.1963 \pm 0.000$	$0.3000 \pm 0.002$
		Non-Collinear	$0.9676 \pm 0.000$	<b><math>0.9417 \pm 0.001</math></b>	$0.2068 \pm 0.001$	$0.1602 \pm 0.001$
	Chinchilla	Collinear	$0.9863 \pm 0.000$	$0.9369 \pm 0.003$	$0.1408 \pm 0.000$	$0.1311 \pm 0.003$
		Non-Collinear	$0.9484 \pm 0.000$	<b><math>0.9482 \pm 0.004</math></b>	$0.1822 \pm 0.001$	$0.1185 \pm 0.004$
Second	Droppo-Elibol	Collinear	$0.9864 \pm 0.000$	$0.9338 \pm 0.004$	$0.1404 \pm 0.000$	$0.1342 \pm 0.004$
		Non-Collinear	$0.9546 \pm 0.000$	<b><math>0.9607 \pm 0.001</math></b>	$0.1709 \pm 0.000$	$0.1037 \pm 0.001$
	Kaplan	Collinear	$0.9834 \pm 0.000$	$0.8692 \pm 0.002$	$0.1553 \pm 0.000$	$0.1893 \pm 0.001$
		Non-Collinear	$0.9455 \pm 0.000$	<b><math>0.9517 \pm 0.001</math></b>	$0.1872 \pm 0.001$	$0.1149 \pm 0.002$

Table 29: peS2o - Holdout-NC ( $\mathcal{H}_{nc}$ ). Mean across 30 seeds; CI = 95% CI on the mean.

Epoch	Law	Design	$R^2$ Train	$R^2 \mathcal{H}_{nc}$	RMSE Train	RMSE $\mathcal{H}_{nc}$
-	Repeated-data	Collinear	$0.9862 \pm 0.000$	$0.8911 \pm 0.000$	$0.1588 \pm 0.000$	$0.1747 \pm 0.000$
		Non-Collinear	$0.9616 \pm 0.000$	<b><math>0.9405 \pm 0.000</math></b>	$0.1836 \pm 0.000$	$0.1291 \pm 0.000$
	Chinchilla	Collinear	$0.9829 \pm 0.000$	$0.8631 \pm 0.002$	$0.1463 \pm 0.000$	$0.1607 \pm 0.001$
		Non-Collinear	$0.9367 \pm 0.000$	<b><math>0.9263 \pm 0.002</math></b>	$0.1833 \pm 0.000$	$0.1179 \pm 0.002$
Final	Droppo-Elibol	Collinear	$0.9833 \pm 0.000$	$0.8783 \pm 0.006$	$0.1447 \pm 0.000$	$0.1513 \pm 0.003$
		Non-Collinear	$0.9426 \pm 0.000$	<b><math>0.9385 \pm 0.001</math></b>	$0.1744 \pm 0.001$	$0.1077 \pm 0.001$
	Kaplan	Collinear	$0.9810 \pm 0.000$	$0.7552 \pm 0.002$	$0.1543 \pm 0.000$	$0.2149 \pm 0.001$
		Non-Collinear	$0.9354 \pm 0.000$	<b><math>0.9252 \pm 0.002</math></b>	$0.1851 \pm 0.001$	$0.1187 \pm 0.001$
	Chinchilla	Collinear	$0.9887 \pm 0.000$	$0.8484 \pm 0.003$	$0.1674 \pm 0.000$	$0.2385 \pm 0.003$
		Non-Collinear	$0.9734 \pm 0.000$	<b><math>0.9223 \pm 0.007</math></b>	$0.1873 \pm 0.001$	$0.1696 \pm 0.007$
First	Droppo-Elibol	Collinear	$0.9887 \pm 0.000$	$0.8423 \pm 0.005$	$0.1675 \pm 0.000$	$0.2431 \pm 0.004$
		Non-Collinear	$0.9810 \pm 0.000$	<b><math>0.9417 \pm 0.000</math></b>	$0.1586 \pm 0.000$	$0.1479 \pm 0.001$
	Kaplan	Collinear	$0.9845 \pm 0.000$	$0.6165 \pm 0.004$	$0.1963 \pm 0.000$	$0.3794 \pm 0.002$
		Non-Collinear	$0.9676 \pm 0.000$	<b><math>0.9476 \pm 0.002</math></b>	$0.2068 \pm 0.001$	$0.1401 \pm 0.002$
	Chinchilla	Collinear	$0.9863 \pm 0.000$	$0.8782 \pm 0.003$	$0.1408 \pm 0.000$	$0.1637 \pm 0.002$
		Non-Collinear	$0.9484 \pm 0.000$	<b><math>0.9274 \pm 0.005</math></b>	$0.1822 \pm 0.001$	$0.1260 \pm 0.004$
Second	Droppo-Elibol	Collinear	$0.9864 \pm 0.000$	$0.8814 \pm 0.007$	$0.1404 \pm 0.000$	$0.1610 \pm 0.005$
		Non-Collinear	$0.9546 \pm 0.000$	<b><math>0.9443 \pm 0.001</math></b>	$0.1709 \pm 0.000$	$0.1106 \pm 0.001$
	Kaplan	Collinear	$0.9834 \pm 0.000$	$0.7428 \pm 0.003$	$0.1553 \pm 0.000$	$0.2379 \pm 0.001$
		Non-Collinear	$0.9455 \pm 0.000$	<b><math>0.9381 \pm 0.001</math></b>	$0.1872 \pm 0.001$	$0.1167 \pm 0.001$

Table 30: RedPajama - Holdout ( $\mathcal{H}$ ). Mean across 30 seeds; CI = 95% CI on the mean.

Epoch	Law	Design	$R^2$ Train	$R^2 \mathcal{H}$	RMSE Train	RMSE $\mathcal{H}$
-	Repeated-data	Collinear	$0.9879 \pm 0.000$	$0.8905 \pm 0.000$	$0.1842 \pm 0.000$	$0.2391 \pm 0.000$
		Non-Collinear	$0.9644 \pm 0.000$	<b><math>0.9290 \pm 0.000</math></b>	$0.2206 \pm 0.000$	$0.1926 \pm 0.000$
	Chinchilla	Collinear	$0.9931 \pm 0.000$	$0.8802 \pm 0.001$	$0.1254 \pm 0.000$	$0.2176 \pm 0.001$
		Non-Collinear	$0.9444 \pm 0.000$	<b><math>0.9079 \pm 0.002</math></b>	$0.2272 \pm 0.000$	$0.1908 \pm 0.002$
Final	Droppo-Elibol	Collinear	$0.9932 \pm 0.000$	$0.8932 \pm 0.008$	$0.1247 \pm 0.000$	$0.2046 \pm 0.007$
		Non-Collinear	$0.9594 \pm 0.000$	<b><math>0.9177 \pm 0.001</math></b>	$0.1941 \pm 0.000$	$0.1803 \pm 0.001$
	Kaplan	Collinear	$0.9866 \pm 0.000$	$0.6643 \pm 0.003$	$0.1750 \pm 0.000$	$0.3642 \pm 0.002$
		Non-Collinear	$0.9189 \pm 0.001$	<b><math>0.8776 \pm 0.003</math></b>	$0.2741 \pm 0.002$	$0.2199 \pm 0.002$
	Chinchilla	Collinear	$0.9851 \pm 0.000$	$0.7692 \pm 0.006$	$0.2236 \pm 0.000$	$0.3902 \pm 0.005$
		Non-Collinear	$0.9790 \pm 0.000$	<b><math>0.9102 \pm 0.004</math></b>	$0.1992 \pm 0.001$	$0.2430 \pm 0.006$
First	Droppo-Elibol	Collinear	$0.9852 \pm 0.000$	$0.7471 \pm 0.009$	$0.2226 \pm 0.000$	$0.4082 \pm 0.007$
		Non-Collinear	$0.9865 \pm 0.000$	<b><math>0.9299 \pm 0.001</math></b>	$0.1595 \pm 0.000$	$0.2152 \pm 0.001$
	Kaplan	Collinear	$0.9838 \pm 0.000$	$0.5222 \pm 0.005$	$0.2332 \pm 0.000$	$0.5618 \pm 0.003$
		Non-Collinear	$0.9571 \pm 0.000$	<b><math>0.9035 \pm 0.001</math></b>	$0.2844 \pm 0.000$	$0.2525 \pm 0.001$
	Chinchilla	Collinear	$0.9923 \pm 0.000$	$0.8823 \pm 0.002$	$0.1388 \pm 0.000$	$0.2252 \pm 0.002$
		Non-Collinear	$0.9538 \pm 0.000$	<b><math>0.9118 \pm 0.004</math></b>	$0.2235 \pm 0.001$	$0.1945 \pm 0.004$
Second	Droppo-Elibol	Collinear	$0.9923 \pm 0.000$	$0.8877 \pm 0.008$	$0.1385 \pm 0.000$	$0.2190 \pm 0.007$
		Non-Collinear	$0.9678 \pm 0.000$	<b><math>0.9217 \pm 0.001</math></b>	$0.1866 \pm 0.000$	$0.1836 \pm 0.001$
	Kaplan	Collinear	$0.9856 \pm 0.000$	$0.6351 \pm 0.006$	$0.1898 \pm 0.000$	$0.3964 \pm 0.003$
		Non-Collinear	$0.9265 \pm 0.001$	<b><math>0.8827 \pm 0.004</math></b>	$0.2819 \pm 0.002$	$0.2246 \pm 0.004$

Table 31: RedPajama - Holdout-CO ( $\mathcal{H}_{\text{col}}$ ). Mean across 30 seeds; CI = 95% CI on the mean.

Epoch	Law	Design	$R^2$ Train	$R^2 \mathcal{H}_{\text{col}}$	RMSE Train	RMSE $\mathcal{H}_{\text{col}}$
-	Repeated-data	Collinear	$0.9879 \pm 0.000$	<b><math>0.9604 \pm 0.000</math></b>	$0.1842 \pm 0.000$	$0.1648 \pm 0.000$
		Non-Collinear	$0.9644 \pm 0.000$	$0.9427 \pm 0.000$	$0.2206 \pm 0.000$	$0.1981 \pm 0.000$
	Chinchilla	Collinear	$0.9931 \pm 0.000$	<b><math>0.9672 \pm 0.001</math></b>	$0.1254 \pm 0.000$	$0.1329 \pm 0.002$
		Non-Collinear	$0.9444 \pm 0.000$	$0.9324 \pm 0.002$	$0.2272 \pm 0.000$	$0.1908 \pm 0.002$
Final	Droppo-Elibol	Collinear	$0.9932 \pm 0.000$	<b><math>0.9635 \pm 0.002</math></b>	$0.1247 \pm 0.000$	$0.1401 \pm 0.003$
		Non-Collinear	$0.9594 \pm 0.000$	$0.9379 \pm 0.001$	$0.1941 \pm 0.000$	$0.1830 \pm 0.001$
	Kaplan	Collinear	$0.9866 \pm 0.000$	$0.8875 \pm 0.002$	$0.1750 \pm 0.000$	$0.2463 \pm 0.002$
		Non-Collinear	$0.9189 \pm 0.001$	<b><math>0.9080 \pm 0.003</math></b>	$0.2741 \pm 0.002$	$0.2226 \pm 0.004$
	Chinchilla	Collinear	$0.9851 \pm 0.000$	$0.8506 \pm 0.005$	$0.2236 \pm 0.000$	$0.3570 \pm 0.006$
		Non-Collinear	$0.9790 \pm 0.000$	<b><math>0.9292 \pm 0.004</math></b>	$0.1992 \pm 0.001$	$0.2454 \pm 0.007$
First	Droppo-Elibol	Collinear	$0.9852 \pm 0.000$	$0.8981 \pm 0.007$	$0.2226 \pm 0.000$	$0.2941 \pm 0.009$
		Non-Collinear	$0.9865 \pm 0.000$	<b><math>0.9416 \pm 0.001</math></b>	$0.1595 \pm 0.000$	$0.2234 \pm 0.001$
	Kaplan	Collinear	$0.9838 \pm 0.000$	$0.8069 \pm 0.003$	$0.2332 \pm 0.000$	$0.4062 \pm 0.004$
		Non-Collinear	$0.9571 \pm 0.000$	<b><math>0.9228 \pm 0.000</math></b>	$0.2844 \pm 0.000$	$0.2569 \pm 0.001$
	Chinchilla	Collinear	$0.9923 \pm 0.000$	<b><math>0.9625 \pm 0.002</math></b>	$0.1388 \pm 0.000$	$0.1471 \pm 0.003$
		Non-Collinear	$0.9538 \pm 0.000$	$0.9374 \pm 0.003$	$0.2235 \pm 0.001$	$0.1901 \pm 0.005$
Second	Droppo-Elibol	Collinear	$0.9923 \pm 0.000$	<b><math>0.9577 \pm 0.003</math></b>	$0.1385 \pm 0.000$	$0.1560 \pm 0.005$
		Non-Collinear	$0.9678 \pm 0.000$	$0.9421 \pm 0.001$	$0.1866 \pm 0.000$	$0.1832 \pm 0.001$
	Kaplan	Collinear	$0.9856 \pm 0.000$	$0.8666 \pm 0.003$	$0.1898 \pm 0.000$	$0.2780 \pm 0.004$
		Non-Collinear	$0.9265 \pm 0.001$	<b><math>0.9099 \pm 0.005</math></b>	$0.2819 \pm 0.002$	$0.2280 \pm 0.006$

Table 32: RedPajama - Holdout-NC ( $\mathcal{H}_{nc}$ ). Mean across 30 seeds; CI = 95% CI on the mean.

Epoch	Law	Design	$R^2$ Train	$R^2 \mathcal{H}_{nc}$	RMSE Train	RMSE $\mathcal{H}_{nc}$
-	Repeated-data	Collinear	$0.9879 \pm 0.000$	$0.7560 \pm 0.000$	$0.1842 \pm 0.000$	$0.2953 \pm 0.000$
		Non-Collinear	$0.9644 \pm 0.000$	<b><math>0.9023 \pm 0.000</math></b>	$0.2206 \pm 0.000$	$0.1868 \pm 0.000$
	Chinchilla	Collinear	$0.9931 \pm 0.000$	$0.6910 \pm 0.001$	$0.1254 \pm 0.000$	$0.2775 \pm 0.001$
		Non-Collinear	$0.9444 \pm 0.000$	<b><math>0.8540 \pm 0.003</math></b>	$0.2272 \pm 0.000$	$0.1907 \pm 0.002$
Final	Droppo-Elibol	Collinear	$0.9932 \pm 0.000$	$0.7403 \pm 0.026$	$0.1247 \pm 0.000$	$0.2523 \pm 0.012$
		Non-Collinear	$0.9594 \pm 0.000$	<b><math>0.8734 \pm 0.002</math></b>	$0.1941 \pm 0.000$	$0.1776 \pm 0.001$
	Kaplan	Collinear	$0.9866 \pm 0.000$	$0.1789 \pm 0.006$	$0.1750 \pm 0.000$	$0.4524 \pm 0.002$
		Non-Collinear	$0.9189 \pm 0.001$	<b><math>0.8108 \pm 0.002</math></b>	$0.2741 \pm 0.002$	$0.2171 \pm 0.001$
	Chinchilla	Collinear	$0.9851 \pm 0.000$	$0.6182 \pm 0.007$	$0.2236 \pm 0.000$	$0.4208 \pm 0.004$
		Non-Collinear	$0.9790 \pm 0.000$	<b><math>0.8750 \pm 0.005</math></b>	$0.1992 \pm 0.001$	$0.2405 \pm 0.005$
First	Droppo-Elibol	Collinear	$0.9852 \pm 0.000$	$0.4679 \pm 0.035$	$0.2226 \pm 0.000$	$0.4948 \pm 0.017$
		Non-Collinear	$0.9865 \pm 0.000$	<b><math>0.9081 \pm 0.001</math></b>	$0.1595 \pm 0.000$	$0.2065 \pm 0.001$
	Kaplan	Collinear	$0.9838 \pm 0.000$	$-0.0044 \pm 0.009$	$0.2332 \pm 0.000$	$0.6827 \pm 0.003$
		Non-Collinear	$0.9571 \pm 0.000$	<b><math>0.8675 \pm 0.003</math></b>	$0.2844 \pm 0.000$	$0.2479 \pm 0.002$
	Chinchilla	Collinear	$0.9923 \pm 0.000$	$0.7156 \pm 0.002$	$0.1388 \pm 0.000$	$0.2823 \pm 0.001$
		Non-Collinear	$0.9538 \pm 0.000$	<b><math>0.8586 \pm 0.005</math></b>	$0.2235 \pm 0.001$	$0.1988 \pm 0.004$
Second	Droppo-Elibol	Collinear	$0.9923 \pm 0.000$	$0.7423 \pm 0.028$	$0.1385 \pm 0.000$	$0.2661 \pm 0.014$
		Non-Collinear	$0.9678 \pm 0.000$	<b><math>0.8792 \pm 0.001</math></b>	$0.1866 \pm 0.000$	$0.1840 \pm 0.001$
	Kaplan	Collinear	$0.9856 \pm 0.000$	$0.1543 \pm 0.010$	$0.1898 \pm 0.000$	$0.4868 \pm 0.003$
		Non-Collinear	$0.9265 \pm 0.001$	<b><math>0.8258 \pm 0.003</math></b>	$0.2819 \pm 0.002$	$0.2209 \pm 0.002$

Table 33: Wikipedia - Holdout ( $\mathcal{H}$ ). Mean across 30 seeds; CI = 95% CI on the mean.

Epoch	Law	Design	$R^2$ Train	$R^2 \mathcal{H}$	RMSE Train	RMSE $\mathcal{H}$
-	Repeated-data	Collinear	$0.9853 \pm 0.000$	$0.8666 \pm 0.000$	$0.2247 \pm 0.000$	$0.2779 \pm 0.000$
		Non-Collinear	$0.9585 \pm 0.000$	<b><math>0.9155 \pm 0.000</math></b>	$0.2594 \pm 0.000$	$0.2212 \pm 0.000$
	Chinchilla	Collinear	$0.9918 \pm 0.000$	$0.8609 \pm 0.002$	$0.1507 \pm 0.000$	$0.2462 \pm 0.002$
		Non-Collinear	$0.9372 \pm 0.000$	<b><math>0.8974 \pm 0.002</math></b>	$0.2626 \pm 0.000$	$0.2115 \pm 0.002$
Final	Droppo-Elibol	Collinear	$0.9919 \pm 0.000$	$0.8701 \pm 0.011$	$0.1500 \pm 0.000$	$0.2366 \pm 0.010$
		Non-Collinear	$0.9567 \pm 0.000$	<b><math>0.9136 \pm 0.001</math></b>	$0.2181 \pm 0.000$	$0.1941 \pm 0.001$
	Kaplan	Collinear	$0.9849 \pm 0.000$	$0.6063 \pm 0.003$	$0.2052 \pm 0.000$	$0.4143 \pm 0.002$
		Non-Collinear	$0.9271 \pm 0.000$	<b><math>0.8850 \pm 0.000</math></b>	$0.2830 \pm 0.000$	$0.2240 \pm 0.000$
	Chinchilla	Collinear	$0.9823 \pm 0.000$	$0.7438 \pm 0.006$	$0.2704 \pm 0.001$	$0.4360 \pm 0.006$
		Non-Collinear	$0.9750 \pm 0.000$	<b><math>0.8947 \pm 0.003</math></b>	$0.2367 \pm 0.001$	$0.2796 \pm 0.004$
First	Droppo-Elibol	Collinear	$0.9823 \pm 0.000$	$0.7450 \pm 0.013$	$0.2704 \pm 0.000$	$0.4342 \pm 0.011$
		Non-Collinear	$0.9847 \pm 0.000$	<b><math>0.9222 \pm 0.001</math></b>	$0.1848 \pm 0.000$	$0.2404 \pm 0.001$
	Kaplan	Collinear	$0.9786 \pm 0.001$	$0.5540 \pm 0.025$	$0.2963 \pm 0.009$	$0.5737 \pm 0.017$
		Non-Collinear	$0.9550 \pm 0.000$	<b><math>0.8903 \pm 0.001</math></b>	$0.3173 \pm 0.000$	$0.2855 \pm 0.001$
	Chinchilla	Collinear	$0.9906 \pm 0.000$	$0.8575 \pm 0.004$	$0.1691 \pm 0.000$	$0.2623 \pm 0.003$
		Non-Collinear	$0.9461 \pm 0.000$	<b><math>0.8804 \pm 0.003</math></b>	$0.2640 \pm 0.000$	$0.2404 \pm 0.003$
Second	Droppo-Elibol	Collinear	$0.9906 \pm 0.000$	$0.8467 \pm 0.012$	$0.1692 \pm 0.000$	$0.2708 \pm 0.010$
		Non-Collinear	$0.9643 \pm 0.000$	<b><math>0.8976 \pm 0.001</math></b>	$0.2148 \pm 0.000$	$0.2225 \pm 0.001$
	Kaplan	Collinear	$0.9843 \pm 0.000$	$0.5652 \pm 0.006$	$0.2193 \pm 0.000$	$0.4584 \pm 0.003$
		Non-Collinear	$0.9314 \pm 0.001$	<b><math>0.8843 \pm 0.000</math></b>	$0.2977 \pm 0.002$	$0.2365 \pm 0.000$

Table 34: Wikipedia - Holdout-CO ( $\mathcal{H}_{col}$ ). Mean across 30 seeds; CI = 95% CI on the mean.

Epoch	Law	Design	$R^2$ Train	$R^2 \mathcal{H}_{col}$	RMSE Train	RMSE $\mathcal{H}_{col}$
-	Repeated-data	Collinear	$0.9853 \pm 0.000$	<b><math>0.9521 \pm 0.000</math></b>	$0.2247 \pm 0.000$	$0.1930 \pm 0.000$
		Non-Collinear	$0.9585 \pm 0.000$	$0.9317 \pm 0.000$	$0.2594 \pm 0.000$	$0.2304 \pm 0.000$
	Chinchilla	Collinear	$0.9918 \pm 0.000$	<b><math>0.9632 \pm 0.002</math></b>	$0.1507 \pm 0.000$	$0.1485 \pm 0.004$
		Non-Collinear	$0.9372 \pm 0.000$	$0.9280 \pm 0.001$	$0.2626 \pm 0.000$	$0.2085 \pm 0.002$
Final	Droppo-Elibol	Collinear	$0.9919 \pm 0.000$	<b><math>0.9611 \pm 0.002</math></b>	$0.1500 \pm 0.000$	$0.1529 \pm 0.004$
		Non-Collinear	$0.9567 \pm 0.000$	$0.9377 \pm 0.001$	$0.2181 \pm 0.000$	$0.1939 \pm 0.001$
	Kaplan	Collinear	$0.9849 \pm 0.000$	$0.8583 \pm 0.002$	$0.2052 \pm 0.000$	$0.2925 \pm 0.002$
		Non-Collinear	$0.9271 \pm 0.000$	<b><math>0.9099 \pm 0.000</math></b>	$0.2830 \pm 0.000$	$0.2333 \pm 0.000$
	Chinchilla	Collinear	$0.9823 \pm 0.000$	$0.8384 \pm 0.005$	$0.2704 \pm 0.001$	$0.3984 \pm 0.007$
		Non-Collinear	$0.9750 \pm 0.000$	<b><math>0.9201 \pm 0.002</math></b>	$0.2367 \pm 0.001$	$0.2803 \pm 0.004$
First	Droppo-Elibol	Collinear	$0.9823 \pm 0.000$	$0.8361 \pm 0.002$	$0.2704 \pm 0.000$	$0.4016 \pm 0.002$
		Non-Collinear	$0.9847 \pm 0.000$	<b><math>0.9371 \pm 0.001</math></b>	$0.1848 \pm 0.000$	$0.2489 \pm 0.001$
	Kaplan	Collinear	$0.9786 \pm 0.001$	$0.8566 \pm 0.018$	$0.2963 \pm 0.009$	$0.3691 \pm 0.025$
		Non-Collinear	$0.9550 \pm 0.000$	<b><math>0.9162 \pm 0.000</math></b>	$0.3173 \pm 0.000$	$0.2872 \pm 0.000$
	Chinchilla	Collinear	$0.9906 \pm 0.000$	<b><math>0.9544 \pm 0.003</math></b>	$0.1691 \pm 0.000$	$0.1733 \pm 0.006$
		Non-Collinear	$0.9461 \pm 0.000$	$0.9138 \pm 0.002$	$0.2640 \pm 0.000$	$0.2394 \pm 0.003$
Second	Droppo-Elibol	Collinear	$0.9906 \pm 0.000$	<b><math>0.9525 \pm 0.005</math></b>	$0.1692 \pm 0.000$	$0.1762 \pm 0.008$
		Non-Collinear	$0.9643 \pm 0.000$	$0.9240 \pm 0.001$	$0.2148 \pm 0.000$	$0.2248 \pm 0.001$
	Kaplan	Collinear	$0.9843 \pm 0.000$	$0.8332 \pm 0.004$	$0.2193 \pm 0.000$	$0.3330 \pm 0.003$
		Non-Collinear	$0.9314 \pm 0.001$	<b><math>0.9059 \pm 0.001</math></b>	$0.2977 \pm 0.002$	$0.2501 \pm 0.001$

Table 35: Wikipedia - Holdout-NC ( $\mathcal{H}_{nc}$ ). Mean across 30 seeds; CI = 95% CI on the mean.

Epoch	Law	Design	$R^2$ Train	$R^2 \mathcal{H}_{nc}$	RMSE Train	RMSE $\mathcal{H}_{nc}$
-	Repeated-data	Collinear	$0.9853 \pm 0.000$	$0.6905 \pm 0.000$	$0.2247 \pm 0.000$	$0.3423 \pm 0.000$
		Non-Collinear	$0.9585 \pm 0.000$	<b><math>0.8817 \pm 0.000</math></b>	$0.2594 \pm 0.000$	$0.2116 \pm 0.000$
	Chinchilla	Collinear	$0.9918 \pm 0.000$	$0.6288 \pm 0.002$	$0.1507 \pm 0.000$	$0.3148 \pm 0.001$
		Non-Collinear	$0.9372 \pm 0.000$	<b><math>0.8276 \pm 0.003</math></b>	$0.2626 \pm 0.000$	$0.2145 \pm 0.002$
Final	Droppo-Elibol	Collinear	$0.9919 \pm 0.000$	$0.6637 \pm 0.037$	$0.1500 \pm 0.000$	$0.2963 \pm 0.016$
		Non-Collinear	$0.9567 \pm 0.000$	<b><math>0.8586 \pm 0.002</math></b>	$0.2181 \pm 0.000$	$0.1943 \pm 0.001$
	Kaplan	Collinear	$0.9849 \pm 0.000$	$0.0343 \pm 0.006$	$0.2052 \pm 0.000$	$0.5078 \pm 0.002$
		Non-Collinear	$0.9271 \pm 0.000$	<b><math>0.8281 \pm 0.000</math></b>	$0.2830 \pm 0.000$	$0.2142 \pm 0.000$
	Chinchilla	Collinear	$0.9823 \pm 0.000$	$0.5555 \pm 0.008$	$0.2704 \pm 0.001$	$0.4707 \pm 0.005$
		Non-Collinear	$0.9750 \pm 0.000$	<b><math>0.8439 \pm 0.004</math></b>	$0.2367 \pm 0.001$	$0.2788 \pm 0.004$
First	Droppo-Elibol	Collinear	$0.9823 \pm 0.000$	$0.5638 \pm 0.037$	$0.2704 \pm 0.000$	$0.4637 \pm 0.018$
		Non-Collinear	$0.9847 \pm 0.000$	<b><math>0.8925 \pm 0.001</math></b>	$0.1848 \pm 0.000$	$0.2315 \pm 0.001$
	Kaplan	Collinear	$0.9786 \pm 0.001$	$-0.0459 \pm 0.045$	$0.2963 \pm 0.009$	$0.7208 \pm 0.016$
		Non-Collinear	$0.9550 \pm 0.000$	<b><math>0.8385 \pm 0.002</math></b>	$0.3173 \pm 0.000$	$0.2838 \pm 0.002$
	Chinchilla	Collinear	$0.9906 \pm 0.000$	$0.6424 \pm 0.004$	$0.1691 \pm 0.000$	$0.3277 \pm 0.002$
		Non-Collinear	$0.9461 \pm 0.000$	<b><math>0.8058 \pm 0.004</math></b>	$0.2640 \pm 0.000$	$0.2414 \pm 0.003$
Second	Droppo-Elibol	Collinear	$0.9906 \pm 0.000$	$0.6117 \pm 0.044$	$0.1692 \pm 0.000$	$0.3375 \pm 0.019$
		Non-Collinear	$0.9643 \pm 0.000$	<b><math>0.8386 \pm 0.002</math></b>	$0.2148 \pm 0.000$	$0.2202 \pm 0.001$
	Kaplan	Collinear	$0.9843 \pm 0.000$	$-0.0303 \pm 0.011$	$0.2193 \pm 0.000$	$0.5563 \pm 0.003$
		Non-Collinear	$0.9314 \pm 0.001$	<b><math>0.8359 \pm 0.002</math></b>	$0.2977 \pm 0.002$	$0.2220 \pm 0.001$

Table 36: Wikipedia (BF16) - Holdout ( $\mathcal{H}$ ). Mean across 30 seeds; CI = 95% CI on the mean.

Epoch	Law	Design	$R^2$ Train	$R^2 \mathcal{H}$	RMSE Train	RMSE $\mathcal{H}$
-	Repeated-data	Collinear	$0.9882 \pm 0.000$	$0.9410 \pm 0.000$	$0.1990 \pm 0.000$	$0.2574 \pm 0.000$
		Non-Collinear	$0.9856 \pm 0.000$	<b><math>0.9729 \pm 0.000</math></b>	$0.1824 \pm 0.000$	$0.1744 \pm 0.000$
	Chinchilla	Collinear	$0.9916 \pm 0.000$	$0.9528 \pm 0.001$	$0.1601 \pm 0.000$	$0.2273 \pm 0.003$
		Non-Collinear	$0.9915 \pm 0.000$	<b><math>0.9675 \pm 0.002</math></b>	$0.1334 \pm 0.000$	$0.1882 \pm 0.005$
Final	Droppo-Elibol	Collinear	$0.9917 \pm 0.000$	$0.9559 \pm 0.001$	$0.1596 \pm 0.000$	$0.2199 \pm 0.002$
		Non-Collinear	$0.9916 \pm 0.000$	<b><math>0.9664 \pm 0.001</math></b>	$0.1328 \pm 0.000$	$0.1918 \pm 0.002$
	Kaplan	Collinear	$0.9915 \pm 0.000$	$0.9453 \pm 0.001$	$0.1612 \pm 0.000$	$0.2450 \pm 0.001$
		Non-Collinear	$0.9898 \pm 0.000$	<b><math>0.9663 \pm 0.000</math></b>	$0.1458 \pm 0.000$	$0.1923 \pm 0.001$
	Chinchilla	Collinear	$0.9857 \pm 0.000$	$0.9061 \pm 0.003$	$0.2331 \pm 0.000$	$0.3303 \pm 0.006$
		Non-Collinear	$0.9893 \pm 0.000$	<b><math>0.9765 \pm 0.002</math></b>	$0.1689 \pm 0.001$	$0.1647 \pm 0.006$
First	Droppo-Elibol	Collinear	$0.9858 \pm 0.000$	$0.9243 \pm 0.002$	$0.2324 \pm 0.000$	$0.2967 \pm 0.004$
		Non-Collinear	$0.9923 \pm 0.000$	<b><math>0.9614 \pm 0.001</math></b>	$0.1438 \pm 0.000$	$0.2118 \pm 0.003$
	Kaplan	Collinear	$0.9856 \pm 0.000$	$0.9249 \pm 0.001$	$0.2342 \pm 0.000$	$0.2957 \pm 0.002$
		Non-Collinear	$0.9922 \pm 0.000$	<b><math>0.9525 \pm 0.000</math></b>	$0.1446 \pm 0.000$	$0.2351 \pm 0.001$
	Chinchilla	Collinear	$0.9920 \pm 0.000$	$0.9550 \pm 0.001$	$0.1578 \pm 0.000$	$0.2217 \pm 0.003$
		Non-Collinear	$0.9918 \pm 0.000$	<b><math>0.9698 \pm 0.002</math></b>	$0.1329 \pm 0.001$	$0.1813 \pm 0.006$
Second	Droppo-Elibol	Collinear	$0.9920 \pm 0.000$	$0.9571 \pm 0.002$	$0.1574 \pm 0.000$	$0.2165 \pm 0.004$
		Non-Collinear	$0.9921 \pm 0.000$	<b><math>0.9635 \pm 0.001</math></b>	$0.1301 \pm 0.000$	$0.1997 \pm 0.003$
	Kaplan	Collinear	$0.9919 \pm 0.000$	$0.9494 \pm 0.001$	$0.1588 \pm 0.000$	$0.2354 \pm 0.001$
		Non-Collinear	$0.9906 \pm 0.000$	<b><math>0.9600 \pm 0.000</math></b>	$0.1419 \pm 0.000$	$0.2091 \pm 0.001$

Table 37: Wikipedia (BF16) - Holdout-CO ( $\mathcal{H}_{col}$ ). Mean across 30 seeds; CI = 95% CI on the mean.

Epoch	Law	Design	$R^2$ Train	$R^2 \mathcal{H}_{col}$	RMSE Train	RMSE $\mathcal{H}_{col}$
-	Repeated-data	Collinear	$0.9882 \pm 0.000$	$0.9639 \pm 0.000$	$0.1990 \pm 0.000$	$0.2244 \pm 0.000$
		Non-Collinear	$0.9856 \pm 0.000$	<b><math>0.9752 \pm 0.000</math></b>	$0.1824 \pm 0.000$	$0.1861 \pm 0.000$
	Chinchilla	Collinear	$0.9916 \pm 0.000$	$0.9699 \pm 0.001$	$0.1601 \pm 0.000$	$0.2046 \pm 0.002$
		Non-Collinear	$0.9915 \pm 0.000$	<b><math>0.9743 \pm 0.001</math></b>	$0.1334 \pm 0.000$	$0.1887 \pm 0.004$
Final	Droppo-Elibol	Collinear	$0.9917 \pm 0.000$	$0.9716 \pm 0.000$	$0.1596 \pm 0.000$	$0.1987 \pm 0.001$
		Non-Collinear	$0.9916 \pm 0.000$	<b><math>0.9738 \pm 0.001</math></b>	$0.1328 \pm 0.000$	$0.1906 \pm 0.002$
	Kaplan	Collinear	$0.9915 \pm 0.000$	<b><math>0.9735 \pm 0.000</math></b>	$0.1612 \pm 0.000$	$0.1918 \pm 0.001$
		Non-Collinear	$0.9898 \pm 0.000$	$0.9719 \pm 0.000$	$0.1458 \pm 0.000$	$0.1978 \pm 0.001$
	Chinchilla	Collinear	$0.9857 \pm 0.000$	$0.9497 \pm 0.002$	$0.2331 \pm 0.000$	$0.2655 \pm 0.004$
		Non-Collinear	$0.9893 \pm 0.000$	<b><math>0.9809 \pm 0.001</math></b>	$0.1689 \pm 0.001$	$0.1633 \pm 0.005$
First	Droppo-Elibol	Collinear	$0.9858 \pm 0.000$	$0.9526 \pm 0.001$	$0.2324 \pm 0.000$	$0.2579 \pm 0.002$
		Non-Collinear	$0.9923 \pm 0.000$	<b><math>0.9750 \pm 0.001</math></b>	$0.1438 \pm 0.000$	$0.1871 \pm 0.003$
	Kaplan	Collinear	$0.9856 \pm 0.000$	$0.9560 \pm 0.001$	$0.2342 \pm 0.000$	$0.2484 \pm 0.002$
		Non-Collinear	$0.9922 \pm 0.000$	<b><math>0.9688 \pm 0.000</math></b>	$0.1446 \pm 0.000$	$0.2094 \pm 0.001$
	Chinchilla	Collinear	$0.9920 \pm 0.000$	$0.9687 \pm 0.001$	$0.1578 \pm 0.000$	$0.2079 \pm 0.002$
		Non-Collinear	$0.9918 \pm 0.000$	<b><math>0.9748 \pm 0.001</math></b>	$0.1329 \pm 0.001$	$0.1862 \pm 0.005$
Second	Droppo-Elibol	Collinear	$0.9920 \pm 0.000$	$0.9704 \pm 0.001$	$0.1574 \pm 0.000$	$0.2023 \pm 0.002$
		Non-Collinear	$0.9921 \pm 0.000$	<b><math>0.9712 \pm 0.001</math></b>	$0.1301 \pm 0.000$	$0.1996 \pm 0.002$
	Kaplan	Collinear	$0.9919 \pm 0.000$	<b><math>0.9731 \pm 0.000</math></b>	$0.1588 \pm 0.000$	$0.1929 \pm 0.001$
		Non-Collinear	$0.9906 \pm 0.000$	$0.9679 \pm 0.000$	$0.1419 \pm 0.000$	$0.2106 \pm 0.001$

Table 38: Wikipedia (BF16) - Holdout-NC ( $\mathcal{H}_{nc}$ ). Mean across 30 seeds; CI = 95% CI on the mean.

Epoch	Law	Design	$R^2$ Train	$R^2 \mathcal{H}_{nc}$	RMSE Train	RMSE $\mathcal{H}_{nc}$
-	Repeated-data	Collinear	$0.9882 \pm 0.000$	$0.9157 \pm 0.000$	$0.1990 \pm 0.000$	$0.2772 \pm 0.000$
		Non-Collinear	$0.9856 \pm 0.000$	<b><math>0.9697 \pm 0.000</math></b>	$0.1824 \pm 0.000$	$0.1662 \pm 0.000$
	Chinchilla	Collinear	$0.9916 \pm 0.000$	$0.9330 \pm 0.002$	$0.1601 \pm 0.000$	$0.2413 \pm 0.004$
		Non-Collinear	$0.9915 \pm 0.000$	<b><math>0.9592 \pm 0.002</math></b>	$0.1334 \pm 0.000$	$0.1879 \pm 0.006$
Final	Droppo-Elibol	Collinear	$0.9917 \pm 0.000$	$0.9376 \pm 0.001$	$0.1596 \pm 0.000$	$0.2330 \pm 0.002$
		Non-Collinear	$0.9916 \pm 0.000$	<b><math>0.9573 \pm 0.001</math></b>	$0.1328 \pm 0.000$	$0.1926 \pm 0.003$
	Kaplan	Collinear	$0.9915 \pm 0.000$	$0.9133 \pm 0.001$	$0.1612 \pm 0.000$	$0.2747 \pm 0.002$
		Non-Collinear	$0.9898 \pm 0.000$	<b><math>0.9591 \pm 0.001</math></b>	$0.1458 \pm 0.000$	$0.1886 \pm 0.001$
	Chinchilla	Collinear	$0.9857 \pm 0.000$	$0.8621 \pm 0.005$	$0.2331 \pm 0.000$	$0.3672 \pm 0.007$
		Non-Collinear	$0.9893 \pm 0.000$	<b><math>0.9717 \pm 0.002</math></b>	$0.1689 \pm 0.001$	$0.1656 \pm 0.006$
First	Droppo-Elibol	Collinear	$0.9858 \pm 0.000$	$0.8954 \pm 0.004$	$0.2324 \pm 0.000$	$0.3200 \pm 0.005$
		Non-Collinear	$0.9923 \pm 0.000$	<b><math>0.9475 \pm 0.001</math></b>	$0.1438 \pm 0.000$	$0.2267 \pm 0.003$
	Kaplan	Collinear	$0.9856 \pm 0.000$	$0.8934 \pm 0.002$	$0.2342 \pm 0.000$	$0.3233 \pm 0.003$
		Non-Collinear	$0.9922 \pm 0.000$	<b><math>0.9358 \pm 0.000</math></b>	$0.1446 \pm 0.000$	$0.2508 \pm 0.001$
	Chinchilla	Collinear	$0.9920 \pm 0.000$	$0.9387 \pm 0.002$	$0.1578 \pm 0.000$	$0.2305 \pm 0.004$
		Non-Collinear	$0.9918 \pm 0.000$	<b><math>0.9632 \pm 0.002</math></b>	$0.1329 \pm 0.001$	$0.1779 \pm 0.006$
Second	Droppo-Elibol	Collinear	$0.9920 \pm 0.000$	$0.9412 \pm 0.003$	$0.1574 \pm 0.000$	$0.2254 \pm 0.006$
		Non-Collinear	$0.9921 \pm 0.000$	<b><math>0.9539 \pm 0.001</math></b>	$0.1301 \pm 0.000$	$0.1998 \pm 0.003$
	Kaplan	Collinear	$0.9919 \pm 0.000$	$0.9222 \pm 0.001$	$0.1588 \pm 0.000$	$0.2599 \pm 0.001$
		Non-Collinear	$0.9906 \pm 0.000$	<b><math>0.9501 \pm 0.001</math></b>	$0.1419 \pm 0.000$	$0.2081 \pm 0.001$

## F Appendix - Fitted scaling law coefficients

Tables 39-43 report the best-fit parameters obtained by multi-start L-BFGS-B with differential evolution polish, on seed 0.  $R^2$  is reported on four splits: training (train), unified holdout (uni), collinear holdout (co), and non-collinear holdout (nc). Please refer to Appendix C.7 for the optimizer bounds we used. Both model designs were trained with the same bounds.

Table 39: Chinchilla fitted parameters:  $L(N, D) = E + A N^{-\alpha} + B D^{-\beta}$ . Final epoch.

Dataset	Design	$E$	$A$	$\alpha$	$B$	$\beta$	$R_{\text{train}}^2$	$R_{\mathcal{H}}^2$	$R_{\mathcal{H}_{\text{col}}}^2$	$R_{\mathcal{H}_{\text{nc}}}^2$
Wikipedia	CO	1.857	4.26e6	0.908	2.99e4	0.518	0.992	0.864	0.966	0.633
	NC	0	239.156	0.260	5.02e4	0.552	0.937	0.898	0.929	0.829
Cosmopedia	CO	1.367	4249.535	0.471	8.53e6	0.874	0.986	0.950	0.961	0.937
	NC	1.174	871.957	0.370	1.37e7	0.902	0.950	0.952	0.956	0.947
RedPajama	CO	2.400	1.87e5	0.706	2.68e4	0.517	0.993	0.880	0.967	0.692
	NC	0.242	118.949	0.209	5.02e4	0.557	0.944	0.916	0.939	0.865
peS2o	CO	2.117	1.66e4	0.566	2.45e5	0.667	0.983	0.896	0.924	0.857
	NC	0	68.799	0.174	2.73e7	0.951	0.935	0.945	0.957	0.929
C4	CO	0.410	47.594	0.161	3.59e7	0.971	0.979	0.945	0.960	0.927
	NC	1.131	82.645	0.216	3.82e4	0.580	0.934	0.954	0.963	0.944

Table 40: Kaplan fitted parameters:  $L(N, D) = [(N_c/N)^{\alpha_N/\alpha_D} + D_c/D]^{\alpha_D}$ . Final epoch.

Dataset	Design	$N_c$	$D_c$	$\alpha_N$	$\alpha_D$	$\alpha_N/\alpha_D$	$R_{\text{train}}^2$	$R_{\mathcal{H}}^2$	$R_{\mathcal{H}_{\text{col}}}^2$	$R_{\mathcal{H}_{\text{nc}}}^2$
Wikipedia	CO	6.78e8	6.90e8	0.382	0.563	0.679	0.985	0.612	0.862	0.045
	NC	1.11e10	2.11e7	0.208	2.000	0.104	0.927	0.884	0.909	0.829
Cosmopedia	CO	1.17e9	1.15e8	0.274	0.841	0.325	0.985	0.942	0.959	0.923
	NC	2.53e9	6.15e7	0.227	1.075	0.211	0.950	0.959	0.961	0.956
RedPajama	CO	3.41e9	10 <sup>9</sup>	0.296	0.512	0.577	0.987	0.666	0.888	0.181
	NC	1.89e11	3.74e7	0.162	1.411	0.115	0.920	0.875	0.904	0.811
peS2o	CO	5.32e9	2.10e8	0.236	0.685	0.345	0.981	0.824	0.881	0.747
	NC	4.67e10	2.76e7	0.169	1.435	0.118	0.936	0.943	0.954	0.928
C4	CO	1.89e11	3.74e7	0.141	1.192	0.118	0.980	0.943	0.956	0.927
	NC	1.89e11	3.74e7	0.140	1.100	0.128	0.928	0.940	0.950	0.929

Table 41: Droppo-Elibol fitted parameters. Final epoch.

Dataset	Design	$L_{\infty}$	$N_C$	$D_C$	$\alpha_N$	$\alpha_D$	$\alpha$	$R_{\text{train}}^2$	$R_{\mathcal{H}}^2$	$R_{\mathcal{H}_{\text{col}}}^2$	$R_{\mathcal{H}_{\text{nc}}}^2$
Wikipedia	CO	2.094	4.64e7	7.72e8	0.735	0.505	0.720	0.992	0.810	0.967	0.456
	NC	0.114	1.36e8	2.57e7	0.298	0.853	2.000	0.957	0.916	0.940	0.861
Cosmopedia	CO	0.509	8.02e7	3.34e7	0.358	1.095	1.476	0.986	0.960	0.966	0.952
	NC	0.556	8.02e7	3.34e7	0.329	1.158	1.481	0.954	0.963	0.966	0.959
RedPajama	CO	1.995	3.69e6	2.61e7	1.016	0.675	1.918	0.993	0.915	0.963	0.811
	NC	0.054	1.61e9	1.97e7	0.215	0.776	2.000	0.959	0.918	0.939	0.875
peS2o	CO	1.047	8.02e7	3.34e7	0.363	0.983	1.393	0.983	0.894	0.916	0.863
	NC	0.534	1.10e8	1.52e7	0.264	1.312	1.833	0.943	0.954	0.964	0.940
C4	CO	0.468	3.48e8	1.49e7	0.205	1.638	1.794	0.981	0.945	0.955	0.933
	NC	0.050	1.23e10	7.80e6	0.153	1.266	1.984	0.940	0.954	0.963	0.944

Table 42: Repeated-data fitted scaling-law parameters. Final epoch.

Dataset	Design	$A$	$\alpha$	$B$	$\beta$	$E$
Wikipedia	CO	4.22e5	0.746	2.19e4	0.515	1.538
	NC	194.407	0.244	9.09e4	0.601	1.86e-11
Cosmopedia	CO	7.22e4	0.656	1.45e6	0.787	1.752
	NC	303.693	0.290	1.46e6	0.790	0.618
RedPajama	CO	1.15e5	0.667	1.26e4	0.485	2.164
	NC	97.241	0.192	4.86e4	0.566	5.23e-12
peS2o	CO	3.07e4	0.600	4.75e5	0.723	2.265
	NC	70.386	0.177	8.92e5	0.762	2.25e-11
C4	CO	1.68e6	0.879	1.84e7	0.963	3.088
	NC	34.408	0.136	1.82e5	0.684	2.94e-11

Table 43: Repeated-data fit quality and repetition factors. Final epoch. Values reported as 0.1 for  $R_N^*$  indicate the L-BFGS-B optimizer terminating at the documented lower bound  $R_N^* \in [0.1, 50.0]$ ; see Appendix C.7 for the full bound list and an explanation of why  $R_N^*$  is not informatively constrained by our grid (epochs vary  $D$  but not  $N$ ).

Dataset	Design	$R_D^*$	$R_N^*$	$R_{\text{train}}^2$	$R_{\mathcal{H}}^2$	$R_{\mathcal{H}_{\text{col}}}^2$	$R_{\mathcal{H}_{\text{nc}}}^2$
Wikipedia	CO	1.074	0.100	0.985	0.867	0.952	0.691
	NC	1.469	0.100	0.959	0.915	0.932	0.882
Cosmopedia	CO	1.500	0.153	0.984	0.950	0.965	0.933
	NC	1.286	0.100	0.966	0.968	0.972	0.965
RedPajama	CO	1.162	0.100	0.988	0.890	0.960	0.756
	NC	1.624	0.100	0.964	0.929	0.943	0.902
peS2o	CO	1.897	0.119	0.986	0.923	0.950	0.891
	NC	2.188	0.100	0.962	0.946	0.951	0.941
C4	CO	0.801	0.564	0.978	0.818	0.857	0.775
	NC	2.352	0.100	0.936	0.957	0.959	0.955

Table 44: BF16 Chinchilla fitted parameters:  $L(N, D) = E + A N^{-\alpha} + B D^{-\beta}$ . Final epoch.

Dataset	Design	$E$	$A$	$\alpha$	$B$	$\beta$	$R_{\text{train}}^2$	$R_{\mathcal{H}}^2$	$R_{\mathcal{H}_{\text{col}}}^2$	$R_{\mathcal{H}_{\text{nc}}}^2$
Wikipedia (BF16)	CO	0	3428.447	0.399	2366.171	0.392	0.992	0.953	0.970	0.933
	NC	0.758	4904.551	0.421	4.82e5	0.713	0.991	0.978	0.981	0.973

Table 45: BF16 Kaplan fitted parameters:  $L(N, D) = [(N_c/N)^{\alpha_N/\alpha_D} + D_c/D]^{\alpha_D}$ . Final epoch.

Dataset	Design	$N_c$	$D_c$	$\alpha_N$	$\alpha_D$	$\alpha_N/\alpha_D$	$R_{\text{train}}^2$	$R_{\mathcal{H}}^2$	$R_{\mathcal{H}_{\text{col}}}^2$	$R_{\mathcal{H}_{\text{nc}}}^2$
Wikipedia (BF16)	CO	1.19e9	2.84e9	0.397	0.394	1.008	0.992	0.946	0.974	0.914
	NC	1.98e9	1.12e8	0.354	0.823	0.430	0.990	0.966	0.972	0.959

Table 46: BF16 Droppo-Elibol fitted parameters. Final epoch.

Dataset	Design	$L_\infty$	$N_C$	$D_C$	$\alpha_N$	$\alpha_D$	$\alpha$	$R_{\text{train}}^2$	$R_{\mathcal{H}}^2$	$R_{\mathcal{H}_{\text{col}}}^2$	$R_{\mathcal{H}_{\text{nc}}}^2$
Wikipedia (BF16)	CO	10 <sup>-6</sup>	9.97e8	1.67e9	0.400	0.388	0.583	0.992	0.956	0.972	0.938
	NC	0.224	1.21e9	1.65e8	0.379	0.612	0.882	0.992	0.965	0.973	0.955

Table 47: BF16 Repeated-data fitted scaling-law parameters. Final epoch.

Dataset	Design	$A$	$\alpha$	$B$	$\beta$	$E$
Wikipedia (BF16)	CO	3125.835	0.392	3300.851	0.427	1.29e-12
	NC	3045.878	0.387	3.49e7	0.995	0.612

Table 48: BF16 Repeated-data fit quality and repetition factors. Final epoch. Values reported as 0.1 for  $R_N^*$  indicate the L-BFGS-B optimizer terminating at the documented lower bound  $R_N^* \in [0.1, 50.0]$ ; see Appendix C.7.

Dataset	Design	$R_D^*$	$R_N^*$	$R_{\text{train}}^2$	$R_{\mathcal{H}}^2$	$R_{\mathcal{H}_{\text{col}}}^2$	$R_{\mathcal{H}_{\text{inc}}}^2$
Wikipedia (BF16)	CO	0.283	0.100	0.988	0.941	0.964	0.916
	NC	0.723	0.100	0.986	0.973	0.975	0.970

# NeurIPS Paper Checklist

## 1. Claims

Question: Do the main claims made in the abstract and introduction accurately reflect the paper’s contributions and scope?

Answer: [Yes]

Justification: The abstract and introduction state five claims; ill-conditioning (Proposition 1), CI inflation (Corollary 1), a TPP-diversity threshold (Proposition 2), NC-vs-CO holdout ordering (Theorem 1, Tables 3-6), and Jacobian-geometry generality (Section 3.2) - each backed by a formal result or empirical table in the body, and constitute the main contributions of the paper.

Guidelines:

- The answer [N/A] means that the abstract and introduction do not include the claims made in the paper.
- The abstract and/or introduction should clearly state the claims made, including the contributions made in the paper and important assumptions and limitations. A [No] or [N/A] answer to this question will not be perceived well by the reviewers.
- The claims made should match theoretical and experimental results, and reflect how much the results can be expected to generalize to other settings.
- It is fine to include aspirational goals as motivation as long as it is clear that these goals are not attained by the paper.

## 2. Limitations

Question: Does the paper discuss the limitations of the work performed by the authors?

Answer: [Yes]

Justification: Section 5 (paragraph 5) discusses theoretical caveats (Theorem 1 gives an ordering not a magnitude; Corollary 1 assumes i.i.d. Gaussian residuals), empirical scope (small-scale models, single architecture, English-only, single fitting protocol, assumption of small loss perturbations due to hyperparameter shifts from dataset-specific values), and generalization limits - softening on Cosmopedia/peS2o, pre-training-only scope, untested cross-domain and downstream tasks transfer.

Guidelines:

- The answer [N/A] means that the paper has no limitation while the answer [No] means that the paper has limitations, but those are not discussed in the paper.
- The authors are encouraged to create a separate “Limitations” section in their paper.
- The paper should point out any strong assumptions and how robust the results are to violations of these assumptions (e.g., independence assumptions, noiseless settings, model well-specification, asymptotic approximations only holding locally). The authors should reflect on how these assumptions might be violated in practice and what the implications would be.
- The authors should reflect on the scope of the claims made, e.g., if the approach was only tested on a few datasets or with a few runs. In general, empirical results often depend on implicit assumptions, which should be articulated.
- The authors should reflect on the factors that influence the performance of the approach. For example, a facial recognition algorithm may perform poorly when image resolution is low or images are taken in low lighting. Or a speech-to-text system might not be used reliably to provide closed captions for online lectures because it fails to handle technical jargon.
- The authors should discuss the computational efficiency of the proposed algorithms and how they scale with dataset size.
- If applicable, the authors should discuss possible limitations of their approach to address problems of privacy and fairness.
- While the authors might fear that complete honesty about limitations might be used by reviewers as grounds for rejection, a worse outcome might be that reviewers discover limitations that aren’t acknowledged in the paper. The authors should use their best judgment and recognize that individual actions in favor of transparency play an important role in developing norms that preserve the integrity of the community. Reviewers will be specifically instructed to not penalize honesty concerning limitations.

## 3. Theory assumptions and proofs

Question: For each theoretical result, does the paper provide the full set of assumptions and a complete (and correct) proof?

Answer: [Yes]

Justification: All assumptions are stated in each theorem environment. Complete proofs are in Appendix B: Proposition 1 in B.3, Corollary 1 in B.11, Proposition 2 in B.12, and Theorem 1 in B.13.

Guidelines:

- The answer [N/A] means that the paper does not include theoretical results.
- All the theorems, formulas, and proofs in the paper should be numbered and cross-referenced.
- All assumptions should be clearly stated or referenced in the statement of any theorems.
- The proofs can either appear in the main paper or the supplemental material, but if they appear in the supplemental material, the authors are encouraged to provide a short proof sketch to provide intuition.
- Inversely, any informal proof provided in the core of the paper should be complemented by formal proofs provided in appendix or supplemental material.
- Theorems and Lemmas that the proof relies upon should be properly referenced.

#### 4. Experimental result reproducibility

Question: Does the paper fully disclose all the information needed to reproduce the main experimental results of the paper to the extent that it affects the main claims and/or conclusions of the paper (regardless of whether the code and data are provided or not)?

Answer: [Yes]

Justification: All architectures, hyperparameters, data splits, fitting protocols, and seed strategies are specified in Section 4 and Appendices C-D.6, with fitted coefficients in Appendix F. An anonymized live online repository link is provided, and the supplementary material includes a ZIP file with a screenshot of that repository, with instructions to reproduce all tables either from pre-computed metrics (~2 CPU-hours) or from scratch (~3,624 GPU-hours).

Guidelines:

- The answer [N/A] means that the paper does not include experiments.
- If the paper includes experiments, a [No] answer to this question will not be perceived well by the reviewers: Making the paper reproducible is important, regardless of whether the code and data are provided or not.
- If the contribution is a dataset and/or model, the authors should describe the steps taken to make their results reproducible or verifiable.
- Depending on the contribution, reproducibility can be accomplished in various ways. For example, if the contribution is a novel architecture, describing the architecture fully might suffice, or if the contribution is a specific model and empirical evaluation, it may be necessary to either make it possible for others to replicate the model with the same dataset, or provide access to the model. In general, releasing code and data is often one good way to accomplish this, but reproducibility can also be provided via detailed instructions for how to replicate the results, access to a hosted model (e.g., in the case of a large language model), releasing of a model checkpoint, or other means that are appropriate to the research performed.
- While NeurIPS does not require releasing code, the conference does require all submissions to provide some reasonable avenue for reproducibility, which may depend on the nature of the contribution. For example
  - (a) If the contribution is primarily a new algorithm, the paper should make it clear how to reproduce that algorithm.
  - (b) If the contribution is primarily a new model architecture, the paper should describe the architecture clearly and fully.
  - (c) If the contribution is a new model (e.g., a large language model), then there should either be a way to access this model for reproducing the results or a way to reproduce the model (e.g., with an open-source dataset or instructions for how to construct the dataset).
  - (d) We recognize that reproducibility may be tricky in some cases, in which case authors are welcome to describe the particular way they provide for reproducibility. In the case of closed-source models, it may be that access to the model is limited in some way (e.g., to registered users), but it should be possible for other researchers to have some path to reproducing or verifying the results.

#### 5. Open access to data and code

Question: Does the paper provide open access to the data and code, with sufficient instructions to faithfully reproduce the main experimental results, as described in supplemental material?

Answer: [Yes]

Justification: Anonymized code: [https://anonymous.4open.science/r/Tokens-per-Parameter\\_Coverage\\_Is\\_Critical\\_for\\_Robust\\_LLM\\_Scaling\\_Law\\_Extrapolation-CC76](https://anonymous.4open.science/r/Tokens-per-Parameter_Coverage_Is_Critical_for_Robust_LLM_Scaling_Law_Extrapolation-CC76). Trained LLMs checkpoints and metrics: [https://huggingface.co/datasets/TPPIsCriticalFor/colinear\\_scaling\\_models](https://huggingface.co/datasets/TPPIsCriticalFor/colinear_scaling_models). All five training corpora are publicly available under permissive licenses.

Guidelines:

- The answer [N/A] means that paper does not include experiments requiring code.
- Please see the NeurIPS code and data submission guidelines (<https://neurips.cc/public/guides/CodeSubmissionPolicy>) for more details.
- While we encourage the release of code and data, we understand that this might not be possible, so [No] is an acceptable answer. Papers cannot be rejected simply for not including code, unless this is central to the contribution (e.g., for a new open-source benchmark).
- The instructions should contain the exact command and environment needed to run to reproduce the results. See the NeurIPS code and data submission guidelines (<https://neurips.cc/public/guides/CodeSubmissionPolicy>) for more details.
- The authors should provide instructions on data access and preparation, including how to access the raw data, preprocessed data, intermediate data, and generated data, etc.
- The authors should provide scripts to reproduce all experimental results for the new proposed method and baselines. If only a subset of experiments are reproducible, they should state which ones are omitted from the script and why.
- At submission time, to preserve anonymity, the authors should release anonymized versions (if applicable).
- Providing as much information as possible in supplemental material (appended to the paper) is recommended, but including URLs to data and code is permitted.

## 6. Experimental setting/details

Question: Does the paper specify all the training and test details (e.g., data splits, hyperparameters, how they were chosen, type of optimizer) necessary to understand the results?

Answer: [Yes]

Justification: All 14 architectures (Table 10), training hyperparameters (Table 11), per-dataset learning rates, data-split procedures, CO/NC grid definitions, holdout partitions, fitting protocol (restart counts, seed strategy), and compute infrastructure are specified in Section 4 and Appendix C.

Guidelines:

- The answer [N/A] means that the paper does not include experiments.
- The experimental setting should be presented in the core of the paper to a level of detail that is necessary to appreciate the results and make sense of them.
- The full details can be provided either with the code, in appendix, or as supplemental material.

## 7. Experiment statistical significance

Question: Does the paper report error bars suitably and correctly defined or other appropriate information about the statistical significance of the experiments?

Answer: [Yes]

Justification: All results report seed-to-seed standard deviations and 95% CIs on the mean across 30 optimizer seeds (Tables 3-4), the overall win rate includes a 95% CI over 1,500 seed-paired comparisons, and the budget-matched subset enumeration (Table 6) reports bootstrap CIs across 22 seeds. A BF16 mixed-precision replication on Wikipedia (Table 5 in the main text and Tables 16-17 in Appendix D.4) independently confirms the same patterns with seed-paired NC win rate 98.7% (296/300).

Guidelines:

- The answer [N/A] means that the paper does not include experiments.
- The authors should answer [Yes] if the results are accompanied by error bars, confidence intervals, or statistical significance tests, at least for the experiments that support the main claims of the paper.
- The factors of variability that the error bars are capturing should be clearly stated (for example, train/test split, initialization, random drawing of some parameter, or overall run with given experimental conditions).
- The method for calculating the error bars should be explained (closed form formula, call to a library function, bootstrap, etc.)
- The assumptions made should be given (e.g., Normally distributed errors).

- It should be clear whether the error bar is the standard deviation or the standard error of the mean.
- It is OK to report 1-sigma error bars, but one should state it. The authors should preferably report a 2-sigma error bar than state that they have a 96% CI, if the hypothesis of Normality of errors is not verified.
- For asymmetric distributions, the authors should be careful not to show in tables or figures symmetric error bars that would yield results that are out of range (e.g., negative error rates).
- If error bars are reported in tables or plots, the authors should explain in the text how they were calculated and reference the corresponding figures or tables in the text.

## 8. Experiments compute resources

Question: For each experiment, does the paper provide sufficient information on the computer resources (type of compute workers, memory, time of execution) needed to reproduce the experiments?

Answer: [Yes]

Justification: Appendix C.6 reports worker type, memory, runtime, and storage for each experiment family:  $\sim 3,624$  GPU-hours for pre-training,  $\sim 5$  wall-clock hours (230 workers) for fitting/visualization, and  $\sim 24$  hours (480 workers) for subset enumeration, plus  $\sim 2.2$  TB total storage. We also disclose that full-project compute exceeded the final reported experiment runs due to pilot and failed sweeps; this additional usage will be reported in the NeurIPS compute-reporting form.

Guidelines:

- The answer [N/A] means that the paper does not include experiments.
- The paper should indicate the type of compute workers CPU or GPU, internal cluster, or cloud provider, including relevant memory and storage.
- The paper should provide the amount of compute required for each of the individual experimental runs as well as estimate the total compute.
- The paper should disclose whether the full research project required more compute than the experiments reported in the paper (e.g., preliminary or failed experiments that didn't make it into the paper).

## 9. Code of ethics

Question: Does the research conducted in the paper conform, in every respect, with the NeurIPS Code of Ethics <https://neurips.cc/public/EthicsGuidelines>?

Answer: [Yes]

Justification: The work uses only publicly available, permissively licensed corpora, involves no human subjects, and releases small-scale checkpoints (5-76.5M parameters) that pose no dual-use risk. See Section 5 for a detailed assessment.

Guidelines:

- The answer [N/A] means that the authors have not reviewed the NeurIPS Code of Ethics.
- If the authors answer [No], they should explain the special circumstances that require a deviation from the Code of Ethics.
- The authors should make sure to preserve anonymity (e.g., if there is a special consideration due to laws or regulations in their jurisdiction).

## 10. Broader impacts

Question: Does the paper discuss both potential positive societal impacts and negative societal impacts of the work performed?

Answer: [Yes]

Justification: Section 5 discusses the corrective intent of the work (deflating overconfident scaling-law extrapolations) and Section 5 addresses the negligible misuse risk of the released checkpoints and the marginal indirect risk of accelerating capability development.

Guidelines:

- The answer [N/A] means that there is no societal impact of the work performed.
- If the authors answer [N/A] or [No], they should explain why their work has no societal impact or why the paper does not address societal impact.
- Examples of negative societal impacts include potential malicious or unintended uses (e.g., disinformation, generating fake profiles, surveillance), fairness considerations (e.g., deployment of technologies that could make decisions that unfairly impact specific groups), privacy considerations, and security considerations.

- The conference expects that many papers will be foundational research and not tied to particular applications, let alone deployments. However, if there is a direct path to any negative applications, the authors should point it out. For example, it is legitimate to point out that an improvement in the quality of generative models could be used to generate Deepfakes for disinformation. On the other hand, it is not needed to point out that a generic algorithm for optimizing neural networks could enable people to train models that generate Deepfakes faster.
- The authors should consider possible harms that could arise when the technology is being used as intended and functioning correctly, harms that could arise when the technology is being used as intended but gives incorrect results, and harms following from (intentional or unintentional) misuse of the technology.
- If there are negative societal impacts, the authors could also discuss possible mitigation strategies (e.g., gated release of models, providing defenses in addition to attacks, mechanisms for monitoring misuse, mechanisms to monitor how a system learns from feedback over time, improving the efficiency and accessibility of ML).

## 11. Safeguards

Question: Does the paper describe safeguards that have been put in place for responsible release of data or models that have a high risk for misuse (e.g., pre-trained language models, image generators, or scraped datasets)?

Answer: [Yes]

Justification: Section 5 describes the safeguards: all corpora are publicly available and pre-filtered, released checkpoints are too small for dual-use capabilities, and the accompanying code targets fitting diagnostics rather than model serving.

Guidelines:

- The answer [N/A] means that the paper poses no such risks.
- Released models that have a high risk for misuse or dual-use should be released with necessary safeguards to allow for controlled use of the model, for example by requiring that users adhere to usage guidelines or restrictions to access the model or implementing safety filters.
- Datasets that have been scraped from the Internet could pose safety risks. The authors should describe how they avoided releasing unsafe images.
- We recognize that providing effective safeguards is challenging, and many papers do not require this, but we encourage authors to take this into account and make a best faith effort.

## 12. Licenses for existing assets

Question: Are the creators or original owners of assets (e.g., code, data, models), used in the paper, properly credited and are the license and terms of use explicitly mentioned and properly respected?

Answer: [Yes]

Justification: All five corpora and every referenced scaling-law formalism are cited at first use (Section 4). The LLaMA architecture is credited to [Touvron et al. \(2023\)](#). Dataset licenses are documented in Appendix C; all are publicly available under permissive terms.

Guidelines:

- The answer [N/A] means that the paper does not use existing assets.
- The authors should cite the original paper that produced the code package or dataset.
- The authors should state which version of the asset is used and, if possible, include a URL.
- The name of the license (e.g., CC-BY 4.0) should be included for each asset.
- For scraped data from a particular source (e.g., website), the copyright and terms of service of that source should be provided.
- If assets are released, the license, copyright information, and terms of use in the package should be provided. For popular datasets, [paperswithcode.com/datasets](https://paperswithcode.com/datasets) has curated licenses for some datasets. Their licensing guide can help determine the license of a dataset.
- For existing datasets that are re-packaged, both the original license and the license of the derived asset (if it has changed) should be provided.
- If this information is not available online, the authors are encouraged to reach out to the asset's creators.

## 13. New assets

Question: Are new assets introduced in the paper well documented and is the documentation provided alongside the assets?

Answer: [Yes]

Justification: We release trained model checkpoints on HuggingFace ([https://huggingface.co/datasets/TPPIsCriticalFor/colinear\\_scaling\\_models](https://huggingface.co/datasets/TPPIsCriticalFor/colinear_scaling_models)) with accompanying documentation describing model configurations, training corpora, and hyperparameters. Experimental code for reproducing scaling law fits and analyses is provided through an anonymized live online repository link, and the supplementary material includes a ZIP file with a screenshot of that repository. All assets use publicly available, permissively licensed training data (RedPajama, Cosmopedia, Wikipedia, peS2o, C4).

Guidelines:

- The answer [N/A] means that the paper does not release new assets.
- Researchers should communicate the details of the dataset/code/model as part of their submissions via structured templates. This includes details about training, license, limitations, etc.
- The paper should discuss whether and how consent was obtained from people whose asset is used.
- At submission time, remember to anonymize your assets (if applicable). You can either create an anonymized URL or include an anonymized zip file.

#### 14. Crowdsourcing and research with human subjects

Question: For crowdsourcing experiments and research with human subjects, does the paper include the full text of instructions given to participants and screenshots, if applicable, as well as details about compensation (if any)?

Answer: [N/A]

Justification: This work does not involve crowdsourcing or human subjects.

Guidelines:

- The answer [N/A] means that the paper does not involve crowdsourcing nor research with human subjects.
- Including this information in the supplemental material is fine, but if the main contribution of the paper involves human subjects, then as much detail as possible should be included in the main paper.
- According to the NeurIPS Code of Ethics, workers involved in data collection, curation, or other labor should be paid at least the minimum wage in the country of the data collector.

#### 15. Institutional review board (IRB) approvals or equivalent for research with human subjects

Question: Does the paper describe potential risks incurred by study participants, whether such risks were disclosed to the subjects, and whether Institutional Review Board (IRB) approvals (or an equivalent approval/review based on the requirements of your country or institution) were obtained?

Answer: [N/A]

Justification: This paper does not involve crowdsourcing nor research with human subjects.

Guidelines:

- The answer [N/A] means that the paper does not involve crowdsourcing nor research with human subjects.
- Depending on the country in which research is conducted, IRB approval (or equivalent) may be required for any human subjects research. If you obtained IRB approval, you should clearly state this in the paper.
- We recognize that the procedures for this may vary significantly between institutions and locations, and we expect authors to adhere to the NeurIPS Code of Ethics and the guidelines for their institution.
- For initial submissions, do not include any information that would break anonymity (if applicable), such as the institution conducting the review.

#### 16. Declaration of LLM usage

Question: Does the paper describe the usage of LLMs if it is an important, original, or non-standard component of the core methods in this research? Note that if the LLM is used only for writing, editing, or formatting purposes and does *not* impact the core methodology, scientific rigor, or originality of the research, declaration is not required.

Answer: [Yes]

Justification: LLM usage is declared in Section 5 (paragraph 5). In short: all research questions, theoretical results, experimental design, and empirical analyses originated with the authors. The primary non-trivial use of LLMs was as a sounding board for candidate proof steps - the authors

drafted the structure of each derivation, asked an LLM to propose intermediate algebraic manipulations, and independently verified, rewrote, or discarded each suggestion before incorporation. Auxiliary uses included exposition,  $\LaTeX$  typesetting, boilerplate code for data loading, training, analysis, and visualization, and prose editing - all reviewed by the authors. We acknowledge Anthropic's Claude Opus 4.7 for its assistance in this capacity.

Guidelines:

- The answer [N/A] means that the core method development in this research does not involve LLMs as any important, original, or non-standard components.
- Please refer to our LLM policy in the NeurIPS handbook for what should or should not be described.